Advanced Oxidation Processes for Organic Contaminant Destruction Based on the Fenton Reaction and Related Chemistry

Joseph J. Pignatello [a]; Esther Oliveros [b]; Allison MacKay [c]
[a] Department of Soil and Water, Connecticut Agricultural Experiment Station, New Haven, Connecticut, USA [b] Lehrstuhl für Umweltmesstechnik, Engler Bunte Institut, Universitaet Karlsruhe, Karlsruhe, Germany [c] Department of Civil and Environmental Engineering, University of Connecticut, Storrs, Connecticut, USA

PLEASE SCROLL DOWN FOR ARTICLE

Advanced Oxidation Processes for Organic Contaminant Destruction Based on the Fenton Reaction and Related Chemistry

JOSEPH J. PIGNATELLO

*Department of Soil and Water, Connecticut Agricultural Experiment Station,
New Haven, Connecticut, USA*

ESTHER OLIVEROS

*Lehrstuhl für Umweltmesstechnik, Engler Bunte Institut, Universitaet Karlsruhe,
Karlsruhe, Germany*

ALLISON MacKAY

*Department of Civil and Environmental Engineering, University of Connecticut,
Storrs, Connecticut, USA*

*Fenton chemistry encompasses reactions of hydrogen peroxide in
the presence of iron to generate highly reactive species such as the
hydroxyl radical and possibly others. In this review, the complex
mechanisms of Fenton and Fenton-like reactions and the important
factors influencing these reactions, from both a fundamental and
practical perspective, in applications to water and soil treatment,
are discussed. The review covers modified versions including the
photoassisted Fenton reaction, use of chelated iron, electro-Fenton
reactions, and Fenton reactions using heterogeneous catalysts. Sec-
tions are devoted to nonclassical pathways, by-products, kinetics
and process modeling, experimental design methodology, soil and
aquifer treatment, use of Fenton in combination with other ad-
vanced oxidation processes or biodegradation, economic compar-
ison with other advanced oxidation processes, and case studies.*

Address correspondence to Joseph J. Pignatello, Department of Soil and Water,
Connecticut Agricultural Experiment Station, PO Box 1106, New Haven, CT 06504-1106, USA.
E-mail: joseph.pignatello@po.state.ct.us

1. BACKGROUND

Fenton and related reactions encompass reactions of peroxides (usually H_2O_2) with iron ions to form active oxygen species that oxidize organic or inorganic compounds when they are present. The history of Fenton chemistry dates to 1894, when Henry J. Fenton reported that H_2O_2 could be activated by Fe(II) salts to oxidize tartaric acid (Fenton, 1894). In the century since then, Fenton and related reactions have become of great interest for their relevance to biological chemistry, synthesis, the chemistry of natural waters, and the treatment of hazardous wastes. A search of the keyword "Fenton reaction" yielded over 2500 scientific articles since 1945.

In 1934 Haber and Weiss (1934) proposed that the active oxidant generated by the Fenton reaction is the hydroxyl radical (HO$^{\bullet}$), one of the most powerful oxidants known ($E^{\circ} = 2.73$ V). Later, in a series of elegant papers on the decomposition of H_2O_2, Barb et al. (1949, 1951a, 1951b) expanded upon and revised the original mechanism proposed by Haber and Weiss (1934) to provide what is now referred to as the "classical" or "free radical" Fenton chain reaction because it involves HO$^{\bullet}$ production as the key step. This sequence of reactions is discussed in detail in this review. Later, others would propose that high-valent oxoiron complexes may also participate in Fenton chemistry. In 1975, Walling published an influential account of his group's research in Fenton oxidation of organic compounds that promoted the free radical pathway over contemporary challenges and served to renew interest in Fenton chemistry among workers in several fields of chemistry.

In the last few decades the importance of HO$^{\bullet}$ reactions in the natural environment, in biological systems, and in useful chemical processes including waste treatment has been recognized, and over 1700 rate constants for HO$^{\bullet}$ reactions with organic and inorganic compounds in aqueous solution have been tabulated (Buxton et al., 1988; University of Notre Dame Radiation Laboratory, Radiation Chemistry Data Center, http://www.allen.rad.nd.edu/). The Fenton and related reactions are viewed as potentially convenient and economical ways to generate oxidizing species for treating chemical wastes. Compared to other bulk oxidants, hydrogen peroxide is inexpensive, safe, and easy to handle, and poses no lasting environmental threat since it readily decomposes to water and oxygen. Likewise, iron is comparatively inexpensive, safe, and environmentally friendly. Research on applications of Fenton chemistry to waste treatment began in academic laboratories only around 1990, although there are anecdotal accounts of its use in industry on a small scale prior to that time (e.g., Eisenhauer, 1964). The number of scientific articles on applications of Fenton chemistry to waste treatment has increased exponentially over the years. Early on it was realized that Fenton reactions were markedly accelerated by light. The photo-assisted Fenton reaction ("photo-Fenton" reaction) typically gives faster rates and a higher degree of mineralization than the thermal ("dark") reaction and can take advantage of
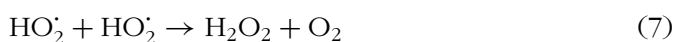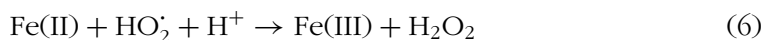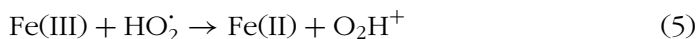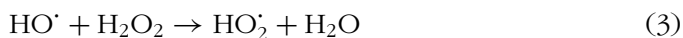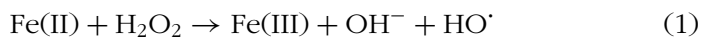
light in the solar spectral region. We now understand the extremely complex chemistry of Fenton systems in considerable detail. Comparisons of Fenton or photo-assisted Fenton systems with other advanced oxidation processes (AOPs) are quite favorable. A few novel variants of the Fenton reaction have been introduced. Investigators have explored the possibility of using Fenton chemistry for degrading contaminants in soil and groundwater. Research on heterogeneous reactions and the preparation of supported iron catalysts continues in an effort to understand and facilitate the reactions in soils and to circumvent the problem of iron oxide sludge generation and disposal inherent in homogeneous Fenton treatment of wastewater.

This review discusses the complex mechanism of Fenton and Fenton-like reactions and the important factors influencing the efficiency of these processes in applications to water and soil treatment. An effort is made to inform the reader on the current state-of-the-art, on the remaining challenges for the development of these processes on the large scale and on the scope of potential applications. Previous recent reviews on the use of Fenton AOPs have focussed on more specific aspects (Tarr, 2003; Burkitt, 2003; Neyens and Baeyens, 2003; Safarzadeh-Amiri et al., 1996) or discuss Fenton more briefly among a list of AOPs (Gogate and Pandit, 2004a, 2004b).

2. FUNDAMENTAL CHEMISTRY OF THE FENTON REACTION

2.1. The Classical Free Radical Mechanism for Decomposition of H_2O_2

The mechanism proposed by Barb et al. (1949, 1951a, 1951b) for decomposition of H_2O_2 in acidic solution in the dark and in the absence of an organic compound consists of the sequence of reactions 1–7. This sequence will be referred to as the thermal Fenton reaction, meaning that it is driven by thermal energy from the surroundings rather than photochemical energy. (The word "thermal" is not meant to imply high temperature.) In this sequence, Fe(II) and Fe(III) are taken to represent all species present in solution in each respective oxidation state.

$$\text{Fe(II)} + H_2O_2 \rightarrow \text{Fe(III)} + OH^- + HO^{\cdot} \tag{1}$$

$$\text{Fe(III)} + H_2O_2 \rightarrow \text{Fe(II)} + HO_2^{\cdot} + H^+ \tag{2}$$

$$HO^{\cdot} + H_2O_2 \rightarrow HO_2^{\cdot} + H_2O \tag{3}$$

$$HO^{\cdot} + \text{Fe(II)} \rightarrow \text{Fe(III)} + OH^- \tag{4}$$

$$\text{Fe(III)} + HO_2^{\cdot} \rightarrow \text{Fe(II)} + O_2H^+ \tag{5}$$

$$\text{Fe(II)} + HO_2^{\cdot} + H^+ \rightarrow \text{Fe(III)} + H_2O_2 \tag{6}$$

$$HO_2^{\cdot} + HO_2^{\cdot} \rightarrow H_2O_2 + O_2 \tag{7}$$

For simplicity, reactions analogous to equations 5–7 involving superoxide anion $O_2^{-\cdot}$, the conjugate base of $HO_2^{\cdot}$ (p$K_a = 4.8$; Sawyer and Valentine, 1981; Bielski and Cabelli, 1991), are omitted (section 2.4). Some of the reactions 1–7 are believed to occur in multiple steps; more details are presented later for those that do.

Some papers have also included reaction 8:

$$HO_2^{\cdot} + H_2O_2 \rightarrow HO^{\cdot} + H_2O + O_2 \qquad (8)$$
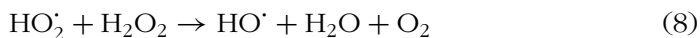
However, reaction 8 is extremely slow ($k_8 = 3$ $M^{-1}\,s^{-1}$; Koppenol et al., 1978) compared to others of $HO_2^{\cdot}$, and can be neglected.

Reactions 1–7 are understood in great detail in simple solutions containing no strongly coordinating ligands other than OH^- and H_2O or other redox species. As can be seen, iron cycles between +II and +III oxidation states. In the absence of any other oxidizable substance the net reaction is the iron-catalyzed conversion of H_2O_2 to molecular oxygen and water according to

$$2H_2O_2 \rightarrow O_2 + 2H_2O \qquad (9)$$

Reaction 9 takes place to a degree even when the target contaminant is present, constituting a waste of bulk oxidant.

The desired oxidant for degrading the target pollutant ($HO^{\cdot}$) is produced by reaction 1. Hydroxyl radical is scavenged by Fe(II) and H_2O_2 (reactions 3 and 4).

The hydroxyl radical may be generated stoichiometrically via reaction 1 simply by combining an Fe(II) salt with H_2O_2. However, this produces a stoichiometric amount of Fe(III) which later precipitates to amorphous ferric oxyhydroxides as the pH is increased from strongly acidic to neutral (section 2.3.1); this generates an undesirable sludge in technological applications. With participation of reaction 2, generation of $HO^{\cdot}$ is catalytic in iron, which can therefore be used in relatively low concentration. Peroxide-to-iron molar ratios employed in water treatment typically lie in the range 100 to 1000. The use of iron catalytically helps to minimize scavenging of $HO^{\cdot}$ by Fe(II) (eq. 4) and also minimizes ferric oxyhydroxides production. Overall, reaction 2 is several orders of magnitude slower than reaction 1, and thus reaction 2 can become the rate-limiting step. However, there are other pathways for reduction of Fe(III) to Fe(II) besides reaction 2, and they are discussed later.

In the literature it is common to refer to reactions initiated by combining H_2O_2 with ferric, as opposed to ferrous, iron as "Fenton-like" reactions and to try to distinguish them mechanistically. However, one can see that both Fe(II) and Fe(III) species are present simultaneously in the chain (reactions 1 to 7), regardless of which is used to initiate the reaction. Consequently, it is usually meaningless *from a mechanistic standpoint* to distinguish "ferrous" from "ferric" type Fenton reactions. This is especially true if a large molar excess of H_2O_2 is present, for in that case all initially added Fe(II) will

quickly be oxidized to Fe(III) and thereafter the system will behave independent of the initial oxidation state of iron. Therefore, this review considers reactions initiated with ferrous and ferric iron as unified. Nevertheless, in practice differences may be, and have been, observed. Starting with Fe(II) can lead to an initial rapid degradation phase resulting from a burst of $HO^{\bullet}$ by reaction 1 (e.g., Bishop et al., 1968; Chen and Pignatello, 1997; Gallard and De Laat, 2000); when H_2O_2 is in large excess the extent of this burst phase will depend on the Fe/contaminant molar ratio because that ratio determines the $HO^{\bullet}$/contaminant ratio in the burst phase. Since reaction 2 is so much slower than reaction 1, starting with Fe(III) salt often results in a slower initial rate—or even a lag phase if aromatic compounds are the targets (section 2.4).

The reactions of $HO^{\bullet}$ with organic compounds lead to the formation of carbon-centered radicals (section 2.6.1). The hydroxyl radical—always present in vanishingly small concentration—reacts in well-known ways with organic compounds, principally by abstracting H from C—H, N—H, or O—H bonds, adding to C=C bonds, or adding to aromatic rings (eqs 10–12) (von Sonntag and Schuchmann, 1997; Buxton et al., 1988):

$$HO^{\bullet} + R - H \rightarrow H_2O + R^{\bullet} \tag{10}$$

$$HO^{\bullet} + C{=}C \rightarrow HO-C-C^{\bullet} \tag{11}$$

$$\tag{12}$$
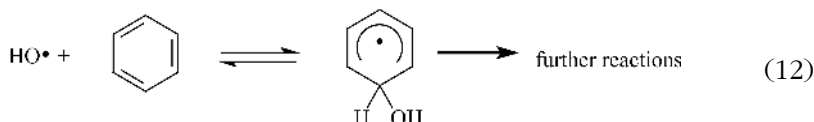
Reactions 10–11 are irreversible but reaction 12 is reversible (von Sonntag and Schuchmann, 1997). The special reactivity of $HO^{\bullet}$ with thioethers in which a radical adduct is formed should be noted (Buxton et al., 1988). Hydroxyl seldom, if ever, undergoes one electron transfer reactions with organics. Section 2.6.1 discusses structure–reactivity relationships for $HO^{\bullet}$ reactions.

When air is present in solution, the radicals produced in reactions 10–12 may react with O_2 to give $HO_2^{\bullet}$ ($O_2^{\bullet-}$), peroxyl radicals $R-OO^{\bullet}$, or oxyl radicals $R-O^{\bullet}$:

$$R^{\bullet} + O_2 \rightarrow \rightarrow R(-H^+) + HO_2^{\bullet} \tag{13}$$

$$R^{\bullet} + O_2 \rightarrow R-OO^{\bullet} \rightarrow \rightarrow R-O^{\bullet} \tag{14}$$

The bimolecular reaction of $R^{\bullet}$ with O_2 is very fast (rate constants are typically in the order of $10^9 \ M^{-1} \, s^{-1}$) and usually irreversible, except notably when $R^{\bullet}$ is a hydoxycyclohexadienyl radical formed as a result of $HO^{\bullet}$ attack on an aromatic ring (eq. 12). The radicals $R^{\bullet}$, $R-OO^{\bullet}$, and $R-O^{\bullet}$ may couple or disproportionate to give relatively stable molecules (section 2.6.2), or they

may react with iron ions (section 2.4). The organic intermediates formed in the first stage of the oxidation may react further with HO$^\bullet$ and oxygen, with the overall process leading eventually to mineralization to CO_2, H_2O, and (if the contaminant contains heteroatoms) inorganic acids. Evolution of CO_2 is slower than dissappearance of the initial compound and ordinarily decreases in rate with time as products become less and less reactive with HO$^\bullet$.

Oxidative degradation of organic contaminants by Fenton reactions usually gives optimal results at a pH slightly below 3; this result is dictated mainly by the speciation of Fe(III) (section 2.3). The presence of coordinating ligands can affect the pH dependence considerably (sections 2.3, 2.4, 3.2).

2.2. Speciation of Iron and Its Effects on Reactivity. Ferrous ion.

In acidic solution without complexing ligands Fe(II) exists predominantly as the hexaquo ion, $Fe(H_2O)_6^{2+}$. This species hydrolyzes according to eq. (15).

$$H_2O + Fe(H_2O)_6^{2+} \rightleftharpoons Fe(H_2O)_5(OH)^+ + H_3O^+$$

$$K_1 = 4.3 \times 10^{-4} M \text{ (ionic strength, 1 } M; 25°C; \text{ Wells and Salam, 1965) (15a)}$$

$$2H_2O + Fe(H_2O)_6^{2+} \rightleftharpoons Fe(H_2O)_4(OH)_2 + 2H_3O^+$$
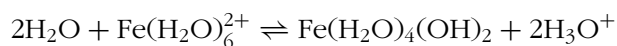
$$\beta_2 = 4.5 \times 10^{-7} M^2 \text{ (ionic strength, 1 } M; 25°C; \text{ Wells and Salam, 1968a)}$$

$$(15b)$$

Hereafter, water ligands are dropped from the formulas and $Fe(H_2O)_6^{2+}$, $Fe(H_2O)_5(OH)^+$, and $Fe(H_2O)_4(OH)_2$ are abbreviated as Fe^{2+}, $FeOH^+$, and $Fe(OH)_2$, respectively. One can see that the majority of ferrous ion will be Fe^{2+} below pH 3 (Figure 1). While ferrous salts are quite soluble in water even at neutral pH, ferrous ion will tend to coprecipitate with Fe(III) oxyhydroxides if the two ions are present together and the pH is brought up above 3.

The reaction between Fe^{2+} and H_2O_2 corresponding to eq. (1) has been assigned a bimolecular rate constant by different researchers that varies from 40 to 80 $M^{-1}\,s^{-1}$ in acidic solution near room temperature (Barb et al., 1951a; Rigg et al., 1954; Walling and Goosen, 1973; Christensen et al., 1993; Gallard et al., 1998). Reaction 1 has a relatively low activation energy (42 ± 1 kJ M^{-1}) between 20 and 300°C (Christensen et al., 1993). Whether it occurs by outer or inner sphere electron transfer has not been firmly established. There is no spectroscopic evidence for a complex between H_2O_2 and aquated Fe^{2+} ion. The outer sphere reaction appears less likely thermodynamically because it requires formation of the transient radical ion, $H_2O_2^{-\bullet}$ (Goldstein et al., 1993; Marsawa et al., 1988). Szulbinski (2000), after having compared two similar macrocyclic complexes, suggested that at least one coordination position on
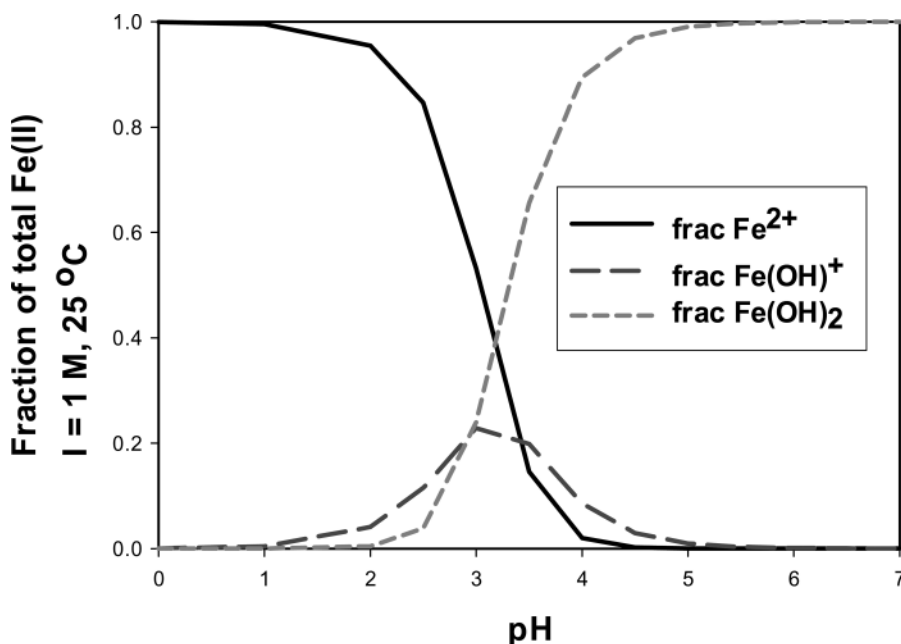
FIGURE 1. Speciation of Fe(II) in water as a function of pH at 1 M ionic strength based on values of hydrolysis constants from Wells and Salam (1965, 1968a).

Fe(II) must be open or else occupied by a labile ligand in order for reaction 1 to occur, implying an inner sphere electron transfer process. Gallard et al. (1998) inferred prior formation of a Fe^{2+}–peroxide complex above pH 4 based on kinetic models. A*b initio* calculations show favorable complexation compared to H_2O and one with end-on geometry in the "gas phase" (Bärsch et al., 2000; Schröder et al., 2000).

It is often stated, incorrectly, that reaction 1 is optimum at pH 3. Rather, reaction 1 for Fe(II) = Fe^{2+} is pH independent below pH $\sim$3 (Barb et al., 1951a; Wells and Salam, 1968a) and *increases* in rate with pH above 3 until it reaches a plateau at about pH 4 corresponding to a value about 7 times greater than at pH 3. This has been attributed to formation of $Fe(OH)_2$, which is about 10 times more reactive than Fe^{2+} ($k_{1,Fe(OH)2} = 586\ M^{-1}\,s^{-1}$ at ionic strength 0.1 M and 25°C) (Wells and Salam, 1968a). The commonly observed pH optimum of the Fenton reaction is due instead to effects on Fe(III) speciation (section 2.3).

Reaction 1 is affected also by other ligands, L, on Fe(II). Wells and Salam (1967, 1968a, 1968b) observed that with increasing concentration of L as halide, sulfate, selenate, trimetaphosphate, or tripolyphosphate, the apparent rate constant for reaction 1 increases up to a limiting value. This increase, however, was only a factor of 2–3 greater than the base-line case with noncoordinating ions such as perchlorate or nitrate. Presumably,

L lowers the reduction potential of the complex by decreasing its positive charge. Some chelating ligands also are known to accelerate the reaction of Fe(II) with H_2O_2. However, one must bear in mind the possiblity that the products of such reactions might be high-valent oxoiron (ferryl) species in addition to, or instead of, HO$^{\bullet}$ (see section 2.9). Fulvic acid, which probably complexes with Fe(II) through carboxylate group(s), accelerates reaction 1 (Voelker and Sulzberger, 1996). The oxalate complex, $Fe^{II}(C_2O_4^{2-})$, reacts rapidly with H_2O_2 ($k = 1 \times 10^4 M^{-1} s^{-1}$) (Park et al., 1997). Fe^{II}–EDTA (EDTA = ethylenediamine tetraacetic acid) also reacts rapidly with H_2O_2 ($k = 1.75 \times 10^4 \ M^{-1} s^{-1}$), but the product behaves more like ferryl than HO$^{\bullet}$ (Rush and Koppenol, 1986). Phosphate ligand seems to suppress reaction 1 (Iwahashi et al., 1990). Further structure–reactivity studies of Fe(II) complexes in reaction 1 are clearly warranted in view of its central role.

2.3. Speciation of Iron and Its Effects on Reactivity: Ferric Ion

2.3.1. INFLUENCE OF pH

In strongly acidic solution containing no H_2O_2 and only noncomplexing counterions such as ClO_4^- or NO_3^-, Fe(III) exists as the hexaaquo ion, $Fe(H_2O)_6^{3+}$. As pH increases, this ion undergoes extensive hydrolysis [eq. (16)], depending on counterion, ionic strength, and total iron concentration, ending in precipitation of amorphous ferric oxyhydroxides (Sylva, 1972).

$$Fe^{3+} \rightleftharpoons FeOH^{2+} \rightleftharpoons Fe(OH)_2^+ \rightleftharpoons Fe_2(OH)_2^{4+}$$

$$\rightleftharpoons \text{other polynuclear species} \rightleftharpoons Fe_2O_3 \cdot nH_2O(s) \qquad (16)$$
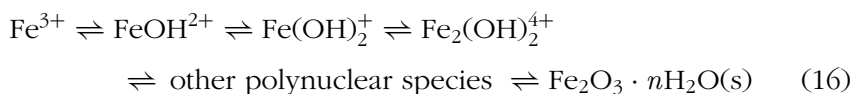
Reaction 16 omits H_2O ligands on iron, as well as H_2O and H^+ involved in the stoichiometry.

All but the first two steps in eq. (16) are slow, and the precipitated species do not redissolve readily. Moreover, the precipitated species are considerably less Fenton-reactive. Because of the complexity of Fe(III) hydrolysis great care is required to obtain well-defined solutions. Some advice to the investigator follows. (a) If concentrated stock solutions are prepared that will later be diluted for experiments, prepare such stock solutions at a concentration below 0.1 M and prepare them in acidified water ($\geq$0.1 M H$^+$), since dissolution of ferric salts in neutral water leads immediately to hydrolysis. (b) Keep total iron below 1×10^{-4} M in solutions less acidic than 10^{-2} M H$^+$. (c) To adjust the pH in the acidic range, use bicarbonate rather than hydroxide solution in order to prevent locally high pH conditions at the point of mixing (the bicarbonate will be volatilized as CO_2). (d) Use solutions within a few hours to minimize interference from colloidal oxides that may form over time. The presence of hydrolyzed species is revealed by turbidity and/or a slight yellow-orange color.
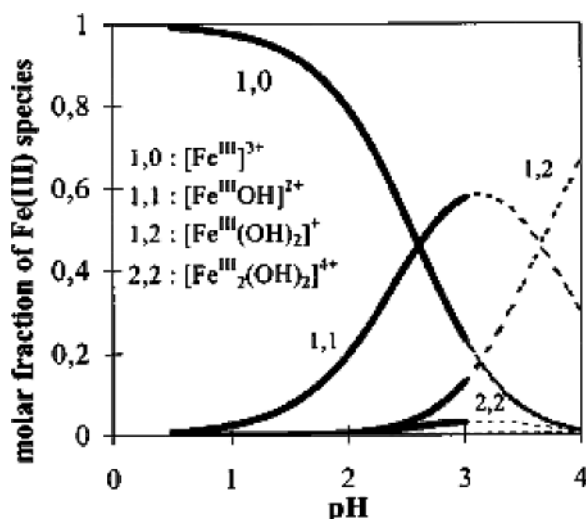
FIGURE 2. Speciation of Fe(III) species in water at 1×10^{-3} *M* total iron, ionic strength 0.1 *M*, and 25°C. Dashed line regions are supersaturated with respect to amorphous ferric oxyhydroxides. Reprinted with permission from Gallard et al. (1999).

Gallard et al. (1999) have plotted the relative abundance of ferric species as a function of pH at 0.1 *M* ionic strength (Figure 2). At pH 2.54, Fe^{3+} and $FeOH^{2+}$ exist in equal concentrations, together with much smaller concentrations of $Fe(OH)_2^+$ and $Fe_2(OH)_2^{4+}$. Colloids begin to form slowly at about pH 3.

2.3.2. FORMATION AND DECOMPOSITION OF Fe(III) COMPLEXES WITH H_2O_2

As already mentioned (section 2.1), hydrogen peroxide forms complexes with Fe(III). In a study of Fe(III) chelates, Graf et al. (1984) found that at least one coordination position on Fe(III) must be open or occupied by a labile ligand (such as H_2O) in order for reaction 2 to occur.

For aqueous Fe(III), the following equilibria have been identified spectrophotometrically:

$$Fe^{3+} + H_2O_2 \rightleftharpoons Fe(HO_2)^{2+} + H^+ \tag{17}$$

$$FeOH^{2+} + H_2O_2 \rightleftharpoons Fe(OH)(HO_2)^+ + H^+ \tag{18}$$
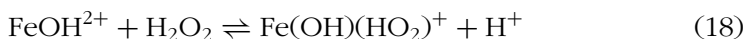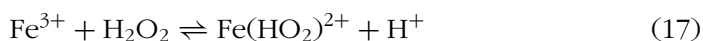
These equilibria, which are attained almost instantly, probably involve innersphere coordination of peroxide with the metal. The first formation constant [eq. (17)] at 25°C ($\mu = 0.1$ *M* $NaClO_4$) has been assigned values of $3.7(\pm0.7) \times 10^{-3}$ (Evans et al., 1949), $9(\pm1.5) \times 10^{-3}$ (Pignatello et al., 1999), on $3.1 (\pm0.4) \times 10^{-3}$ (Gallard et al., 1999). The second formation constant (eq. 18) has been assigned the value $2(\pm0.5) \times 10^{-4}$ (Gallard et al., 1999). Lewis et al. (1963) suggest the formation of $Fe(H_2O_2)^{3+}$ and

$Fe(H_2O_2)(HO_2)^{2+}$ at very high H_2O_2 concentration (~ 9 *M*), but such complexes could not be verified spectrophotometrically (Pignatello et al., 1999). The geometry of Fe(III) complexes with HO_2^- is unknown but is most likely end on (i.e., Fe–OOH).

Fe(III)–EDTA forms a well-known purple peroxide complex (Walling et al., 1970; Ahmad et al., 1988; Francis et al., 1985). Using Raman spectroscopy, Ahmad et al. (1988) established the structure to be Fe^{III}–EDTA(O_2^{2-}) where the peroxide ligand has side-on (η^2) geometry. The peroxide ligand most likely displaces an H_2O or OH^- ligand at the seventh coordination site. Szulbinski (2000) also established the η^2 geometry for peroxide in its complex with Fe^{III}–DPC (DPC = *N*,*N'*-di-2-picolyl-4,7-diaza-1-oxacyclononane).

$$Fe^{III}\diagdown\!\!\!\diagup \begin{matrix} O \\ | \\ O \end{matrix}$$

$$\eta^2$$
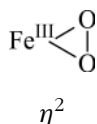
The rate-limiting step in Fe(III)-catalyzed decomposition of H_2O_2 is usually reductive dissociation of the Fe(III)–peroxide complex:

$$Fe^{III}(HO_2^-) \rightarrow Fe^{II} + HO_2^{\cdot} \tag{19}$$

$$Fe^{III}(OH^-)(HO_2^-) \rightarrow Fe^{II} + HO_2^{\cdot} + OH^- \tag{20}$$
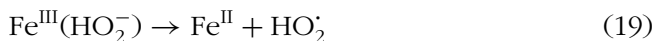
Reactions 19 and 20 are sources of Fe(II), which reacts in eq. (1) to form $HO^{\cdot}$. In a kinetic model, De Laat and Gallard (1999) estimated the effective rate constant for combined reactions 19 and 20 to be 0.0027 s^{-1}. The individual rate constants are unknown.

Since net reaction 2 (collectively, reactions 17–20) is so much slower than reaction 1, organic compound removal in reaction mixtures starting with Fe^{2+} and having H_2O_2 in large stoichiometric excess will generally exhibit two-stage kinetics: a fast stage attributable to reaction 1 as the rate-limiting step, and a much slower stage attributable to net reaction 2 as the rate-limiting step. This was shown nicely for atrazine degradation by Gallard and De Laat (2000). The contribution of the fast stage depends, of course, on the molar ratio of target compound to Fe(II) starting concentration.

As mentioned before, the rates of Fe(III)-catalyzed Fenton reactions usually reach a maximum at a pH slightly below 3 (Eisenhauer, 1964; Bishop et al., 1968; Feuerstein et al., 1981; Pignatello, 1992). This occurs for two reasons. First, unless chelating ligands are present, the Fe(III) catalyst begins to precipitate above pH 3 in the form of relatively inactive hydrous oxyhydroxides (section 2.3.1). Second, $[Fe(HO_2)^{2+}]$ reaches a maximum around pH 3 (Gallard et al., 1999). Although in theory $[Fe(OH)(HO_2)^+]$ continues to grow above pH 3, Fenton reaction rates tend to decrease anyway due to catalyst precipitation.

The influence of ligand structure on reactions 17–20 is unknown. Few researchers have attempted to distinguish reactions 19–20 as written (i.e., with HO$_2^{\cdot}$ as a product) either from reactions that produce other species, such as high-valent oxoiron species (section 2.9), or from indirect effects due to ligand scavenging of HO$^{\cdot}$. Decomposition of the peroxide–Fe(III)–EDTA complex, ostensibly to O$_2^{\cdot-}$ and Fe(II), is about 30 times faster than the corresponding peroxide–Fe(III)–aquo complex (Francis et al., 1985). By contrast, the reaction between H$_2$O$_2$ and Fe^{III}–DTPA (DTPA = diethylenetriamine pentaacetic acid) is about 4×10^5 times faster than that of the aquo complex, but the product is not scavenged by typical HO$^{\cdot}$ scavengers, like methanol or *t*-butanol, suggesting formation of a high-valent oxoiron complex instead of Fe(II) and HO$^{\cdot}$ (Rahhal and Richter, 1988).

2.3.3. INFLUENCE OF INORGANIC IONS

Fenton and photo-Fenton oxidations of organic compounds are inhibited in varying degrees by phosphate, sulfate, organosulfonate, fluoride, bromide, and chloride ions, depending on their concentrations. Such anions may be present initially in the wastewater or formed as end products from the compounds undergoing degradation. Inhibition by these species may be due to precipitation of iron, scavenging of HO$^{\cdot}$, or coordination to dissolved Fe(III) to form a less reactive complex. The practitioner and researcher is well advised to be aware of such effects. Nitrate or perchlorate ions do not complex with Fe^{3+} or Fe^{2+} measurably, nor do they react with HO$^{\cdot}$, making them the counterions of choice for fundamental studies.

Iron(III) forms complexes with phosphate that are quite insoluble in neutral or mildly acidic solution. Lu et al. (1997) studied oxidation of dichlorvos [2,2-dichloroethenyl dimethyl phosphate] using Fe^{2+} and an excess of H$_2$O$_2$ and observed the typical two-stage (fast-slow) rate profile. In 0.2 *M* phosphate, the fast stage, which is rate-limited by reaction 1, was not much affected, but the slow, Fe(III)-catalyzed stage was completely stopped, presumably by precipitation of Fe(III) phosphate complexes. In reactions of sulfonic acid dyes, precipitation of Fe(III) may take place by coordination of Fe(III) with the aryl sulfonate group (Ar-SO$_3^-$) (Arslan and Balcioglu, 1999; MacKay and Pignatello, 2001).

Inhibition of Fenton reactions by Cl$^-$ and Br$^-$ is due to scavenging of HO$^{\cdot}$ [eq. (21), X = Cl, Br], as these ions are relatively weak ligands of Fe(III).

$$HO^{\cdot} + X^- \rightleftharpoons HOX^{\cdot-} \stackrel{H^+(-H_2O)}{\rightleftharpoons} X^{\cdot} \stackrel{X^-}{\rightleftharpoons} X_2^{\cdot-} \qquad (21)$$
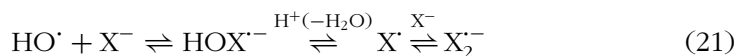
This limits Fenton treatment of waste streams containing high concentrations of halide salts. Reaction 21 is fast, reversible, and dependent on [X$^-$] and [H$^+$] (Jayson et al., 1973). Inhibition of Fenton reactions by chloride scavenging is noticeable above 0.01 *M* Cl$^-$ at pH 2.8 (Pignatello, 1992). Fenton reaction kinetics in the presence of high chloride concentrations are complicated by

reactions of chlorine radicals with H_2O_2, iron species and the organic compound itself. Kiwi et al. (2000) observed Cl^- inhibition of orange II dye degradation and noted the appearance of unidentified organochlorine by-products in 3 to 33% yield. Bromide is a potent $HO^\cdot$ scavenger, since equilibrium of reaction 21 lies strongly to the right (Zehavi and Rabani, 1972). (Bromide natural abundance in seawater is 0.15 mole percent of chloride.) Under Fenton conditions, degradation of the soil pesticide 1,2-dibromoethane at 0.1 mM displayed autoinhibition by Br^- released during its mineralization, and was stopped almost completely in 1 mM NaBr (Figure 3). Halide radicals ($X^\cdot$) and dihalide radical anions ($X_2^{\cdot-}$), especially the former, are reactive with organic compounds in aqueous media and proceed by H-abstraction addition to alkenes and alkynes and one-electron oxidation pathways, but products and rate constants are scarce. H-abstraction and one electron oxidation is beneficial to the goal of mineralization, while addition forms organohalogen compounds.

Sulfate (Jones et al., 1959; Pignatello, 1992; De Laat and Le, 2005) and fluoride (Barb et al., 1951a) ions inhibit the Fenton reaction even though they are poor $HO^\cdot$ scavengers (Buxton et al., 1988) and their complexes with Fe are soluble. These ions reduce the reactivity of Fe(III) through coordination. Iron(III) forms a mixture of $FeSO_4^+$ and $Fe(SO_4)_2^-$ complexes in the presence
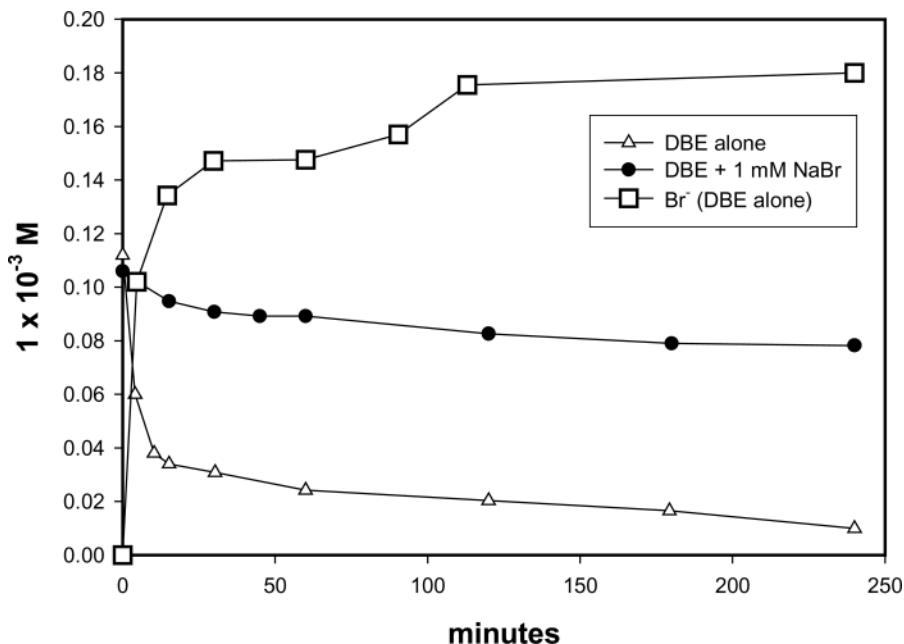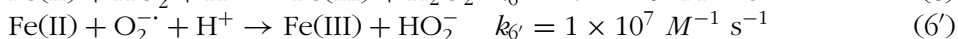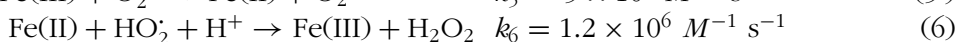

FIGURE 3. Photo-Fenton reaction of 1,2-dibromoethane showing auto-inhibition by the released bromide ion, and strong inhibition by added NaBr. 1.0 mM Fe(ClO$_4$)$_3$; 10.1 mM H$_2$O$_2$; pH 2.75; 25°C; fluorescent black-lamp irradiation.

of sulfate. Evidently H_2O_2 does not coordinate with Fe(III)–sulfato complexes (De Laat and Le, 2005). The rate of 2,4-dichlorophenoxyacetic acid (2,4-D) oxidation was inhibited 6-fold in 0.1 *M* sulfate, and that of H_2O_2 decomposition was inhibited 20-fold in 1 *M* sulfate (Pignatello, 1992). It is likely, however, that the millimolar concentrations of sulfate introduced by adding iron in the form of a sulfate salt will have little effect on Fenton reaction performance.

The affinity of ferric ion for fluoride is very high, with successive formation constants for the mono-, di-, and trifluoride complex of ${\sim}10^5$, 10^5, and 10^3 M^{-1}, respectively (Sillén and Martell, 1964). Even the monofluoride complex is catalytically inactive in the Fenton reaction (Jones et al., 1959).

2.4. Reactions of Inorganic and Organic Free Radicals with Iron Species

Hydroperoxyl radical, $HO_2^{\cdot}$, and its conjugate base, $O_2^{-\cdot}$, can both reduce and oxidize iron by the following,

$$Fe(III) + HO_2^{\cdot} \rightarrow Fe(II) + O_2 + H^+ \qquad k_5 < 2 \times 10^3\ M^{-1}\ s^{-1} \qquad (5)$$
$$Fe(III) + O_2^{-\cdot} \rightarrow Fe(II) + O_2 \qquad k_{5'} = 5 \times 10^7\ M^{-1}\ s^{-1} \qquad (5')$$
$$Fe(II) + HO_2^{\cdot} + H^+ \rightarrow Fe(III) + H_2O_2 \quad k_6 = 1.2 \times 10^6\ M^{-1}\ s^{-1} \qquad (6)$$
$$Fe(II) + O_2^{-\cdot} + H^+ \rightarrow Fe(III) + HO_2^- \quad k_{6'} = 1 \times 10^7\ M^{-1}\ s^{-1} \qquad (6')$$

The ratio of reduction to oxidation rates by $HO_2^{\cdot}$ ($O_2^{-\cdot}$) radicals depends on pH and the instantaneous Fe(III) and Fe(II) concentrations according to:

$$\frac{\text{rate}_{\text{red}}\,(5 + 5')}{\text{rate}_{\text{ox}}\,(6 + 6')} = \frac{k_5 + k_5 K_{\text{a}}/[\text{H}^+]}{k_6 + k_6 K_{\text{a}}/[\text{H}^+]} \cdot \frac{[\text{Fe(III)}]}{[\text{Fe(II)}]} \qquad (22)$$

where K_{a} is the acidity constant of $HO_2^{\cdot}$ (1.58×10^{-5}). Assuming the reported rate constants for reactions 5, 5′, 6, and 6′ given here (De Laat and Gallard, 1999) are valid below pH 3.5, eq. (22) equals $0.39 \times [\text{Fe(III)}]/[\text{Fe(II)}]$ at pH 2.8. Thus, $HO_2^{\cdot}$ ($O_2^{-\cdot}$) carries out net reduction at [Fe(III)]/[Fe(II)] ratios above 2.5 and net oxidation at ratios below 2.5. The speciation of iron during Fenton reactions has been monitored in some studies (Sun and Pignatello, 1993c; Chen and Pignatello, 1997). The [Fe(III)]/[Fe(II)] ratio at any given instant depends on the H_2O_2 concentration (Sun and Pignatello, 1993c), the concentration of organic intermediates capable of oxidizing or reducing iron (Chen and Pignatello, 1997), and radiant power when photoassistance is employed (section 3.1). Typically, Fe(III) predominates when the molar ratio of H_2O_2 to total Fe is high; under those conditions reduction of iron by $HO_2^{\cdot}$ ($O_2^{-\cdot}$) is more favorable. Regardless, $HO_2^{\cdot}$ ($O_2^{-\cdot}$) radicals are decomposed to give one or the other of the Fenton reactants, Fe(II) or H_2O_2, and thereby propagate the Fenton reaction.

Iron plays an important role in the fate of organo-oxyl radicals (RO$^{\cdot}$, ROO$^{\cdot}$) and carbon-centered radicals (R$^{\cdot}$). Organoperoxyl radicals consume Fe(II) by the following sequence of reactions (Mansano-Weiss et al., 2002):

$$Fe^{II} + R\text{–}OO^{\cdot} \ \smallint \ Fe^{III}\text{–}OOR \tag{23}$$

$$Fe^{III}\text{–}OOR + H^+ \rightarrow R\text{-}OOH + Fe(III) \tag{24}$$

$$Fe^{III}\text{–}OOR + Fe^{II} + 3H^+ \rightarrow 2Fe^{III} + ROH + H_2O \tag{25}$$

$$Fe^{III}\text{–}OOR + R\text{–}OO^{\cdot} \rightarrow Fe^{II} + O_2 + ROH + R(\text{–}H)\text{=}O \tag{26}$$
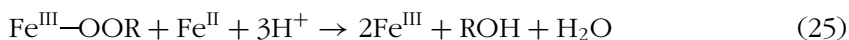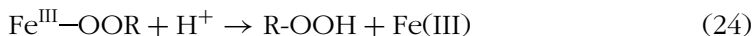
Reaction 25 is three orders of magnitude faster than reaction 1. The combination of equilibrium 23 and reaction 26 represents Fe(II)-catalyzed disproportionation of organoperoxyl radicals.

Alkoxyl radicals consume Fe(II) rapidly according to eq. (27):

$$R\text{–}O^{\cdot} + Fe(II) + H^+ \rightarrow R\text{–}OH + Fe(III) \tag{27}$$

Carbon-centered radicals may reduce Fe(III) [eq. (28)] or oxidize Fe(II) [eq. (29)] depending on their structure. Both reactions are essentially irreversible.

$$Fe(III) + R^{\cdot} \rightarrow Fe(II) + R^+ \tag{28}$$

$$Fe(II) + R^{\cdot} + H^+ \rightarrow Fe(III) + RH \tag{29}$$
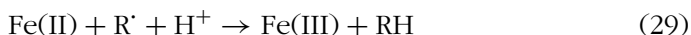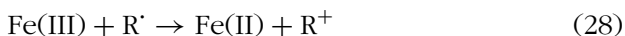
The carbocation produced in reaction 28 may, (a) loose a proton from a position adjacent to the positive carbon to form a double bond, or (b) react with water to form an alcohol. Iron species in reactions 28 and 29 must compete with O_2 for reaction with R$^{\cdot}$ (eqs. 13 and 14).

Few rate constants are available for reaction 28. Tertiary alkyl radicals and radicals α to –OH, –OR, or –amide N groups are most reactive; for example (Buxton and Green, 1978):

$$Fe^{3+} + {}^{\cdot}CH_2OH \rightarrow Fe^{2+} + H_2C\text{=}O + H^+ \quad k = 8 \times 10^7 M^{-1}s^{-1} \tag{28'}$$
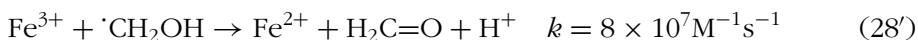
Allylic and benzylic radicals are intermediate in reactivity, and ordinary primary and secondary alkyl radicals are inert (Walling, 1975; http://www.rcdc.nd.edu/compilations/Ali/Ali.htm; Neta et al., 1996). However, since the rate constant of even the fastest reactions (e.g., reaction 28′) are still an order of magnitude smaller than rate constants typical for reactions of R$^{\cdot}$ with O_2 (eqs. 13–14) reduction of Fe^{3+} by carbon-centered radicals in the presence of O_2 is probably minor.

Oxidation of Fe(II) by carbon radicals (reaction 29) is common for vinyl radicals and radicals α to a carbonyl group. When R$^{\cdot}$ originates from HO$^{\cdot}$ attack, its reduction back to starting compound amounts to a waste of reagents,

since the net reaction is simply reduction of hydrogen peroxide to water "catalyzed" by RH:

$$2Fe(II) + H_2O_2 + 2H^+ \xrightarrow{RH} 2Fe(III) + 2H_2O \tag{30}$$
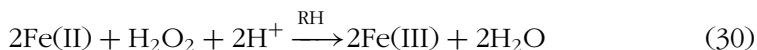
Compounds showing this behavior include acetone, acetic acid, succinic acid and malonic acid (Merz and Waters, 1947; Walling, 1975), and diuron [3-(3,4-dichlorophenyl)-1,1-dimethylurea] and isoproturon [3-(4-(2-methylethyl-phenyl)-1,1-dimethylurea] (Gallard and De Laat, 2001).

Hydroxycyclohexadienyl radicals formed by reaction of HO· with aromatic rings [eq. (12)] can reduce Fe(III) indirectly through the catalytic mediation of quinone molecules (Chen and Pignatello, 1997, 1999). An example is shown in eq. (31) using a substituted 1,4-benzoquinone.

$$\tag{31a}$$

$$\tag{31b}$$

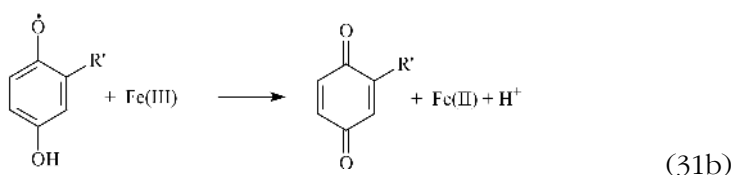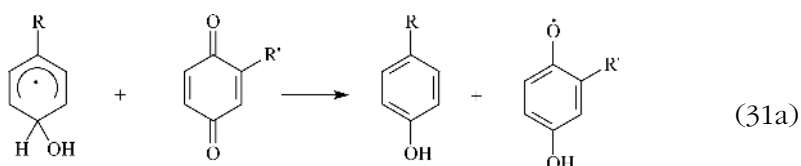As quinones build up in solution, the fraction of Fe in the +II state increases. Reaction 31 has been demonstrated for phenol and nitrobenzene oxidation catalyzed by substituted and unsubstituted benzoquinones and naphthoquinones. The example of nitrobenzene is shown in Figure 4. Reaction 31a is rate-limiting. Electron-donating substituents on the quinone ring inhibit the reaction, and naphthoquinones are better catalysts than benzoquinones (Chen and Pignatello, 1999). By this electron-shuttle mechanism, quinones, which themselves are by-products of aromatic compound degradation, play an important role in Fenton oxidation of aromatic compounds by catalyzing the hydroxylation of aromatic rings:

$$Ar{-}H + H_2O_2 \xrightarrow[\text{quinone}]{Fe^{III}} A{-}OH + H_2O \tag{32}$$
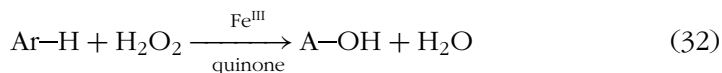
Equation (32) can be seen as the net of reactions 1, 12, 31a, and 31b. Electron shuttle catalysis by quinones is tempered by the reality that quinones are readily attacked by HO·. Further effort in identifying more stable quinone catalysts is needed.
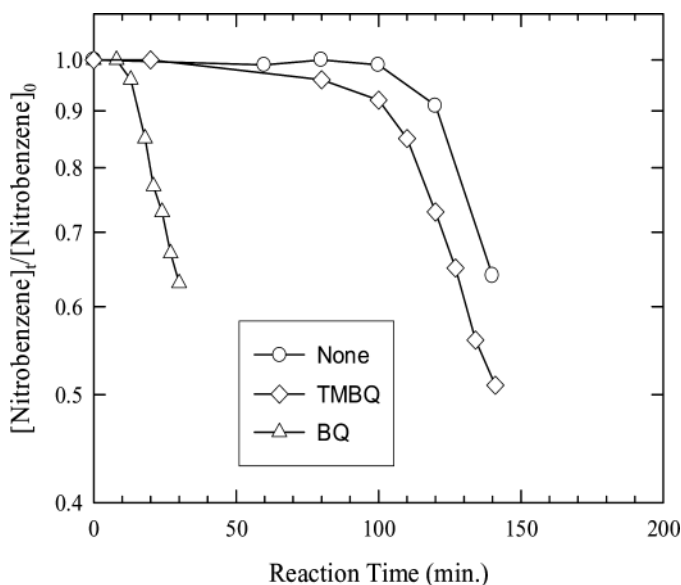
FIGURE 4. Nitrobenzene degradation by Fe(III) and H_2O_2 in the presence or absence of added quinone catalysts. BQ, benzoquinone, TMBQ, *tetra*-methyl benzoquinone. From Chen and Pignatello (1999) with permission.

2.5. Reactions of Organic Molecules With Iron Species

The Fe^{2+} ion in water is a weak reductant and, therefore, not very reactive toward most organic pollutants. Likewise, Fe(III) containing only aquo ligands is a poor oxidant. Nevertheless, iron species are known to react directly with some types of compounds of interest in Fenton applications, most notably organoperoxides, hydroquinones and certain dyes.

Organoperoxide molecules are usually unstable in the presence of Fe(II):

$$R\text{—}OOH + 2Fe(II) + 2H^+ \rightarrow R\text{—}OH + H_2O + 2Fe(III) \qquad (33)$$

Reaction 33 involves two steps, the first of which produces alkoxyl and/or hydroxyl radicals, depending on R. Reaction 33 is so fast that it hinders efforts to detect organoperoxide products in Fenton reaction mixtures.

Ortho- or *para*-substituted dihydroxybenzenes (hydroquinones) can reduce Fe(III) by successive one-e^- transfer steps via the semiquinone radical— for example, eq. (34) followed by eq. (31b).

$$(34)$$
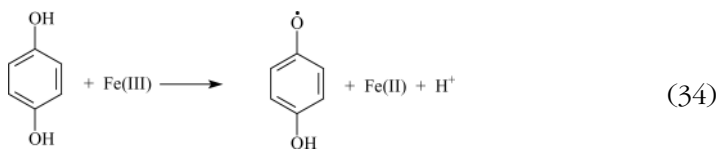
Hydroquinones can be produced in the Fenton reaction by repeated hydroxylation of aromatic rings. *Meta*-dihydroxy groups are far less oxidizable because they lack the special stability of the semiquinone structure and cannot give a quinone.

Through reactions like 31 and 34, the oxidation of substituted benzenes by Fe(III)/H_2O_2 system shows autocatalysis (Chen and Pignatello, 1997). After a lag phase, the reaction cascades into a fast phase, as hydroquinone and quinone products build up. This is accompanied by a sharp increase in [Fe^{2+}]. Similarly, Fe(III)/H_2O_2 degradation of atrazine was accelerated when 1,2,4-trichlorobenzene was added, presumably due to facilitated regeneration of Fe(II) by hydroquinone/quinone intermediates from trichlorobenzene degradation (Gallard and De Laat, 2001).

Iron(III) also rapidly oxidizes the *p*-hydroxyazo dye Acid Orange 20 (AO20), producing two equivalents of Fe(II), an unidentified product that forms a reversible complex with Fe(II), and a minor yield (4%) of 1,4-naphthoquinone (MacKay and Pignatello, 2001). AO20 is shown here in its hydrazone form, the predominant tautomer in polar solvents. Interestingly, *o*-hydroxyazo analogs, Acid Orange 7 and Acid Orange 10, are inert.

Acid Orange 20

2.6. Reactions of Organic Molecules With Radical Species

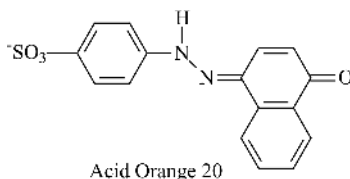In this section, the reactivities of the most important radical species involved in oxidative degradation of contaminants are summarized. These are the hydroxyl radical, peroxyl radicals (ROO˙), and the hydroperoxyl radical (HO$_2^˙$) and its conjugated base, the superoxide anion (O$_2^{-˙}$). The interested reader is referred to the corresponding literature for detailed reviews on these topics. This chemistry is not specific to the Fenton reaction, but occurs in all AOPs based on hydroxyl radical processes in aqueous media.

2.6.1. REACTION OF ORGANIC MOLECULES WITH THE HYDROXYL RADICAL

In Fenton systems, the fate of the target organic compound, as well as of many of its degradation by-products, is dependent principally on its reactions with HO˙. As discussed in section 2.1, HO˙ reacts mainly by abstracting H atoms or adding to unsaturated bonds (reactions 10–12). A great deal is known about the reactivity of HO˙ in aqueous media. Second-order rate constants k_{HO} fall in the range 10^7 to 10^{10} $M^{-1}\,s^{-1}$ (Buxton et al., 1988; University of Notre Dame Radiation Laboratory, Radiation Chemistry Data Center: http://www.allen.rad.nd.edu/).

Although highly reactive and indiscriminate, HO$^\bullet$ appears to be weakly electrophilic. The Hammett sensitivity parameter ρ for substituted benzenes and benzoic acids is -0.41, which corresponds to a $\sim$3–4 fold increase in rate constant on going from a ring with a strongly electronegative substituent ($-NO_2$) to one with a strongly electropositive substituent ($-NH_2$) (Anbar et al., 1966). Another indication of the electrophilic character of HO$^\bullet$ is the reduced rate of H-abstraction when an electron-withdrawing carbonyl group is located in the alpha position (e.g., $k_{HO} = 1 \times 10^8 \ M^{-1}\,s^{-1}$ for acetone versus $k_{HO} = 1.4 \times 10^9 M^{-1}\,s^{-1}$ for ethane), which is not the case for an electro-neutral radical such as methyl (Smith and March, 2001).

Nevertheless, other factors besides the electrophilic character of HO$^\bullet$ can be important, even dominant. These include: (a) strength of the C$-$H bond; (b) stability of the nascent organoradical; (c) statistical factors, that is, the number of equivalent H atoms or positions of attack; and (d) steric effects. Some of these factors are interrelated; for example, (a) depends on the electronegativity of substituents and (a) and (b) are inversely related. Solvent, pH, and ionic strength effects are expected to be minor.

For alkane functional groups the order in C$-$H reactivity is typically *tertiary > secondary > primary*. This is the same as the order in electron density on C, but it is also the same as the order in stability of the nascent organoradical and the inverse order in C$-$H bond strength (Lide, 1998). Addition to alkenes is favored over H-abstraction (per-H from $-CH_2-$ or R_2CH-), especially when the double bond is substitued with electron-donating substituents, $-R$ or $-OR$ (Moise et al., 2005).

A comparison of gaseous- and aqueous phase k_{HO} for halogenated alkanes and alkenes (Atkinson, 1989; Notre Dame Radiation Laboratory Radiation Chemistry Data Center, http://allen.rad.nd.edu/) shows that aliphatic halogen has a dual effect on organic reactivity:

1. A deactivating effect due to the strong electronegativity of halogen. Halogenation at the β-position of ethanes is rate-retarding in the order F > Cl.
2. An activating effect at the α position due to its ability to stabilize the organoradical—or weaken the C$-$H bond. The α-stabilizing ability follows the order Cl > Br > F. Per hydrogen atom, successive substitution of Cl in methane progressively increases C$-$H reactivity. Perhaloalkanes are unreactive because HO$^\bullet$ does not readily attack halogen. The α-stabilizing ability of Cl is exemplified in trichloroethene, where HO$^\bullet$ favors the *less* substituted carbon, leaving the radical on the carbon bearing the most Cl atoms.

For aromatic compounds, observed substituent effects on rates of Fenton reactions are mixed and not always consistent with expectation based on the electron-withdrawing ability of the substituents and the electrophilic nature of HO$^\bullet$. This may in part be due to attack of HO$^\bullet$ on a substituent rather than
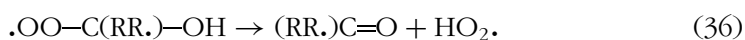
on the ring. It may also be due to statistical factors having to do with the number of sites available for attack. Sedlak and Andren (1991) found that k_{HO} for di- through penta-chlorobiphenyls in water varied by less than twofold. On the basis that Cl blocks attack on its own C, each additional Cl prevented ~10% of collisions from leading to reaction, with sites *ortho* to the biphenyl link being slightly more reactive than *meta* and *para*.

For attack on C=C bonds in alkenes and aromatic rings, frontier orbital theory predicts radical attack at the position corresponding to the highest sum of single-electron densities in the highest occupied molecular orbital (HOMO) and in the lowest unoccupied molecular orbital (LUMO). Using this theory, Lee et al. (2001) successfully predicted the initial position of reaction on four polycyclic aromatic hydrocarbons—acenaphthylene, anthracene, benz[a]anthracene, and benzo[a]pyrene—after reaction with Fenton's reagent ($Fe^{2+} + H_2O_2$).

2.6.2. REACTIVITY OF PEROXYL AND HYDROPEROXYL/SUPEROXIDE RADICALS

Carbon-centered free radicals react with O_2 to form peroxyl radicals [$ROO^{\cdot}$, eq. (14), section 2.1]. Peroxyl radical chemistry in aqueous solution has been extensively reviewed by Von Sonntag and Schuchmann (1991, 1997). While not very reactive toward other organic compounds, decomposition of $ROO^{\cdot}$ contributes to the oxidative degradation of organic contaminants.

Peroxyl radicals eliminate $O_2^{-\cdot}$ or $HO_2^{\cdot}$ when an α-substituent is an amino or hydroxyl group, respectively [eqs. (35)–(36)], or when rearomatization is possible.

$$^{\boldsymbol{\cdot}}OO\text{---}C(RR\boldsymbol{.})\text{---}N(R..R...) \rightarrow (RR\boldsymbol{.})C=N^+(R..R...) + O_2^{-}\boldsymbol{.} \qquad (35)$$

$$^{\boldsymbol{\cdot}}OO\text{---}C(RR\boldsymbol{.})\text{---}OH \rightarrow (RR\boldsymbol{.})C=O + HO_2\boldsymbol{.} \qquad (36)$$

Peroxyl radicals also may decay bimolecularly through a short-lived tetroxide intermediate:

$$2RC(HR')\text{---}OO^{\cdot} \leftrightarrows RC(HR')\text{---}OOOO\text{---}C(HR')\text{---}R \qquad (37)$$

Reaction 37 is fast for primary ($RCH_2OO^{\cdot}$) and secondary ($R_2CHOO^{\cdot}$) peroxyl radicals, but much slower for tertiary. Tetroxides decompose by various pathways, eliminating O_2 or H_2O_2 and giving alcohols, ketones, aldehydes, esters, and/or acids, depending on the precursor:

$$RC(HR)\text{---}OOOO\text{---}C(HR)\text{---}R \rightarrow O_2 + R_2CHOH + R_2C=O \qquad (38a)$$

$$\rightarrow O_2 + 2RCHO + 2R^{\cdot} \qquad (38b)$$

$$\rightarrow H_2O_2 + 2R_2C=O \qquad (38c)$$

$$\rightarrow O_2 + 2RC(HR)\text{---}O^{\cdot} \qquad (38d)$$
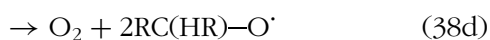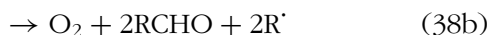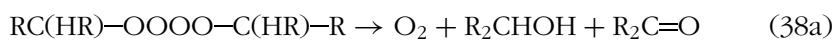
Oxyl radicals (RO˙) formed in reaction 38d may undergo either *β*-fragmentation [eq. (39)] or a water-assisted 1,2-H-shift [eq. (40)] provided an *α*-H atom is present.

$$RC(HR)\!-\!O^{\bullet} \rightarrow RCHO + R^{\bullet} \tag{39}$$

$$RC(HR)\!-\!O^{\bullet} \rightarrow RC^{\bullet}(R)\!-\!OH \tag{40}$$

The 1,2-H shift is fast, explaining why H-abstraction reactions of RO˙, typical in organic solvents, are not observed in water. The ensemble of reactions starting from ROO˙ leads to oxidation, as well as fragmentation of the starting organic compound.

It is of interest to note peroxyl radical chemistry related to reaction of aromatic compounds. Compared to ordinary C-centered radicals, reaction of dioxygen as in eq. (14) with the hydroxycyclohexadienyl radical is slower and reversible. It usually occurs at the *ortho* or *para* position relative to the ─OH group. The resulting peroxyl radical can either rearomatize by eliminating $HO_2^{\bullet}$ or undergo an intramolecular addition to one of the double bonds in the ring leading to a new C-centered radical. That radical can undergo rearrangement, cleavage reactions, and/or react with another dioxygen molecule. In further steps the ring is ultimately cleaved and fragmented, and halogens, nitro groups, and sulfonate substituents are often eliminated as their inorganic acids during the process.

Peroxyl radicals are far less reactive than HO˙ in water with respect to H-abstraction and addition to unsaturated bonds. They may act as one-electron oxidants 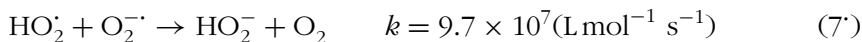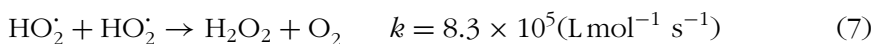but only toward strong electron donor compounds such as N,N,N′,N′-tetramethylphenyldiamine (TMPD) or ascorbic acid, especially if R in ROO˙ is strongly electron-withdrawing (e.g., $CCl_3OO^{\bullet}$).

The $HO_2^{\bullet}$ and $O_2^{-\bullet}$ radicals originate both from added H_2O_2 (section 2.1) and decomposition of ROO˙ [eqs. (35)–(36)]. A principal reaction is disproportionation [eq. 7, 7˙, 7¨) with the rate constants given (Notre Dame Radiation Laboratory Radiation Chemistry Data Center, http://allen.rad.nd.edu/). The relative contributions of 7 and 7˙ to Fenton chemistry depends on the pH.

$$HO_2^{\bullet} + HO_2^{\bullet} \rightarrow H_2O_2 + O_2 \quad\quad k = 8.3 \times 10^5 (\mathrm{L\,mol^{-1}\,s^{-1}}) \tag{7}$$

$$HO_2^{\bullet} + O_2^{-\bullet} \rightarrow HO_2^- + O_2 \quad\quad k = 9.7 \times 10^7 (\mathrm{L\,mol^{-1}\,s^{-1}}) \tag{7˙}$$

$$O_2^{-\bullet} + O_2^{-\bullet} \rightarrow \text{very slow} \tag{7¨}$$

In aqueous solution $HO_2^{\bullet}(O_2^{-\bullet})$ radicals are quite unreactive compared to HO˙ toward most organic substrates (Bielski et al., 1985; Bielski and Cabelli, 1991). They may reduce peroxyl radicals to ROOH, with rate constants an order of magnitude lower for $HO_2^{\bullet}$ than for $O_2^{-\bullet}$. Superoxide ion is a sufficiently strong reductant [E˙ $(O_2/O_2^{-\bullet})$ = −0.16 V vs. NHE, pH 7; Sawyer and

Valentine, 1981] that it can reduce many quinones to the semiquinone radical anion. Hydroperoxyl may undergo H-abstraction reactions, but with very small rate constants. Superoxide is not an effective one-electron oxidant because of the instability of the resulting peroxide anion (O_2^{2-}). Superoxide is a strong nucleophile in aprotic media but not in water.

2.7. By-Products of Fenton Reactions

Determination of organic byproducts is crucial on the chance some may be of comparable or greater hazard than the target pollutant. Table 1 gives organic by-products found in selected studies. It should be noted that most studies do not report intermediates or by-products. In practice, total organic carbon (TOC) or dissolved organic carbon (DOC) concentration and toxicity may be the parameters of greatest concern. It is beyond the scope of the article to discuss pathways for all the by-products listed in Table 1. However, a few gereralizations are appropriate.

Since HO$^{\cdot}$ is so indiscriminate in its reactivity, a multitude of by-products can be expected in most cases. For example, the herbicide metolachlor gives several metolachlor derivatives with the aromatic ring intact along with chloroacetate, oxalate, formate, and serine (Figure 5) (Sun and Pignatello, 1995).

As the Fenton degradation proceeds, low-molecular-weight acids such as glyoxylic, maleic, oxalic, acetic, and formic acids accumulate if the reaction is carried out in the dark. This is because many of these acids, and/or their complexes with Fe(III), are weakly reactive toward HO$^{\cdot}$. In light, however, these acids may be mineralized via Fe(III)-catalyzed photoreactions (section 3.1), which helps explain the incomplete removal of DOC often found in dark systems.

When the organic substrate contains heteroatoms, mineralization often leads to the formation of inorganic acids (HCl, HNO_3, NH_4^+, H_2SO_4, etc.). Nitrogen-containing compounds may form HNO_3 exclusively (e.g., from nitrophenols; Kavitha and Planivelu, 2005) or a mixture of NH_4^+ and HNO_3 (e.g. from linuron, a phenylurea herbicide; Katsumata et al., 2005). The influence of contaminant structure and reaction conditions on the relative yields of NH_4^+ and HNO_3 are not well known. Redox interconversion of NH_4^+ and NO_3^- during HO$^{\cdot}$-intiated reactions involve a number of intermediate steps and species (e.g., NH_2OH, $NH_2^{\cdot}$, NO$^{\cdot}$) whose importance is governed by pH, and presence of electron, proton, or hydrogen donors or acceptors and O_2 (Gonzalez et al., 2004). In the presence of O_2 and absence of organic matter, NH_4^+ is oxidized to NO_3^-, but this reaction can be very slow.

In some cases a small yield of reduced organic product may be observed. For example, hexachloroethane in a soil slurry gave a low yield of pentachloroethane above 0.3 *M* H_2O_2, which was attributed to reduction

TABLE 1. Reported Organic By-Products of Fenton and Photo-Fenton Reactions

Type	Rection system	Organic intermediates	References
Thermal	Fe(II) + H$_2$O$_2$ + 2-chlorobiphenyl	Hydroxychlorobiphenyls; some dihydroxylated products	Sedlak and Andren, 1991
Thermal and photo-Fenton	Fe(III) + H$_2$O$_2$ (+ hv) + 2,4-dichlorophenoxy-acetic acid	2,4-Dichlorophenol; 2,4-dichlorophenylformate; 2,4-dichloro-1-(chloromethoxy)-benzene; 6,8-dichloro-2H-1,4-benzodioxan-3-one; oxalic acid; formic acid	Pignatello, 1992; Sun and Pignatello, 1993a; Sun and Pignatello, 1993b
Thermal and photo-Fenton	Fe(III) + H$_2$O$_2$ (+ hv) + 2,4,5-Trichloro-phenoxyacetic acid	2,4,5-Trichlorophenol	Pignatello, 1992
Photo-Fenton	Fe(III) + H$_2$O$_2$ + hv+ metolachlor or methyl parathion	MET: see Figure 5. MP: oxalate; 4-nitrophenol; dimethylphosphate; O,O-dimethyl-4-nitrophenyl phosphate	Sun and Pignatello, 1995
Chelated iron, thermal (soil)	Fe(III)-NTA or -HEIDA + methyl parathion	Dimethyl phosphate	Pignatello and Day, 1996
Thermal	Fe(III) + H$_2$O$_2$ + phenol	1,4-Benzoquinone	Chen and Pignatello, 1997
Photo-Fenton	Fe(III) + H$_2$O$_2$ + hv + 1,1,2-trichloroethane (TCA) or trichloroethene (TCE) or tetrachloroethene (TeCE) or cyclohexene (CE)	TCA: dichloroacetaldehyde; mono- and dichloroacetic acids. TCE: dichloroacetaldehyde; di- and trichloroacetic acids. TeCE: di- and trichloroacetic acids. CE: epoxide of cyclohexene; 2-cyclohexen-1-ol; cyclohexanone; 2-cyclohexen-1-one	Pignatello et al., 1999
Thermal	Fe(III) only (no peroxide) + acid orange 20	1,4-Naphthoquinone (minor); unidentified Fe(II) complex	MacKay and Pignatello, 2001
Thermal	Fe(II) + H$_2$O$_2$ + various PAHs in ethanol	Quinone products of PAHs	Lee et al., 2001
Electro-Fenton	Cathodic reduction of O$_2$; Fe(II) + 4-nitrophenol	Hydroquinone; benzoquinone; 4-nitrocatechol; 1,2,4-trihydroxybenzene; 3,4,5-trihdyroxynitrobenzene	Oturan et al., 2000
Photo-Fenton	Fe(III) + H$_2$O$_2$ + UV + ethylene glycol	Formic acid (major), glycolaldehyde, acetic acid	McGinnis et al., 2000
Photo-Fenton	Fe(III) + H$_2$O$_2$ + UV + humic acid + aniline	p-Aminophenol, p-hydroquinone, maleic acid, fumaric acid, covalent coupling products with humic acid	Fukushima et al., 2000

(Continued on next page)

TABLE 1. Reported Organic By-Products of Fenton and Photo-Fenton Reactions (*Continued*)

Type	Rection system	Organic intermediates	References
Photo-Fenton	Fe(III) + H_2O_2 + UV + 4-nitrophenol	1,2,4-Trihydroxybenzene, 2-hydroxybenzoquinone, hydroquinone, *p*-benzoquinone, 4-nitrocatechol, 4-nitrophenol	Lipczynska-Kochany, 1991
Photo-Fenton	Fe(III) + H_2O_2 + UV + quinoline	2-Quinolinone, 4-quinolinone, 5-hydroxyquinoline, 8-hydroxyquinoline, quinoline-5,8-dione	Cermenati et al., 1997
Thermal Fenton	Fe(III) + H_2O_2 + enediol (e.g., catechol) + X-benzene (X = NO_2, Cl, or CH_3O)	Corresponding hydroxylated compound	Hamiliton et al., 1966
Thermal Fenton	Fe(II) + H_2O_2 + metol (*N*-methyl-4-aminophenol)	Polyhydroxylated dimer products, and tartaric, malonic, malic, and maleic acids	Lunar et al., 2000b
Thermal Fenton	Fe(II) + H_2O_2 + 2,4-Dimethyl aniline (xylidine)	2,4-Dimethyl phenol (major) Oxalic acid (stable product)	Bossmann et al., 1998
Photo-Fenton	Fe(II) + H_2O_2 + hv + 2,4-dimethyl aniline (xylidine)	2,4-Dimethyl phenol Oxalic acid (mineralized)	Bossmann et al., 1998
Thermal Fenton	Fe(II) + H_2O_2 + polyvinyl alcohol (PVA)	Super-macromolecules (oxidized PVA and iron(III)), partly resistant to degradation No low-molecular-weight intermediates About 60% residual DOC	Lei et al., 1998; Bossmann et al., 2001a
Photo-Fenton	Fe(II) + H_2O_2 + hv + polyvinyl alcohol (PVA)	Super-macromolecules (oxidized PVA and iron (III)) No low-molecular-weight intermediates about 10% residual DOC (super-macromolecules)	Lei et al., 1998; Bossmann et al. 2001a
Photo-Fenton	Fe(III) + H_2O_2 + hv + methyl orange in methanolic solution	4-Dimethylamino aniline 2-Butenedioic acid Oxalic acid	Chen et al., 2001b
Photo-Fenton	Fe(III) + H_2O_2 + hv + acridine orange and alizarine violet 3B	*N,N*-Dimethyl formaldehyde *N,N*-Dimethyl acetamide	Xie et al., 2000
Thermal Fenton	Fe(II) + H_2O_2 + mandelic acid	Benzaldehyde (major) Benzoic acid Ring hydroxylated products (*o*-, *m*-, *p*-phenols) (pH dependent)	Walling and Amarnath, 1982
Electro-Fenton H_2O_2; electro-regenerated Fe^{2+}	(0.1-1 m*M* phenol or 1 m*M* chlorobenzene) 0.01 m*M* $FeSO_4$, 0.1 *M* H_2SO_4, O_2	Phenol: hydroquinone, cathechol, resorcinol Chlorobene: *p*-chlorophenol, phenol	Hsaio and Nobe, 1993

(Continued on next page)

TABLE 1. Reported Organic By-Products of Fenton and Photo-Fenton Reactions (*Continued*)

Type	Rection system	Organic intermediates	References
Electro-Fenton Pt anode, carbon PTFE cathode	Aniline (100 ppm), 10 mM FeSO$_4$, 25°C, pH 3	Benzoquinone, nitrobenzene, NH$_4^+$, maleic and fumaric acid	Brillas, 1998a
Thermal Fenton	0.2 mM Substituted benzenes 8 mM H$_2$O$_2$ 0.1 mM ferrous ammonia sulfate pH 3	Major path through chlorophenol→ chlorodihydroxybenzene→ chlorohydroquinone Minor path chlorophenol–phenol– dihydroxybenzene–quinone	Augusti et al., 1998
Thermal Fenton	FeSO$_4$ 0.73 mM Atrazine 140 μM H$_2$O$_2$ 0.73 mM Reaction time 24 h	4-Acetamido-2-chloro-6-(isopropylamino)-s-triazine deethylatrazine; 4-acetamido-2-chloro-6-(ethylamino)-s-triazine; deisopropylatrazine; 4-acetamido-2-hydroxy-6-(isopropylamino)-s-triazine; 4-acetamido-6-amino-2-chloro-s-triazine; diaminoatrazine	Arnold et al., 1995
Electro-Fenton and photo electro-Fenton	FeSO$_4$ 1 mM H$_2$O$_2$ generated by anodic reduction of O$_2$ 230 ppm 2,4-D	2,4-Dichlorophenol; 4,6-dichlororesorcinol; chlorohydroquinone; chlorobenzoquinone; glycolic, glyoxylic, maleic, fumaric and oxalic acids.	Brillas et al., 2000
Thermal Fenton	Metol removal		Lunar et al., 2000b
Electrochemical Fenton	Wastewater with 3680 mg/L hexamine 380 g/L H$_2$O$_2$ 5000 mg/L as ferric sulfate	Formaldehyde (intermediate) Formate CO$_2$ NH$_4^+$, NO$_3^-$	Chou et al., 1999
Electro-Fenton	Pentachlorophenol; working electrode 10 cm^2 carbon felt, −0.5 V (SCE), 50 mA, 1 cm^2 platinum counterelectrode with catalytic amount of Fe^{2+}	1,2- and 1,4-tetrachlorocatechol; tetrachloro-o-quinone; tetrachloro-p-quinone; hydroxyquinone	Oturan et al., 2001
Electro-Fenton, thermal Fenton	Ethylene thiourea	Ethylene urea, 2-imidazolin-2-yl sulfonic acid	Saltmiras and Lemley, 2000
Electro-Fenton	Chlorophenoxyacid herbicides 1 mM (no reported meas. of avg. H$_2$O$_2$ or Fe^{2+} conc., pH 2)	Prod. dependent on current applied; chlorinated phenol to hydroxylated chlorobenzene to chloroaliphatic alcohols, ketones, carboxylic acids, alkenes	Oturan et al., 1999
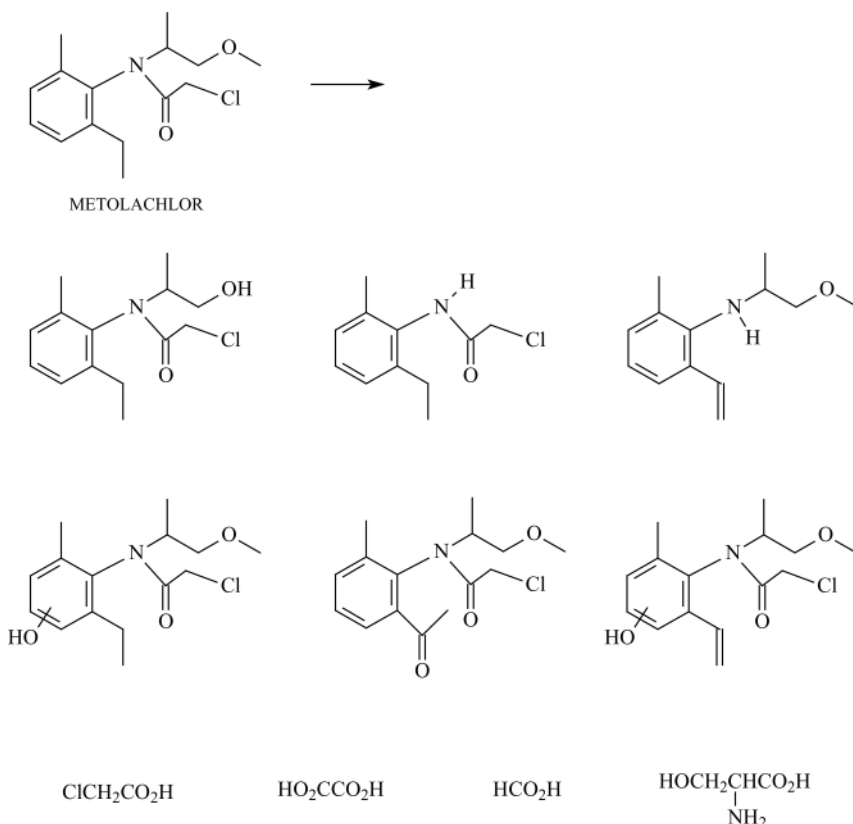
FIGURE 5. Some degradation products of the herbicide, metolachlor, in the photoassisted Fenton reaction (Sun and Pignatello, 1995). The alkenes likely arise from dehydration of precursor products in which the side chain is hydroxylated in the inlet of the gas chromatograph.

by superoxide ion (Watts et al., 1999). Another possible reductant is the alcoholate radical anion, $R_2C^{\cdot}{-}O^-$, which can be formed by reaction of $HO^{\cdot}$ with primary or secondary alcohol groups on natural organic matter (NOM) or other components of the waste stream (Peyton et al., 1995). NOM may serve as a trap for organoradicals, yielding covalently linked products, as for pentachlorophenol (Fukushima and Tatsumi, 2001).

Lastly, in an accounting of by-products one must also consider reactions of organic molecules or radicals with Fe(II) and Fe(III) (sections 2.4 and 2.5), ferryl species (section 2.9), and halogen radicals (section 2.3.3).

2.8. Role of Dioxygen in Fenton Reactions

Having dioxygen (O_2) present almost invariably leads to greater mineralization of the target pollutant to CO_2. Dioxygen acts in two ways: It serves as a supplemental bulk oxidant and it accelerates the rate.

Since dioxygen is practically free, it is desirable to channel reaction pathways toward consumption of it rather than H_2O_2. Every mole of O_2 replaces two moles of H_2O_2. Hydrogen peroxide O is incorporated into organic compounds principally by reactions 11 and 12. Dioxygen O is incorporated into organic compounds by reaction 14. In the Fenton reaction of benzene in the presence of $^{18}O_2$, the isotope label was $\sim$20% incorporated into phenol and 100% incorporated into benzoquinone by-products (Kunai et al., 1986). As a cautionary note, labeling experiments may be ambiguous because O exchange is possible between H_2O_2 and O_2 and vice versa in Fenton systems: that is, $H_2^{18}O_2 \rightarrow {}^{18}O_2$ via reaction 2 and reaction 5 or 7, and $^{18}O_2 \rightarrow H_2^{18}O_2$ via reaction 13 and reaction 6 or 7.

Complete mineralization of 2,4-D during Fe(III)-catalyzed photo-Fenton treatment resulted in incorporation of O_2 according to the following stoichiometry (Pignatello, 1992):

$$C_8H_6Cl_2O_3 + 7H_2O_2 + 4O_2 \xrightarrow{\text{Fe(III)}} 2HCl + 8CO_2 + 9H_2O \qquad (41)$$
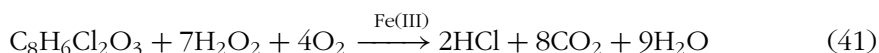
Utset et al. (2000) observed partial replacement of H_2O_2 by O_2 in the Fenton reaction of aniline. The degree of replacement increased with [aniline], decreased with [H_2O_2], and increased slightly with temperature.

Dioxygen usually accelerates the rate of mineralization in photo-Fenton reactions (Sun and Pignatello, 1993c; Kim and Vogelpohl, 1998; Bossmann et al., 2001a). It is likely that dioxygen increases the steady-state concentration of $HO_2^{\cdot}$ via reaction of organoradicals with O_2 [eqs. (35)–(36)]. As indicated in section 2.4, this would lead to an increase in either [Fe^{2+}] [eqs. (5) and (5′)] or [H_2O_2] [eqs. (6) and (6′)], depending on the Fe(III)-to-Fe(II) ratio.

One exception to the "rule" that dioxygen accelerates Fenton reactions was discovered by Duesterberg et al. (2005) in a study of formic acid. The reason is that the initial product of $HO^{\cdot}$ attack on HCO_2H—namely, $CO_2^{-\cdot}$— reduces Fe(III) under deaerated conditions, propagating the Fenton cycle, but preferentially reduces dioxygen under aerated conditions forming $HO_2^{\cdot}(O_2^{-\cdot})$, which both propagates and terminates the Fenton cycle.

Direct oxidation of Fe(II) species by dioxygen,

$$Fe(II) + O_2 \rightarrow Fe(III) + O_2^{-\cdot} \qquad (42)$$
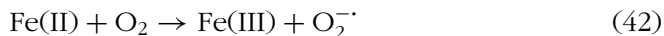
is exceedingly slow at pH levels where Fe(III) is soluble (King, 1998) and therefore ordinarily does not contribute to Fenton reactions below pH 4. Above pH 4, though, it could be important.

2.9. Nonclassical Fenton Pathways: Formation of High-Valent Oxoiron Complexes

Several transition metal ions, iron among them, can form high-valent oxo complexes, which are usually written as M=O. Certain chelated forms of

Fe(II) and/or Fe(III), where the chelating agent is a polycarboxylate ligand or macrocyclic ligand (e.g., porphyrin and pyridyl-type ligands), may react with H_2O_2, organoperoxides or dioxygen to form a complex containing a high-valent oxoiron ("ferryl") moiety, Fe=O. The iron in the ferryl moiety may be in the +IV or +V formal oxidation state. There is general agreement that ferryl participates in both O insertion and electron transfer reactions of many heme and nonheme enzymes (Rush and Koppenol, 1986; Fujii et al., 1996; Dong et al., 1995; Arasasingham et al., 1989; Rahhal and Richter, 1988; Meunier, 1994; Feig and Lippard, 1994) and may be involved in other processes such as aging and chemical toxicity.

Reactions that ferryl can undergo with organic compounds include hydroxylation, methylene ketonization, olefin epoxidation, α-diol cleavage, α-ketoalcohol cleavage, dehydrogenation, oxidative cleavage of olefins, N-, S-, or O-demethylation, and S-, or P-oxygenation (Sheldon and Kochi, 1981; Nam et al., 1991; Sawyer et al., 1993; Tung et al., 1992; Sheu et al., 1990; Leising et al., 1991; Fish et al., 1993; Song et al., 1993; Natrajan et al., 1990; Sheu and Sawyer, 1990a, 1990b; Sugimoto et al., 1988). The mechanisms are not well established. Possibilities include single-step O insertion, a two-step electrophilic mechanism, or a two-step free radical mechanism, depending on the ligand field on the metal.

Some contaminants or their by-products are capable of chelating iron, and thus the formation of ferryl complexes originating from such chelates in Fenton AOPs is plausible, and more effort in this area is warranted. A question that arises is whether ferryl species can form when only aquo ligands are present on the metal, as is the more usual situation. Although suitable organic ligands may be better able to delocalize the spin or charge on Fe=O, short-lived intermediates having only aquo ligands are certainly attainable. Rush and Bielski (1994) observed transient $H_3Fe^VO_4$ and its deprotonated forms after pulse-radiolysis reduction of potassium ferrate [eq (43)]. (The +VI oxidation state of Fe (ferrate) is relatively stable.) Rush and Bielski (1986) also gave spectroscopic evidence for $[(OH)_n Fe^{IV}=O]^{2-n}$ as a product of Fe(III) oxidation by radiolysis-generated HO· in alkaline solution:

$$Fe^{VI}O_4^{2-} + [e^-] \rightarrow Fe^VO_4^{3-} \tag{43}$$

$$Fe^{III}(OH)_4^- + HO· \rightarrow [(OH)_nFe^{IV}=O]^{2-n} \tag{44}$$
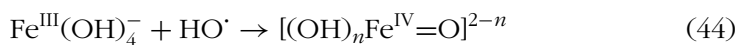
Jacobsen et al. (1997, 1998) formed the Fe(IV) ferryl complex quantitatively in water by reacting Fe^{2+} with ozone:

$$Fe^{2+} + O_3 \rightarrow Fe^{IV}O^{2+} + O_2 \tag{45}$$
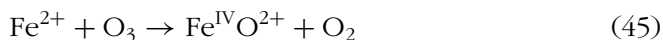
Based mainly on kinetic data, Kremer has argued for replacing the free-radical chain mechanism of the thermal Fenton reaction [eqs. (1)–(7) and related reactions] with mechanisms involving high-valent oxoiron species

(Kremer, 1985, 1999, 2000). He suggested that reaction of Fe^{2+} with H_2O_2 produces a mononuclear Fe(IV) oxo complex and a mixed-valent binuclear Fe(IV)–Fe(III) oxo complex (Kremer, 1999):

$$Fe^{2+} + H_2O_2 \rightarrow FeO^{2+} + H_2O \underset{Fe^{3+}}{\overset{Fe^{3+}}{\rightleftharpoons}} FeOFe^{5+} \tag{46}$$
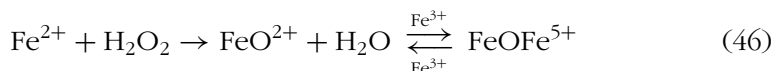
Decomposition of H_2O_2 by Fe^{3+} was suggested to go by the "complex mechanism," which involves an Fe(V) oxo intermediate (Kremer, 1985):

$$Fe^{3+} + HO_2^- \rightleftharpoons FeHO_2^{2+} \rightarrow FeO^{3+} + HO^- \tag{47}$$

Proposed non-hydroxyl radical schemes for the Fenton reaction have been controversial (Walling, 1975, 1998; Walling and Goosen, 1973; Wink et al., 1994; Sawyer et al., 1996; MacFaul et al., 1998). In the absence of spectroscopic identification, the involvement of ferryl proves difficult if it gives products similar to HO˙, or if it is generated concurrently with HO˙ but reacts slower with a probe molecule than HO˙, failing to leave its mark. For example, free radical spin-trapping experiments may be inconclusive because they cannot rule out the existence of a transient that is not trapped, or a transient that yields the same spin trap product as HO˙ (Jiang et al., 1993; Lloyd et al., 1997). Thus, conclusions based solely on structure–reactivity relationships, kinetics, or the identity or yields of products must be interpreted with great caution.

Bossmann et al. (1998) published evidence against the formation of HO˙ as the main oxidizing intermediate in thermal and photo-assisted Fenton reactions of dimethylanilines (xylidines). Although hydroxylated anilines were formed by HO˙ attack during H_2O_2 photolysis (which forms only free HO˙), these products could not be detected during the Fenton and photo-Fenton reactions. In these cases, 2,4-dimethyl phenol was the most important intermediate. The authors proposed that 2,4-dimethyl phenol was formed by an electron transfer mechanism where 2,4-xylidine was oxidized by an Fe(IV) oxoiron moiety. The latter may be formed by an inner-sphere two-electron transfer reaction taking place within a hydrated iron(II)–H_2O_2 complex (section 2.2).

Pignatello et al. (1999) gave evidence for an alternative oxidant in photo-Fenton reactions (refer to Figure 6). Using competitive kinetic experiments they showed that the kinetic deuterium isotope effect (KDIE $= k_H/k_D$) for the photo-Fenton reaction of cyclohexane/cyclohexane-d_{12} was 1.22–1.26, significantly greater than values of 1.06–1.12 obtained using known or reputed HO˙-generating reactions, including H_2O_2 photolysis, Fe^{3+} photolysis, and (interestingly) $Fe^{2+} + H_2O_2$. Addition of *t*-butanol—a strong HO˙ scavenger, but weak ferryl scavenger—increased the cyclohexane KDIE of the photo-Fenton reaction to a maximum of 1.40 depending on [*t*-butanol], but
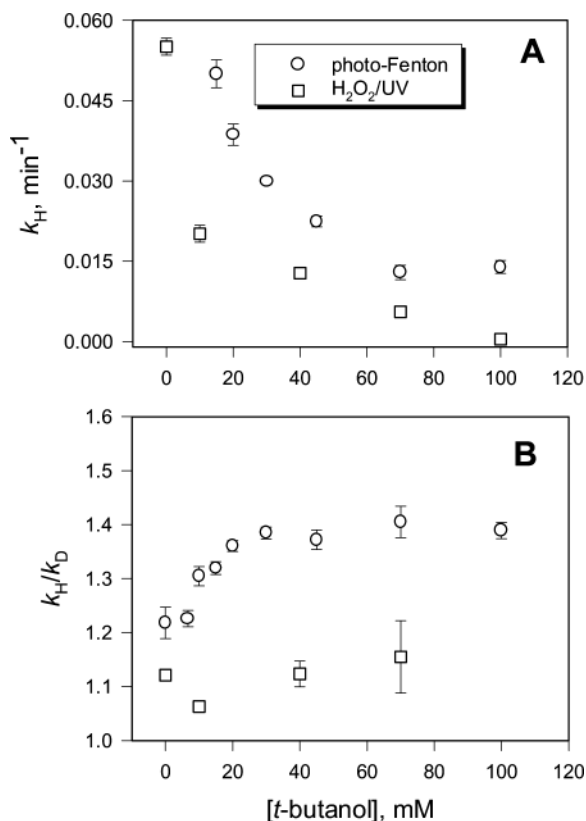
FIGURE 6. Reaction of cyclohexane under photo-assisted Fenton conditions (section 3) compared to photo-peroxidation ($H_2O_2 + UV \rightarrow 2HO^\cdot$) supporting an additional oxidant in photo-Fenton reaction. (A) Photoperoxidation is completely inhibited by the $HO^\cdot$ scavenger *t*-butanol, but the photo-Fenton reaction leaves a residual reactivity at high [*t*-butanol]. (B) The kinetic deuterium isotope effect (C_6H_{12} vs. C_6D_{12}) increases with [*t*-butanol] for the photo-Fenton reaction but remains constant for photoperoxidation. From Pignatello et al. (1999) with permission.

had no effect on the same KDIE for H_2O_2 photolysis (Figure 6b). At high [*t*-butanol], significant residual reactivity toward cyclohexane was left in the photo-Fenton reaction that did not exist in H_2O_2 photolysis.

These results clearly indicate the presence of an additional oxidant other than $HO^\cdot$, but produced in minor yield. Nanosecond laser flash photolysis detected a transient intermediate with broad absorbance in the visible spectrum and a lifetime of $\sim$100 ns (Pignatello et al., 1999). This transient was suggested to be either an excited state of a Fe(III) hydrogen peroxide complex or a ferryl species, according to the following reactions:

$$[Fe^{III}\!-\!OOH]^{2+} \overset{h\nu}{\rightleftharpoons} [Fe^{III}\!-\!OOH]^{2+*} \tag{48}$$

$$[Fe^{III}\!-\!OOH]^{2+*} \rightarrow \{Fe^{III}\!-\!O^\cdot \leftrightarrow Fe^{IV}\!\!=\!\!O\} + HO^\cdot \tag{49}$$
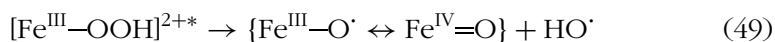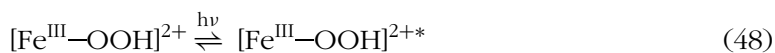
where an asterisk designates the photoexcited state. Ferryl species is thus generated along with HO$\cdot$.

The existence of ferryl species in Fenton reactions can influence product distribution. Alkene epoxidation, for example, is a well-known reaction for ferryl but uncharacteristic of HO$\cdot$. Pignatello et al. (1999) found a small yield of cyclohexene oxide (reaction 50) in photo-Fenton reactions, but not in photolysis of H_2O_2 alone, where HO$\cdot$ only is produced.

$$\text{(50)}$$
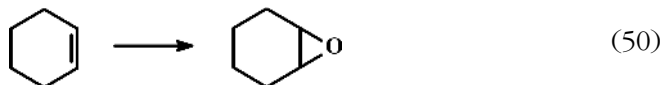
These authors also found that trichloroethene and tetrachloroethene gave radically different ratios of chlorinated acetic acid by-products in photo-Fenton reaction compared to those obtained during photolysis of H_2O_2 alone, possibly due to epoxidation.

In ^{17}O labeling experiments Lloyd et al. (1997) showed that all of the spin-trapped active oxygen generated in the thermal $Fe^{2+} + H_2O_2$ reaction originated from H_2O_2 and none from H_2O; this means either that a ferryl complex is not formed in that reaction, or that the O does not undergo exchange with water:

$$Fe=^{17}O + H_2O \int Fe=O + H_2{}^{17}O \qquad (51)$$

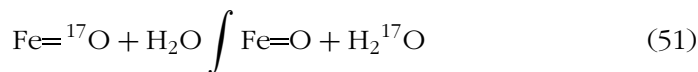The ferryl complex generated by reaction of Fe^{2+} and ozone [eq. (45)] seems to be a much weaker oxidant than HO$\cdot$, with rate constants of $1 \times 10^3 M^{-1} s^{-1}$ for nitrobenzene and $\sim 1 \times 10^4 \ M^{-1} s^{-1}$ for phenol and the three nitrophenol isomers (Mártire et al., 2002). These rate constants are several orders of magnitude smaller than the corresponding rate constants with HO$\cdot$, so their role in the Fenton reaction of the species $Fe^{IV}O$, if it is formed is likely minor.

3. MODIFIED FENTON REACTIONS

3.1. The Photoassisted Fenton Reaction

Irradiation of reaction solutions with ultraviolet (UV) or UV/visible light almost invariably leads to faster rates and higher yields of inorganic products (e.g., Pignatello, 1992; Ruppert et al., 1993; Kiwi et al., 1994; Lei et al., 1998; DeLaat et al., 1999; Balanosky et al., 2000; Benitez et al., 2000b). Photoenhancement will be observed even in the presence of ordinary overhead fluorescent light used to illuminate laboratory space. Enhancement is due nearly entirely to the photochemistry of Fe(III). Fe(III) complexes undergo ligand-to-metal charge transfer (LMCT) excitation, dissociating to give Fe(II) and an oxidized ligand, L_{ox} (Balzani and Carassiti, 1970; Sima and Makanova, 1997):

$$Fe^{III}(L)_n + h\nu \rightarrow Fe^{II}(L)_{n-1} + L_{ox}^{\cdot} \qquad (52)$$
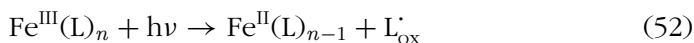
The photochemistry of Fe(III) is advantageous to Fenton AOPs because the reduced iron can then react with H_2O_2 to produce $HO^\cdot$ [eq. (1)] and because oxidation of the ligand may lead to further degradation of the target pollutant (e.g., Pignatello, 1992; Sun and Pignatello, 1993c; Safarzadeh-Amiri et al., 1996; Bandara et al., 1997; Bossmann et al., 1998). The photolysis of Fe(II) species is unimportant at wavelengths employed in Fenton AOPs.

Hydrogen peroxide also photolyzes with UV light (section 3.1.5):

$$H_2O_2 + h\nu \rightarrow 2HO^\cdot \tag{53}$$

3.1.1. PHOTOLYSIS OF AQUATED Fe(III) SPECIES

Fe(III) hydroxy complexes present in mildly acidic solution, such as $Fe(OH)^{2+}$ and $Fe_2(OH)_2^{4+}$ (section 2.3.1), absorb light appreciably in the UV and into the visible region. These complexes undergo photoreduction to give $HO^\cdot$ and Fe(II). The most important species is $Fe(OH)^{2+}$ due to a combination of its relatively high absorption coefficient and concentration relative to other Fe(III) species under typical conditions:

$$Fe(OH)^{2+} \xrightarrow{h\nu} Fe^{2+} + HO^\cdot \tag{54}$$

The quantum yield Φ for Fe^{2+} formation in eq. (54) is wavelength dependent (Faust and Hoigné, 1990; Langford and Carey, 1975; Benkelberg and Warneck, 1995): It is 0.14–0.19 at 313 nm and 0.017 at 360 nm (Faust and Hoigné, 1990). In technical applications, quantum efficiency under polychromatic irradiation, symbolized by $\langle\Phi\rangle$, is of interest (section 3.1.4). The $\langle\Phi\rangle$ for Fe^{2+} production from ferric sulfate at pH 3 using a medium-pressure mercury arc (Heraeus Noblelight, TQ 718) is 0.21 (Bossmann et al., 1998).

Excitation of Fe(III) aquo complexes alone (i.e., without peroxide) can be used to promote degradation of pollutants since $HO^\cdot$ is formed in reaction 54 (Larson et al., 1991; Kawaguchi and Inagaki, 1994; Mazellier et al., 1997, 1999; Brand et al., 1998, 2000a, 2000b; Mailhot et al., 1999). However, photolysis of Fe(III) alone appears to offer little, if any, advantage over the photo-Fenton reaction. Fe(III) is required in stoichiometric amount unless a pathway for its regeneration from Fe^{2+} is available. While regeneration is possible from intermediates in the reaction (e.g., $HO_2^\cdot$, H_2O_2, $Cl^\cdot$), or air, it is not very efficient. Furthermore, care has to be taken to keep the pH in a range (2.5 < pH < 3–4) where the $Fe(OH)^{2+}$ species exists in appreciable concentration and the bulk of the iron remains soluble (section 2.3.1).

3.1.2. PHOTOLYSIS OF Fe(III)—OOH COMPLEXES

As discussed in section 2.3, the rate-limiting step in the thermal Fenton reaction is usually the thermal decomposition of an Fe(III)–peroxide intermediate [eqs. (19)–(20)]. Photoexcitation of the Fe(III)—OOH complex in mixtures of Fe(III) and H_2O_2 enhances the rate of H_2O_2 decomposition (Bossmann et al.,

1998) and dioxygen evolution (Behar and Stein, 1986; Sun and Pignatello, 1993c) compared to the corresponding thermal reaction. Reaction 55 has been proposed (Behar and Stein, 1986).

$$[\text{Fe}^{\text{III}}\text{–OOH}]^{2+*} \rightarrow \text{Fe(II)} + \text{HO}_2^{\cdot} \tag{55}$$
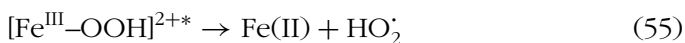
where the asterisk signifies the charge-transfer photo-excited state of the complex formed in reaction 17. The $\langle \Phi \rangle$ for Fe(II) production (medium-pressure mercury arc, pH 3) is about 0.33 (Bossmann et al., 1998). Reaction 55 may compete with reaction 49, which produces ferryl (section 2.9).

3.1.3. PHOTOLYSIS OF Fe(III) COMPLEXES WITH ORGANIC LIGANDS

Fe(III) may complex with certain target compounds or their byproducts, especially those acting as polydentate ligands. These complexes typically have higher molar absorption coefficients in the near-UV and visible regions than do the aquo complexes. Their excitation leads to the production of Fe^{2+} and a ligand radical by the generalized reaction 52 with quantum yields that are wavelength dependent. Polychromatic quantum efficiencies ($\langle \Phi \rangle$) in the UV/visible for different complexes range from ~0.05 to ~0.95 (Ronco and Aymonino, 1987; Pohl et al., 1988; Andrianirinaharivelo et al., 1995; Bandara et al., 1996; Van der Zee et al., 1993).

The photoreactivity of Fe(III)–carboxylate or Fe(III)–polycarboxylate complexes is well-known and usually leads to decarboxylation of the organic ligand (Balzani and Carassiti, 1970):

$$\text{R–CO}_2\text{–Fe(III)} + h\nu \rightarrow \text{R–CO}_2^{\cdot} + \text{Fe(II)} \rightarrow \text{R}^{\cdot} + \text{CO}_2 \tag{56}$$
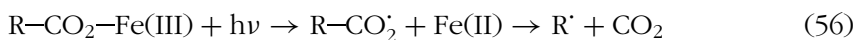
An interesting and potentially useful modification of the photo-Fenton reaction takes advantage of the photo-lability of Fe(III)–oxalate complexes (Safarzadeh-Amiri et al., 1996, 1997; Hislop and Bolton, 1999), which is efficient up to 500 nm ($\Phi = 1.0$–1.2). [Ferric oxalate is commonly used as a chemical actinometer (Hatchard and Parker, 1956; Braun et al., 1991).] Bolton and coworkers added oxalate to reaction solutions and obtained photoreduction of the resulting ferrioxalate complexes in situ, such as

$$[\text{Fe}(\text{C}_2\text{O}_4)_3]^{3-} \rightarrow \text{Fe}^{2+} + 2\text{C}_2\text{O}_4^{2-} + \text{C}_2\text{O}_4^{-\cdot} \tag{57}$$
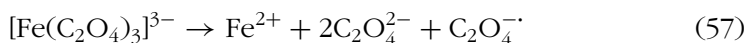
and obtained degradation of aromatic and chlorinated aromatic hydrocarbons, chlorinated ethenes, ethers, alcohols, and ketones (Safarzadeh-Amiri et al., 1996, 1997). Oxalate addition also enhanced photo-Fenton degradation of the herbicide diuron in goethite suspensions by accelerating photoreductive dissolution of iron (Mazellier and Sulzberger, 2001):

$$\equiv\text{Fe}^{\text{III}}\text{–}(\text{C}_2\text{O}_4^{-}) + h\nu \rightarrow \text{Fe}^{2+}(\text{aq}) + \text{C}_2\text{O}_4^{-\cdot} \tag{58}$$
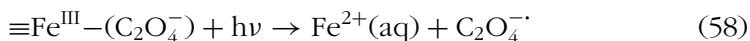
where $\equiv$ represents the surface-bound metal.

At low Fe(III) concentrations the oxalyl radical anion, $C_2O_4^{-\cdot}$, rapidly decomposes to give carbon dioxide and the carboxylate radical anion (59, $k_{59} = 2 \times 10^6 \text{ s}^{-1}$). The latter reacts with dioxygen (when present) to yield the superoxide anion:

$$C_2O_4^{-\cdot} \rightarrow CO_2 + CO_2^{-\cdot} \tag{59}$$

$$O_2 + CO_2^{-\cdot} \rightarrow CO_2 + O_2^{-\cdot} \tag{60}$$
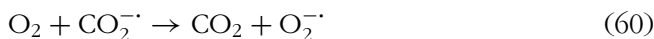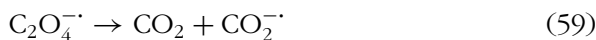
At high Fe(III) concentrations, $C_2O_4^{-\cdot}$ reduces Fe(III) to Fe(II).

The carboxylate radical anion $CO_2^{-\cdot}$ is a sufficiently strong reducing agent that it can, in the absence of peroxide and dioxygen, reduce perchloroalkanes such as tetrachloromethane and hexachloroethane, which are normally inert to $HO^{\cdot}$ (Huston and Pignatello, 1996):

$$CCl_4 \xrightarrow{h\nu, Fe(C_2O_4)_3^{3-}} CCl_3CCl_3(\text{major}) + CHCl_3(\text{minor}) \tag{61}$$

$$CCl_3CCl_3 \xrightarrow{h\nu, Fe(C_2O_4)_3^{3-}} CCl_2{=}CCl_2 \tag{62}$$

The products $CHCl_3$ and $CCl_2{=}CCl_2$ could later be degraded by adding hydrogen peroxide.

An example of Fe(III) complexes with macromolecules is discussed here because it shows photochemical behavior different from complexes of small molecules. Iron(III) is known to form stable complexes with polyvinylalcohol (PVA), a polymer of great importance in many industrial applications (Bossmann et al., 2001). PVA degradation by the Fenton reaction was found to be independent of molecular weight (MW = 15,000, 49,000, and 100,000). Interestingly, in early stages of the reaction, macromolecules or macromolecular aggregates of very high mass (MW $\gg 2 \times 10^6$) were formed between iron(III) and the oxidized PVA-chains. Since low-molecular-weight intermediates, su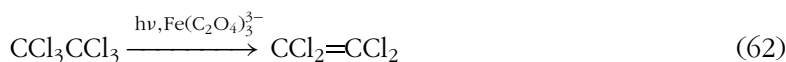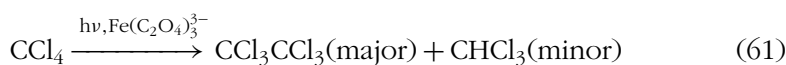ch as oxalic acid, formic acid or formaldehyde were not observed, it was deduced that the degradation took place within the supramacromolecular complexes, producing CO_2 directly.

3.1.4. CALCULATION OF POLYCHROMATIC QUANTUM EFFICIENCIES FOR Fe(II) PRODUCTION

The efficiency of Fe(III) photoreduction is critical for optimizing the photo-assisted Fenton reaction. Technical applications employ radiation sources emitting in the UV/visible region, such as medium or high pressure mercury arc lamps, or solar radiation. The polychromatic quantum efficiency for Fe(II) production $\langle \Phi(Fe^{2+}) \rangle$ is (Bossmann et al., 2001a):

$$\langle \Phi(Fe^{2+}) \rangle = \frac{d[Fe^{2+}]}{dt} \frac{1}{P_a} \tag{63}$$

where $d[Fe^{2+}]/dt$ $(M\,s^{-1})$ is the rate of Fe(II) formation and P_a (einstein $L^{-1}\,s^{-1}$) is the photon flux absorbed by the Fe(III) complex over the entire wavelength range, which is given by:

$$P_a = \sum P_{a,\lambda} = \left(\frac{RP_e}{V \cdot N_A} \right) \cdot \sum \left[\frac{S_{e,\lambda}(1 - 10^{-A_\lambda})}{E_{ph,\lambda}} \right] \qquad (64)$$

where $P_{a,\lambda}$ (einstein $L^{-1}\,s^{-1}$) is the photon flux absorbed at wavelength λ; N_A is Avogadro's number; V is the total volume of solution (L); RP_e (W) is the total radiant power emitted by the lamp; $S_{e,\lambda}$ is the spectral distribution of radiant power emitted by the lamp (usually obtained from the provider); $E_{ph,\lambda}$ is the energy of a photon of wavelength λ (J); and A_λ is the average absorbance of the solution at wavelength λ during irradiation. This relationship may be used if A_λ is equal to or greater than 2, or does not vary by more than 10% during the irradiation.

   RP_e may be determined by performing ferrioxalate actinometry (Hatchard and Parker, 1956; Braun et al., 1991) directly in the reactor. The radiant power is then given by:

$$RP_e = \frac{n_{Fe^{2+}}}{t} \left\{ \sum \left[\frac{S_{e,\lambda}\Phi_{ac,\lambda}(1 - 10^{-A_{ac,\lambda}})}{E_{ph,\lambda}} \right] \right\}^{-1} \qquad (65)$$

where n_{Fe2+} is the number of Fe(II) species formed during the irradiation time t (s); $A_{ac,\lambda}$ is the average absorbance of the ferrioxalate actinometric solution at wavelength λ during irradiation; and $\Phi_{ac,\lambda}$ is the quantum yield of the actinometer at wavelength λ. Iron(II) may be determined by, for example, the absorbance of its 1,10-phenanthroline complex.

3.1.5. CONTRIBUTION OF DIFFERENT PHOTOCHEMICAL REACTIONS TO THE ENHANCEMENT OF THE FENTON REACTION

Clearly, many photochemical reactions are possible in irradiated Fenton systems. The contribution of a given reaction to degradation depends on the emission spectrum of the source, the concentration and absorbance of the photoactive species, the quantum efficiency for the given reaction, and the presence and concentration of other light-absorbing species in the system— that is, the inner filter effect. The inner filter effect limits the reactor volume. The concentration and absorbance of photoactive and non-photoactive species change during the course of the reaction. Further research is needed to establish the contributions of individual reactions. However, a few conclusions may be reached from existing knowledge.

First, Fe(III) complexes often exhibit higher absorbances and higher quantum yields than simple aquated Fe(III) species, and therefore may be more important in photo-Fenton systems. For example, the mixture of 2,4-dimethylaniline and Fe(III) at pH 3 photolyzes with a quantum yield of 0.92 for Fe(II) production (Bossmann et al., 1998), compared to ≤0.2 for aquated complexes. The photolysis of Fe(III)–carboxylate or –polycarboxylate complexes likely play a dominant role when they are present. Photodecarboxylation, in fact, often accounts for a substantial fraction of carbon mineralization, especially when the target compound is aromatic (Casado et al., 2005; Sun and Pignatello, 1993b, 1993c). For example, 60% of CO_2 evolved from 2,4-D was attributed to Fe(III)-catalyzed photodecarboxylation principally of oxalic acid resulting from advanced degradation of the aromatic ring (Sun and Pignatello, 1993b, 1993c) (Figure 7). Oxalic acid is a major product of aromatic ring degradation and its complexes with Fe(III) are very stable to HO· attack in the dark. These examples help explain why complete mineralization often cannot be achieved using the Fenton reaction in the dark.

Second, although photolysis of H_2O_2 (reaction 53) has a relatively high quantum yield (Φ is ~1 for HO· production, and ~0.5 for H_2O_2 loss), its

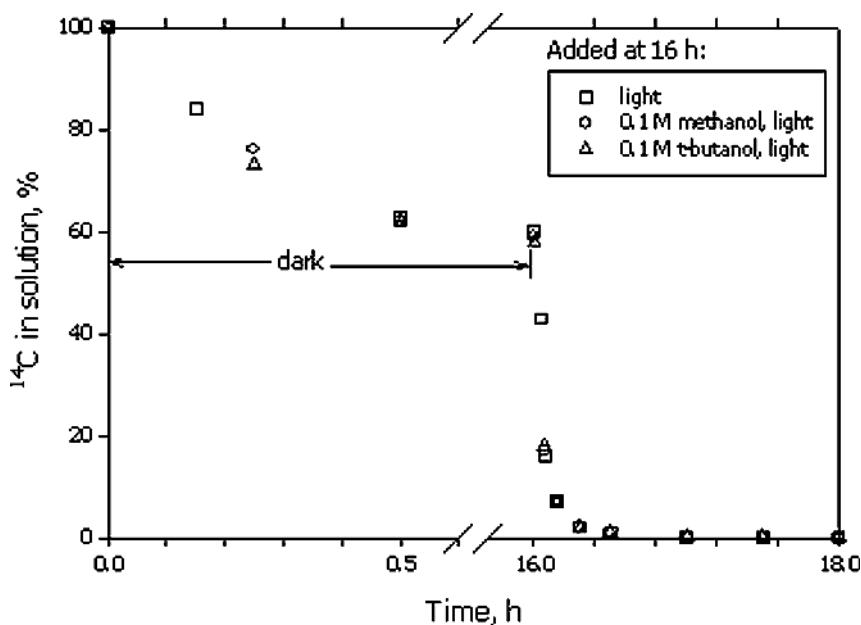**FIGURE 7.** Mineralization of ring-^{14}C-labeled 2,4-dichlorophenoxy acetic acid under photo-assisted Fenton conditions. After the dark reaction leveled off, irradiation resulted in further mineralization of the ring independent of the HO· scavengers methanol and *t*-butanol. The ^{14}C in solution that persisted in the dark was later identified as being associated with oxalic acid. Redrawn from Sun and Pignatello (1993c).

contribution in photo-Fenton applications is limited by the weak absorption of light by H_2O_2 (the molar absorption coefficient of H_2O_2 is only 18.7 $M^{-1}\,cm^{-1}$ at 254 nm and becomes vanishingly small above 350 nm) and the strong "inner filter effect" due to absorption of light by iron and organic solutes (especially aromatics). However, H_2O_2 photolysis may contribute to HO˙ production at low concentration of iron and organic absorbers or at very large concentrations of H_2O_2.

Third, while in theory rate should increase with radiant power, in practice there may be an upper limit reached when photoreduction of iron outpaces its reoxidation—that is, when iron in the +III state becomes a small fraction of total iron.

3.2. Iron Complexes as Fenton Catalysts

Chelated forms of iron have been used to carry out Fenton degradation of pollutants in a few cases. Chelation extends the pH range over which iron is soluble because the chelating ligand competes favorably with hydroxide ion for coordination, and chelated complexes typically are soluble. Chelation may also accelerate reaction 1 (section 2.2). On the other hand, (1) chelation may retard reaction 2 (section 2.3); (2) the chelating agent—free or complexed— may scavenge HO˙; and (3) chelation may divert reactions of bulk oxidant to ferryl species, which seem to be intrinsically less reactive than HO˙ toward most functional groups (section 2.9).

Sun and Pignatello (1992) found many organic and inorganic polydentate ligands to be effective in catalyzing the thermal Fe(III) Fenton oxidation of 2,4-D at pH 6 in homogeneous solution compared to a control containing precipitated iron oxyhydroxides at pH 6. Reactions with chelate were not, however, faster than the Fenton reaction at its optimized pH. Active chelating agents were found among aminopolycarboxylates (e.g., nitrilotriacetic acid, or NTA), polycarboxylates (e.g., mucic acid), *N*-heterocyclic carboxylates (e.g., picolinic acid), and polyhydroxy aromatics (e.g., 1,2-dihyroxybenzoic acid). Selected chelates were active toward other insecticides and herbicides at pH 6 (Sun and Pignatello, 1993b), and in soils at pH ~6 (Baehr and Pignatello, 1994; Pignatello and Day, 1996). In water the chelates were able to bring about extensive mineralization of the aromatic ring of 2,4-D (Sun and Pignatello, 1992). The NTA chelate is also effective for tetrachloroethylene degradation in water (Howsawkeng et al., 2001). Polyhydroxy aromatic compounds may be active by virtue of their ability to reduce Fe(III) (section 2.4; also Rodriguez et al., 1999). Macrocyclic chelating agents have also been employed. The iron(III) porphyrin, heme, was used to catalyze the degradation of phenol and crystal violet by hydrogen peroxide in soil, but was not compared with the heme-free Fenton system (Chen et al., 1999). Likewise, iron sulfophthalocyanine, used to catalyze the degradation

of chlorinated phenols (Sorokin et al., 1995), was not compared with an inorganic control.
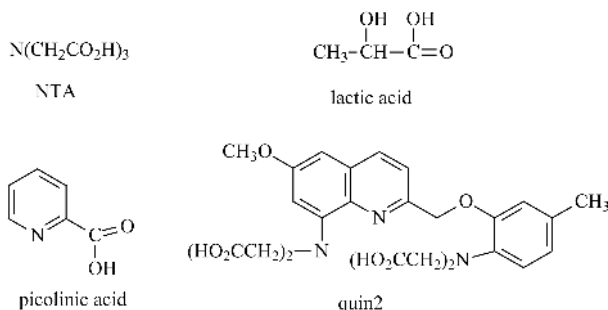
When added to Fenton systems certain chelating agents have been found to increase the EPR signal for the HO˙ spin trap adduct of DMPO (5,5′-dimethyl-1-pyrroline N-oxide) and to accelerate hydroxylation reactions. The exact causes of their effects remain speculative. Lactic acid, 2-methyllactic acid, and 3-hydroxypyruvic acid form complexes with Fe(III) (Ali and Konishi, 1998; Ali et al., 2000). Pyridine-2,6-dicarboxylic acid and the pyridine-2-carboxylates, picolinic acid, quinolinic acid, and fusaric acid, apparently form complexes with Fe(II) (Iwahashi et al., 1999). Quin2 shows a stronger affinity for Fe(II) than Fe(III) and accelerates the reduction of Fe(III) in the presence of H_2O_2 (Sandström et al., 1997).

Further efforts are needed to identify chelating agents that accelerate oxidation of the target organic yet are stable to the reaction conditions and safe to add to the wastestream.

3.3. Electro-Fenton Methods

Electro-Fenton methods broadly include electrochemical reactions that are used to generate in situ one or both of the reagents for the Fenton reaction. The reagent(s) generated depend on cell potential, solution conditions and the nature of the electrodes. Several different types of electro-Fenton reactions have been described, as summarized in Table 2.

TABLE 2. Types of Electrochemical Fenton Reactions, with the Fenton Reagent Generated Shown in boldface

Type	Anode reaction	Cathode reaction	Reagent introduced externally
1	$Fe° \rightarrow \mathbf{Fe^{2+}} + 2e^-$	$2H_2O + 2e^- \rightarrow H_2 + 2OH^-$	H_2O_2
2	$Fe° \rightarrow \mathbf{Fe^{2+}} + 2e^-$	$O_2 + 2H^+ + 2e^- \rightarrow \mathbf{H_2O_2}$	—
		$Fe^{3+} + e^- \rightarrow \mathbf{Fe^{2+}}$	
3	$2H_2O \rightarrow 4H^+ + O_2 + 2e^-$	$O_2 + 2H^+ + 2e^- \rightarrow \mathbf{H_2O_2}$	Fe^{2+}
4	$2H_2O \rightarrow 4H^+ + O_2 + 2e^-$	$Fe^{3+} + e^- \rightarrow \mathbf{Fe^{2+}}$	H_2O_2

Ferrous ions may be produced by oxidative dissolution of sacrificial anodes such as iron metal (Pratap and Lemley, 1994; Roe and Lemley, 1997; Wang and Lemley, 2001; Saltmiras and Lemley, 2001; Chou et al., 1999; Arienzo et al., 2001a, 2001a, 2001b) or titanium and iron (Huang et al., 1999):

$$Fe^0 \rightarrow Fe^{2+} + 2e^- \tag{66}$$
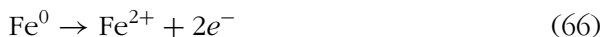
The electrodes must have sufficiently high specific surface area to achieve optimum dissolved iron concentrations (Savall, 1995).

Ferrous ion may also be produced by reduction of ferric ions at an inert cathode, such as platinum (Hsaio and Nobe, 1993; Oturan et al., 1999; Brillas, et al., 1998b; Qiang et al., 2003):

$$Fe^{3+} + e^- \rightarrow Fe^{2+} \tag{67}$$

Hydrogen peroxide may be produced by reduction of dioxygen at the cathode (Chou et al., 1999; Brillas et al., 1998b, 2000; Oturan et al., 1999; Sudoh et al., 1986; Casado et al., 2005):

$$O_2 + 2H^+ + 2e^- \rightarrow H_2O_2 \tag{68}$$
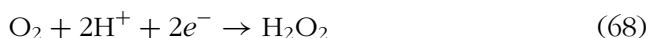
In situ generation of reagents might be an advantage in some applications over pumping the same reagents from an external reservoir using conventional technology. However, the electro-Fenton reaction faces several obstacles that must be overcome first. The production of H_2O_2 in reaction 68 is slow because oxygen has low solubility in water (Savall, 1995) and because current efficiency under acidic conditions is low (Chou et al., 1999). Porous gas dispersion electrodes appear to be a promising solution to the former problem (Shen et al., 2005). Stoichiometric electro-generated Fe^{2+} can be carried out near neutral pH (Pratap and Lemley, 1998), thus overcoming the need for acidic conditions, a fundamental disadvantage of Fenton reactions in general. However, formation of ferric oxyhydroxide sludge is still a problem here. The sludge can be electrochemically reduced to Fe^{2+}, but this requires a step in which the pH is lowered below 1 (Qiang et al., 2003; Chou et al., 1999). Gradual corrosion of electrodes can be expected in many electro-Fenton applications. H_2O_2 produced at the cathode is destroyed at the anode unless the cells are separated by an electrolyte bridge. Shen et al. (2005) studied acid red B dye degradation in such a dual-chamber cell. They achieved both anodic oxidation of the dye in the anode chamber and H_2O_2 oxidation (accelerated by addition of Fe^{2+}) in the cathode chamber.

In principle the most promising electro-Fenton mode is Type 4 (Table 2), in which ferric ion is reduced to ferrous at the cathode. However, Fe^{2+} regeneration is slow even at optimal current density, and both current density and current efficiency drop off precipitously above pH $\sim$2.5 (Figure 8). As
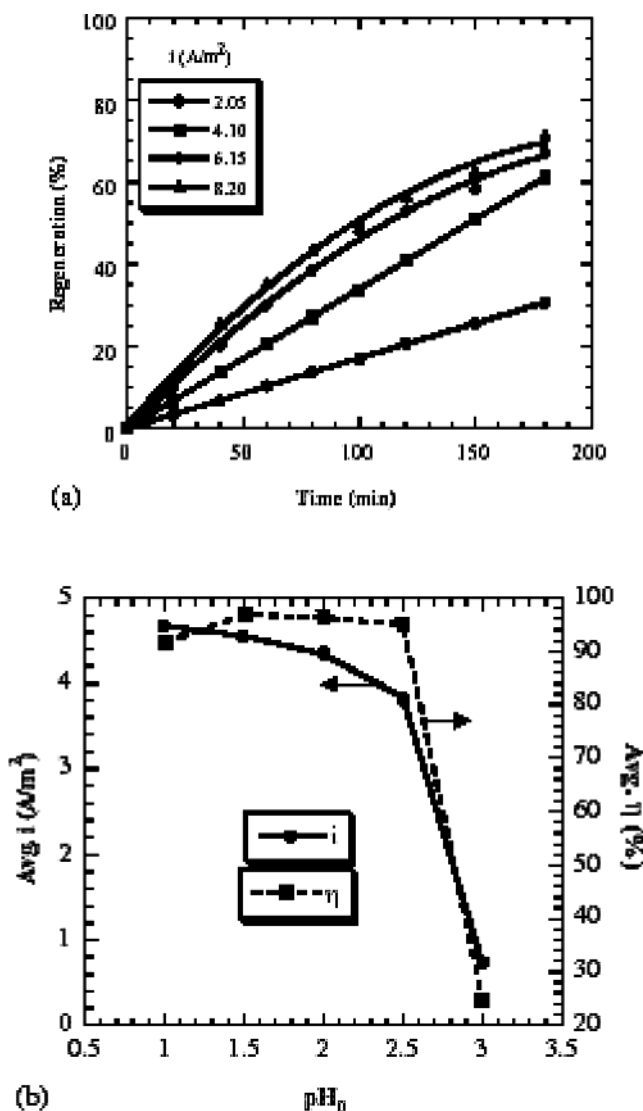
FIGURE 8. (a) Effect of current density on accumulated regeneration percentage of Fe^{2+} ($pH_0 = 2$; $[Fe^{3+}]_0 = 500$ mg/L). (b) Effect of initial pH on average current density and average current efficiency ($E_c = -0.1$ V vs. SCE; $[Fe^{3+}]_0 = 500$ mg/L; 3 h). Reprinted from Qiang et al. (2003) with permission.

an active area of research, further advances are expected in electro-Fenton reactions.

3.4. Fenton Reactions Using Iron From Solid Sources

A number of researchers have investigated the potential use of solid iron compounds or solid materials rich in iron. In such cases, oxidation may

potentially occur via iron ions released into solution or via reactions that take place between solutes and surface-bound species.

Iron powder has been used as a source of iron to oxidize azo dyes and phenolic compounds by H_2O_2. At pH below 2.5, dye removal occurred mainly by adsorption; whereas, at higher pH where adsorption was less important, addition of H_2O_2 doubled (at pH 3) or quintupled (at pH 3.5) dye removal to >90% of initial concentration (Tang and Chen, 1996). Iron powder and iron-impregnated activated carbon were shown to catalyze oxidation of 4-chlorophenol by homogeneous reactions (Lucking et al., 1998). At an application rate of 1 g/L, iron powder achieved stoichiometric production of Cl^- and 50% DOC removal after 2 h using 5.3 g/L H_2O_2. These results were more favorable than the Fenton reaction (1 mg/L Fe^{2+}, added as $FeSO_4$), which gave only 40% Cl^- production and 5% DOC removal after 150 h. Takemura et al. (1994) investigated steel wool, steel foil, and recticulated iron (manufactured by impregnating urethane foam with an iron powder slurry, then sintering) in the presence of hydrogen peroxide to oxidize perchloroethylene (PCE). All solids reduced the PCE concentration from 100 mg/L to less than 0.1 mg/L in 24 h, but the reaction with recticulated iron could be conducted at pH 5–9 with no apparent iron oxide by-product.

Waite and coworkers have observed surrepetitious oxidation of some compounds in aqueous solution when mixed with nanoscale zero-valent iron particles in the presence of air and no added H_2O_2 (Joo et al., 2005). Evidently, H_2O_2 and Fe^{2+} are generated by dioxygen corrosion of the metal and released into solution, or react on the surface, it's hard to say. This represents a novel use of zero-valent iron—normally a reducing agent—for oxidation reactions that has potential application for soil treatment.

Several researchers have used iron minerals in combination with H_2O_2 to study the natural attenuation of organic compounds in the environment, or to serve as an alternative Fenton-type treatment (reviewed by Tarr, 2003). Although oxidation is generally much slower than the corresponding solution reactions at the same mole per liter reagent concentrations, the heterogeneous reactions are sometimes more efficient; that is, they consume less peroxide per mole contaminant degraded. Oxidation at the surface is often speculated but there is little compelling evidence and further study is clearly warranted.

Petroleum contaminated soil (200–1000 mg/kg diesel fuel) was treated with a mixture of silica sand and goethite or magnetite in water at pH 2–3 (Kong et al., 1998). For magnetite the rate of hydrocarbon removal slowed over time despite the high (up to 8 mg/L) dissolved iron, suggesting heterogeneous reactions. The authors hypothesized that precipitation of ferric oxide on the magnetite surface slowed surface electron transfer. Lu (2000) found that the rate of 2-chlorophenol oxidation increased with decreasing size of goethite particles due to release of Fe^{2+} into solution, suggesting that homogeneous reactions were more important. It is not clear whether

heterogeneous reactions played a role in the H_2O_2 oxidation of 2,4,6-trinitrotoluene by pyrite (Arienzo, 1999). Li et al. (1999) showed that basic oxygen furnace waste slag (BOF) could decolorize naphthol blue black (acid black 1, a diazo acid dye) at pH 2.8. BOF is a porous waste product of steel manufacture that contains appreciable FeO and Fe_2O_3.

3.5. Fenton Reactions Using Designed Heterogeneous Catalysts

Investigators have explored the use of iron ions immobilized on a solid support as a strategy to avoid sludge formation and to expand the effective pH range of the Fenton reaction. Some success in this regard has been achieved, notably with iron-exchanged Nafion membranes and iron-modified clays. The advantage of a suitable heterogeneous catalyst is its separability from the waste stream. Unless the catalyst is designed to provide a steady-state source of iron in solution for the homogeneous reaction, a fundamental disadvantage is that dissolved target molecules must diffuse to the surface to reach active oxidant sites before they decay (for example, adsorbed hydroxyl radicals may self-annihilate).

Nafion is a perfluorinated oxyalkyl polymer with sulfonate groups capable of binding cations.

$$[(-CF_2CF_2-)_x-CF-]_y \quad (OCF_2CF)_z-OCF_2CF_2-\underset{\underset{O}{\|}}{\overset{\overset{O}{\|}}{S}}-OH$$
$$CF_3$$
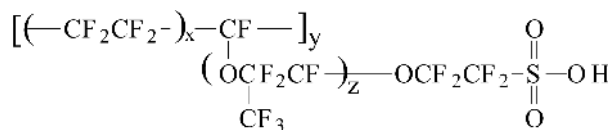
Nafion in protonated form

Ferric-exchanged Nafion membrane is claimed to be an effective photo-Fenton catalyst (Kiwi et al., 2002; Fernandez et al., 1999; Dhananjeyan et al., 2001; Sabhi and Kiwi, 2001). Activity under simulated solar irradiation correlates with the presence of Fe(III) species such as

$$Fe(H_2O)_6{}^{+3}, \quad [(H_2O)_5Fe \overset{\overset{H \diagdown O \diagup H}{}}{\underset{\underset{H}{O}}{}} Fe(H_2O)_5]^{5}, \quad [(H_2O)Fe\text{-}O-Fe(H_2O)_5]^{+4}$$
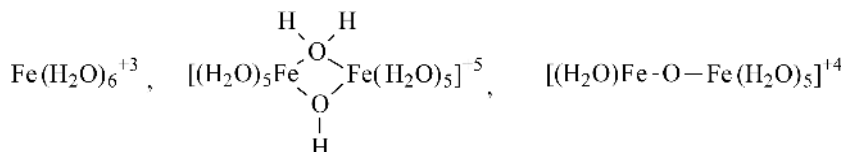
electrostatically associated with sulfonate groups. Iron oxide crystalites on the surface are much less active. Fe-Nafion membranes appear to be effective up to at least pH 5.4. Although it was possible to achieve mineralization of 2,4-dichlorophenol at higher initial pH (up to 11), the pH (unbuffered) always drifted quickly to a value below 5 (Sabhi and Kiwi, 2001). Orange II
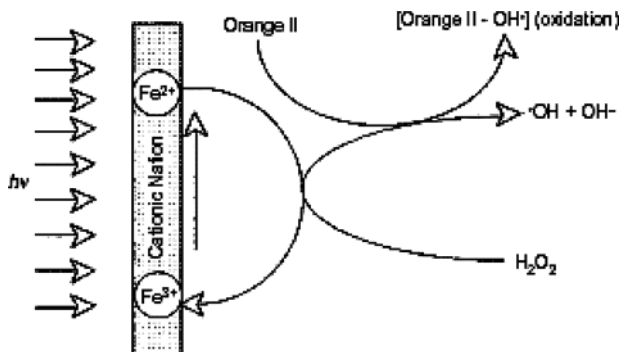
FIGURE 9. Proposed mechanism for Fe^{3+}-catalyzed photo-Fenton degradation of organic compounds in water using an Fe^{3+}-exchanged Nafion membrane. From Fernandez et al. (1999) with permission.

decoloration was effective in the initial pH range 2.8 to 4.8, but was much slower at pH 6.5 and 7.5 (Fernandez et al., 1999).

The detailed mechanism concerning the role of surface reactions and of adsorption/desorption of iron ions and reactants in Fe–Nafion systems is unclear at this time. Fernandez et al. (1999) proposed that Nafion-bound Fe(III) is photoreduced to Fe(II), which subsequently undergoes the Fenton reaction (Figure 9). Whether H_2O_2 reacts with surface-bound or desorbed Fe(II) species is uncertain. Dissolved methanol inhibited orange II decoloration, which suggests that HO$\cdot$ is generated in solution, or at least desorbs before it reacts. If H_2O_2 reacts in solution then the Fe(III) product must re-adsorb faster than it precipitates, since membranes retain activity over several cycles without sludge production (Sabhi and Kiwi, 2001; Dhananjeyan et al., 2001). The question of the involvement of dissolved Fe(III) species in these systems is appropriate, yet still unanswered.

Another innovative approach is the use of Fe-exchanged Al-pillored beidellite (a 2:1 dioctahedral smectite clay) (Catrinescu et al., 2003). The exact form of iron in the catalyst is unknown. The interlayer spacing was 1.7 nm. Phenol was mineralized to a considerable degree within 3 h at initial pH values from 2.5 to 5.0. The authors note that as the reaction proceeds the pH drops (to unspecified values) and the rate accelerates. Catalyst activity appears to decline with use (Figure 10). Less than 18 μM Fe was found in solution at 1 g L^{-1} catalyst (which contains 1.8% Fe), suggesting homogeneous reactions contributed negligibly to phenol removal.

Feng et al. (2003) obtained encouraging results in irradiated solutions of Orange II dye and H_2O_2 using a nanocomposite material composed of crystalites of Fe_2O_3 (maghemite) and laponite RD clay ($Fe_2Si_4O_{10}$) at pH 3. Although the catalyst bleeds iron into solution (up to 3 mg L^{-1} during the run), the rates were faster than in homogeneous reactions containing 3 mg L^{-1} ferric ion, and catalyst efficiency did not decline much in repreated runs.
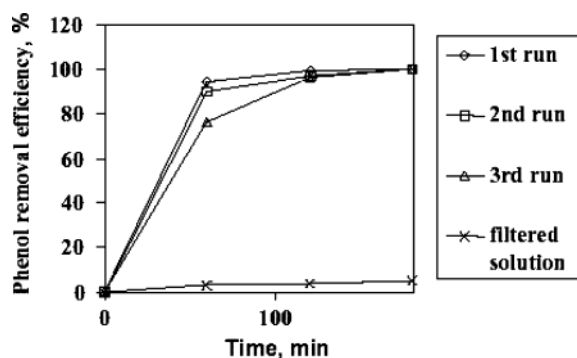
FIGURE 10. Conversion of phenol in successive runs by Fe-exchanged Al-pillored beidellite and by the filtered solution: 50°C, 250 mg L^{-1} phenol, 37 mM H_2O_2, 0.5 g L^{-1} catalyst, initial pH 3.5. From Catrinescu et al. (2003) with permission.

The performance of an Fe^{3+}-exchanged zeolite Y as a heterogeneous photo-Fenton catalyst was tested on degradation of polyvinyl alcohol (Bossmann et al., 2001b) and xylidines (dimethyl anilines, Rios-Enriquez et al., 2004). Although some leaching of Fe^{3+} was observed, it amounted to only 2.2% percent of the total iron(III) present in the zeolite, less than 3.3×10^{-5} M in solution, and was thought not to play an important role in the reaction.

Bossmann et al. (2002) employed a novel zeolite Y photo-Fenton catalyst encapsulating $Fe(bpy)_3^{2+}$ [bpy = 2,2′-bipyridine] and containing TiO_2 nanoparticles deposited inside ($\sim$72%) and outside ($\sim$28%) the zeolite Y support. These TiO_2 nanoparticles interconnect individual $Fe(bpy)_3^{2+}$ complexes, located within the supercages of zeolite Y. Activity was observed only for the combined $Fe(bpy)_3^{2+}/TiO_2$/zeolite Y when tested for 2,4-xylidine degradation.

4. KINETICS AND PROCESS MODELING

4.1. Mechanistic Kinetic Modeling

The kinetics of Fenton reactions can be quite complex because of the large number of steps involved. The general elementary rate law for reaction of the target organic compound (RH) can be written as:

$$-\frac{d[\text{RH}]}{dt} = k_{\text{HO}}[\text{HO}^{\bullet}][\text{RH}] + \sum_i k_{\text{ox}_i}[\text{ox}_i][\text{RH}] \tag{69}$$

where ox_i represents oxidants other than $\text{HO}^{\bullet}$ that may be present, such as ferryl (section 2.9). Equation (69) based on the assumption—valid in most cases—that photolysis of RH and reactions of RH with organoradicals, such

as R·, RO·, and ROO·, are comparatively unimportant. Hydroxyl radical is usually regarded as the sole or most important reactive species. Values of k_{HO} are available for many organic compounds. But the identities of possible alternative oxidants such as ferryl are not well established (section 2.6.1.), much less their rate constants with specific compounds. Hydroxyl is produced in thermal and photochemical reactions and destroyed by reaction with target pollutant, pollutant by-products, and scavengers. Thus, [HO·] can change during the course of the reaction as reagent and organic concentrations change. Obviously, HO· cannot be monitored conveniently. Simple reaction-rate expressions can be employed under certain limiting conditions; otherwise, the kinetics must be solved numerically using multistep computational models (Chen and Pignatello, 1997; Gallard et al., 1998; Gallard and De Laat, 2000; Duesterberg et al., 2005). The use of multistep models can provide valuable information on reaction mechanism, as illustrated next.

Gallard et al. (1998) followed the kinetics of atrazine or 1,2,4-trichlorobenzene loss in the Fe(II) Fenton reaction (i.e., with Fe(III)-catalyzed reactions suppressed). At pH <3, multistep modeling of the rate profiles was consistent with the free radical chain mechanism in reactions 1–7 and 10 (section 2.1). However, above pH 4 the model overestimated the rate, suggesting formation of an Fe(II)-peroxide complex of unknown structure (possibly ferryl) that either decomposes to HO· or oxidizes another Fe(II) species.

Gallard and De Laat (2000) also studied the decomposition of atrazine under Fe(III)-catalyzed conditions and conditions in which secondary reactions and scavenging by byproducts were suppressed. Again, the kinetics were consistent with the radical chain mechanism. At pH ≤3, the rate of atrazine depletion, beyond a short induction period of several minutes for HO· to reach steady-state concentration, was first-order each in atrazine and Fe(III) [eq. (70)].

$$-\frac{d[\text{Atr}]}{dt} = k_{\text{obs}}[\text{Fe(III)}][\text{Atr}] \tag{70}$$

The dependence of the rate on [H_2O_2] and pH is more complicated. The effect of [H_2O_2] could be divided into three regions (Figure 11). (1) From 0 to 10 mM H_2O_2 the reaction was first-order in H_2O_2, reflecting reaction 2 as the rate-limiting step. (2) From ~10 mM to ~50 mM H_2O_2 the reaction was zero-order in H_2O_2 because most hydroxyl radicals were consumed by H_2O_2 in reaction 3. (3) Above ~50 mM H_2O_2, the rate was inhibited by hydrogen peroxide due to the buildup of Fe(III)–peroxo complexes, such as those in reactions 17–18 (section 2.3.2), which do not participate in propagation reactions.

The influence of pH on k_{obs}, shown in Figure 12 reflects, (1) the difference in reactivity between protonated atrazine ($k_{HO} = 1.6 \times 10^9\,M^{-1}\,\text{s}^{-1}$) and neutral atrazine ($k_{HO} = 2.9 \times 10^9\,\text{M}^{-1}\,\text{s}^{-1}$) (atrazine has a p$K_a$ of 1.6); and

FIGURE 11. Influence of initial [H_2O_2] on the observed rate constant for reaction of atrazine (k_{obs}) and H_2O_2 (k'_{obs}) in the thermal Fenton reaction at pH 3. From Gallard and De Laat (2000) with permission.

(2) the inverse dependence on [H^+] of the stability constant for the Fe(III)–peroxo complex [eqs. (17)–(18), section 2.3.2], whose decomposition is the source of Fe(II) for the Fenton reaction. The latter effect applies to all target chemicals.

In many studies, complex multistep mechanistic rate laws are avoided and instead the optimum conditions for removal of a particular organic

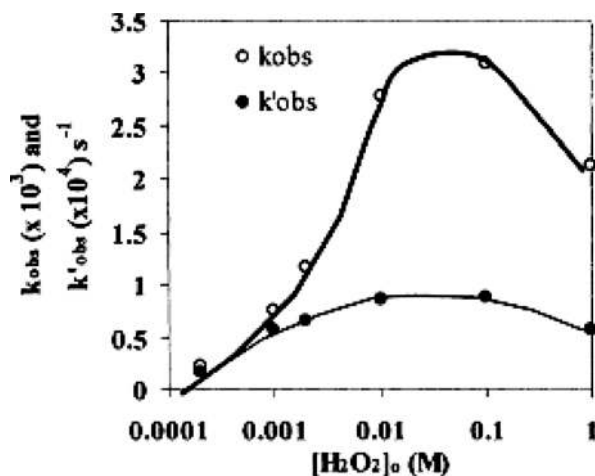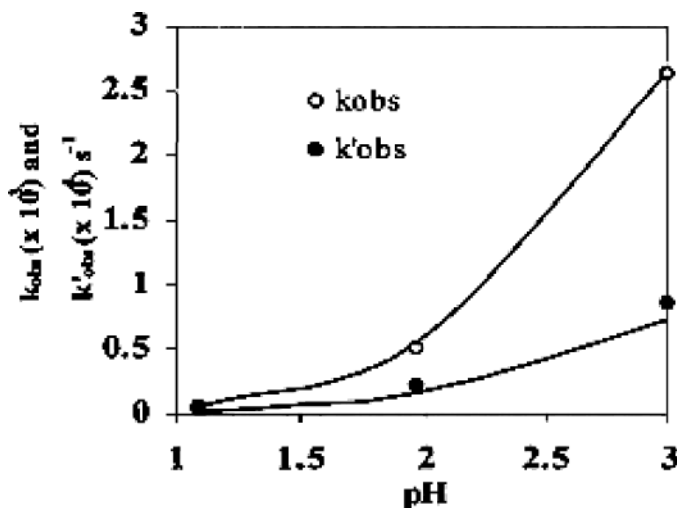**FIGURE 12.** Influence of pH on the observed rate constant for reaction of atrazine (k_{obs}) and H_2O_2 (k'_{obs}) in the thermal Fenton reaction. Curves represent simulation by a kinetic model. From Gallard and De Laat (2000) with permission.

J. J. Pignatello et al.
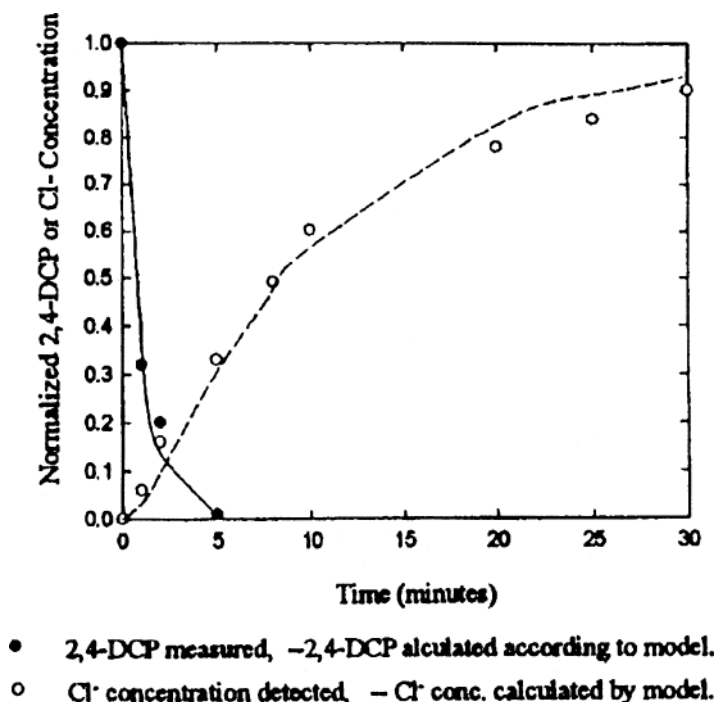
FIGURE 13. Oxidation of 2,4-dichorophenol (2,4-DCP) under classic Fenton conditions. Kinetic modeling of 2,4-DCP removal and Cl^- production gave first order rate constants of 0.995 min^{-1} and 0.092 min^{-1}, respectively. Experimental conditions: 2,4-DCP = 5×10^{-4} M, H_2O_2 = 5×10^{-3} M, $Fe(ClO_4)_2 = 2 \times 10^{-4}$ M, pH 3.5, ionic strength 0.05 M as Na_2SO_4. Figure from Tang and Huang (1996) with permission from Selper, Ltd.

compound are determined by varying pH, iron and hydrogen peroxide concentrations and reporting the conditions under which the highest rate constant, or the greatest compound removal, within a specified time period was observed. In one notable example (Figure 13), Tang and Huang (1996) developed a kinetic model to predict the optimal ratio of $[H_2O_2]$ to $[Fe^{2+}]$ for Fenton oxidations. The optimal $[H_2O_2]/[Fe^{2+}]$ ratio for 2,4-dichlorophenol degradation matched the theoretical prediction of 11 (Tang and Huang 1996). Optimal $[H_2O_2]/[Fe^{2+}]$ ratios for chlorinated ethenes ranged from 5 to 11 (Tang and Huang, 1997); these authors also reported iso-contour plots of the percent chlorinated ethene transformed as a function of initial H_2O_2 concentration and initial compound concentration. Lemley and coworkers developed a kinetic model to calculate organic compound removal and optimal reagent concentrations for anodic Fenton treatment (Saltmiras and Lemley, 2001; Wang and Lemley, 2001).

In photo-Fenton reactions the rate obviously depends strongly on the properties of the lamp and reactor.

4.2. Empirical Kinetic Modeling

Oxidation by Fenton reagents, particularly under irradiation, involves complex mechanisms in which rate constants for individual steps are not easy to determine. This poses a challenge for the design and scale-up of photochemical reactors to be used in an industrial setting, where cost and material limitations demand that optimal operating conditions be reached through minimal experimentation. Accordingly, some researchers have turned to empirical modeling based on *experimental design methodology* (EDM) (Box et al., 1978; Khuri and Cornell, 1987; Cochran and Cox, 1992; Droesbeke et al., 1997) and *artificial neural networks* (ANN; e.g., Rumelhart et al., 1986; Zupan and Gasteiger, 1993). Such approaches may be particularly useful when the mechanism is not well understood. It should be noted that empirical modeling rarely gives information on mechanism.

4.2.1. EXPERIMENTAL DESIGN AND RESPONSE SURFACE METHODOLOGIES

EDM is based on multivariate methods whereby the values of the independent variables (*e.g.*, processing conditions) are modified in a systematic manner. EDM provides the means of building a *statistically significant model* of a phenomenon by performing a *minimum set of experiments* adequately distributed in the *experimental region*. A large number of experimental designs (matrices) adapted to various types of problems are available—complete and fractional factorial designs, central composite matrices, and Doehlert uniform arrays, to cite only a few. In these designs, the *experimental response of interest* (dependent variable y; e.g., degradation rates, pollutant and/or TOC contents at a given irradiation time, apparent rate constants, CO_2 evolution, etc.) is usually represented as a function of the normalized independent variables x_i (e.g., concentrations of hydrogen peroxide and iron salt, temperature, etc.), using a polynomial model [$y = f(x_i)$]. The least-square estimates of the coefficients of the model are calculated by multilinear regression of the values of the response y for the series of experiments included in the chosen experimental matrix. The resulting model for each given response allows the drawing of contour plots (lines or curves of constant response value), and once the validity of the model has been tested, the value of the response at any point in the experimental region of interest may be predicted (*response surface methodology*; Khuri and Cornell, 1987).

Experimental design methodology has recently been applied by a few authors to wastewater treatment by the Fenton reaction. Oliveros and coworkers used Doehlert uniform arrays to investigate the photo-Fenton removal of xylidines (methyl anilines) and TOC in wastewater both at the laboratory (Oliveros et al., 2000) and pilot scales (Oliveros et al., 1997a, 1997b; see section 5.1.6 for experiments at the pilot scale). In the laboratory study, the effects of the temperature and reagent concentrations (Fe(II) or Fe(III) salt, H_2O_2) on the degradation of 2,4-xylidine by the photo-Fenton

reaction were studied. Experimental data were obtained by performing the series of designed experiments of a Doehlert uniform array for 3 variables (13 experiments). The analysis was carried out using the pseudo-first-order apparent rate constant of 2,4-xylidine disappearance ($y = k_{ap}$) to represent the degradation efficiency. As an example, contour plots representing the variations of k_{ap} as a function of the temperature and the initial concentration of iron(III) ([iron(III)]) are shown in Figure 14 for various initial hydrogen peroxide concentrations ([HP]). In the ranges investigated, k_{ap} increases with

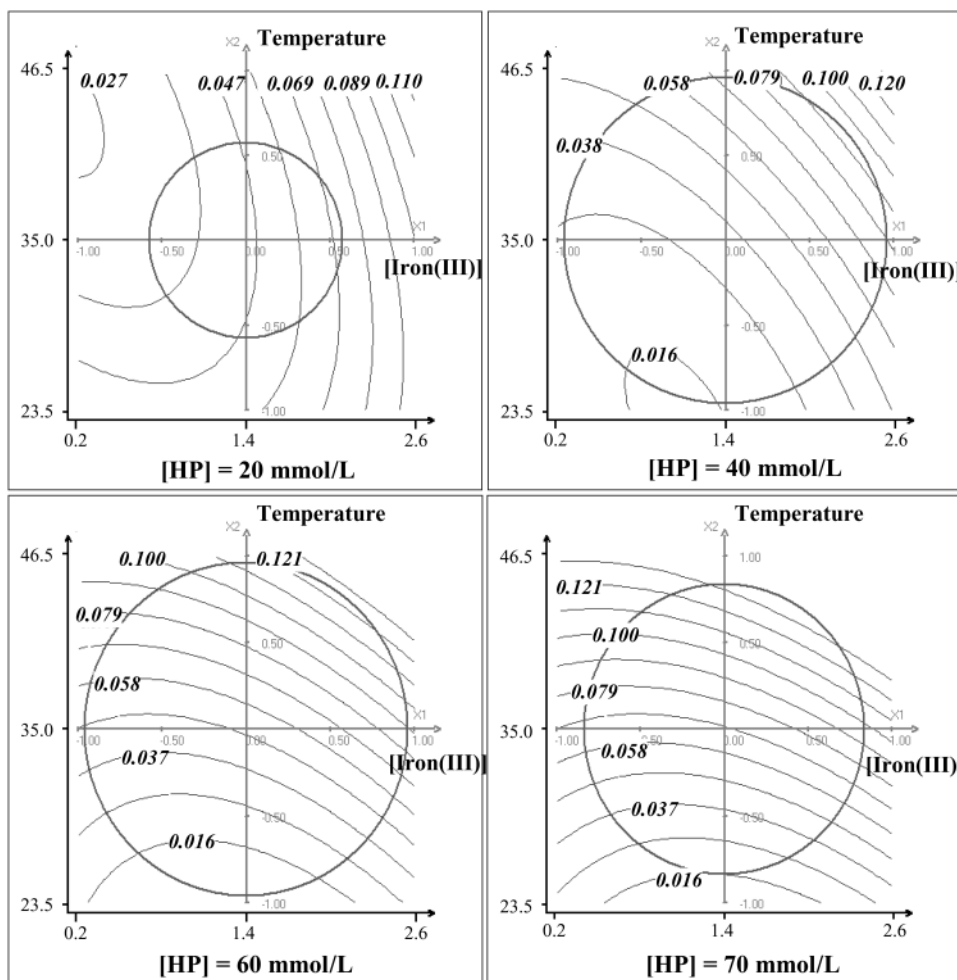**FIGURE 14.** Contour plots for the apparent rate constant of 2,4-xylidine disappearance (k_{ap}, min^{-1}, values in italics) as a function of the [iron(III)] (0.2 to 2.6 mmol L^{-1}) and the temperature (23.5 to 46.5°C), for various concentrations of hydrogen peroxide (HP) (Doehlert matrix for three variables; the circles represent the limit of the experimental domain). From Oliveros et al. (2000) with permission.

increasing [iron(III)] and temperature, independently of [HP], but the increase of k_{ap} reaches a plateau above a certain concentration of [HP]. These observations are the basis for chosing the optimal operating conditions. In this case, mechanistic conclusions could also be drawn: For the lowest [HP] used (20 mmol/L), the rate-limiting step is the photochemical reduction of iron(III) to iron(II) (k_{ap} sensitive to the concentration of iron(III) but hardly affected by temperature), whereas at relative high [H_2O_2] (60–70 mmol/L), the thermal reactions control predominantly the degradation rate (k_{ap} mostly dependent on the temperature, Figure 14).

Büyüksönmez et al. (1999) investigated the simultaneous optimization of chemical and biological mineralization of perchloroethylene (PCE) by a modified Fenton's reagent in the presence of microorganisms. The authors used a central composite design of four variables (concentrations of PCE, H_2O_2, Fe^{2+}, and cells). Response surface contour plots for PCE mineralization showed that PCE concentration had no significant effect on the mineralization extent within the tested limits of the experimental region, and that simultaneous chemical and biological reactions increased the extent of mineralization.

Kiwi and coworkers published several reports on the treatment of textile waste waters by the Fenton and the photo-assisted Fenton reactions (Balanosky et al., 1998a, 1998b, 1999, 2000; Herrera et al., 2000). The authors also employed a Nafion–Fe^{3+} membrane as an immobilized Fenton reagent (Balanosky et al., 1999). Statistical modeling of reactor performance for the degradation of model pollutants (naphthalene 1,5-disulfonate, *p*-nitrotoluenesulfonate, reactive dye Uniblue A, and others) and textile waste waters from nanofiltration of biologically treated secondary textile industry effluents was performed. Although the authors did not make use of planned experimental designs, they constructed single exponential functions of the response of interest (*Z*, e.g., TOC) in order to fit the observed degradation data, as a function of the independent variables (e.g., concentrations of reagents and pollutant, recirculation flow, residence time, power of the light source). The function *Z* was used for optimization purposes through contour plots and two and three-dimensional response surfaces.

4.2.2. ARTIFICIAL NEURAL NETWORKS

An alternative to polynomial models is ANN. ANNs have attracted great interest over the last decade as predictive models, as well as for pattern recognition (see, e.g., Rumelhart et al., 1986; Zupan and Gasteiger, 1993). The potential for fruitfully employing ANNs in data treatment is especially high in the case of systems presenting nonlinearities and complex behavior. Indeed, ANNs possess the ability to "learn" from a set of processing conditions (input variables, x_j) and corresponding experimental responses (output variables, y_k), without actual knowledge of the physical and chemical laws that govern the system (supervised learning). A series of input–output pairs of

experimental data (*X*, *Y*) are used for training the network (*learning set*). Schematically, input variables are converted into output variables through a series of mathematical operations (weighted sums, transfer function) taking place in the processing units (called neurons). The weights are modified by an iterative technique (back-propagation algorithm) in order to minimize the quadratic deviation between the calculated and the experimental values of the response variable(s). Once a network of given characteristics (e.g., number of neurons, weight values) is validated, it may be used for simulations and optimizations. Response surfaces and contour plots may be drawn as in the case of polynomial models (section 4.2.1). ANNs have been proven useful in simulating and optimizing complex photochemical systems (Braun et al., 1993; Nascimento et al., 1994; Oliveros et al., 1998; Goeb et al., 1999).

Teixeira et al. (2003, 2004) applied neural network modeling to the photo-Fenton treatment of aqueous emulsions containing an aminosilicone polymer in a bench-scale photochemical reactor and in a solar reactor. The modeling was useful in adapting concentrations of additives (iron salt and H_2O_2) to operation during cloudy days.

Oliveros and coworkers have used an approach combining experimental design and ANNs for the investigation of 2,4-xylidine degradation by the photo-Fenton reaction (Goeb et al., 1999, 2001; Oliveros et al., 2000). Experimental data used for training the ANN were obtained by performing the series of designed experiments of two- and three-dimensional Doehlert matrices (independent variables: amounts of H_2O_2 and Fe(II) or Fe(III) salt, and temperature, section 4.2.1). In the case of ANN modeling, no global parameter for pollutant degradation (e.g., k_{ap}) is necessary: the output variable *y* was the xylidine concentration analysed at different reaction times ($y =$ $[Xyl]_t$) and the irradiation time (*t*) was an additional input variable. Response surfaces of the pollutant oxidation rates showed that the normalized effects of temperature and iron salt concentration on the 2,4-xylidine degradation rate were similar, but that the process efficiency was much more sensitive to iron salt concentration than to H_2O_2 concentration, which is advantagous in terms of economic feasibility. Moreover, under otherwise similar conditions, degradation was faster when the reaction was started with iron(II) than with iron(III), as already observed for the oxidation of other organic compounds by the Fenton reaction (section 2.1).

5. APPLICATIONS OF THE FENTON REACTION

5.1. Water Treatability Studies

Fenton and modified Fenton processes have few documented industrial applications. (The three most frequently applied non-Fenton AOPs are O_3/H_2O_2, H_2O_2/UV, and O_3/UV.) Limitations of Fenton-based AOPs for wastewater treatment stem mainly from the need for pH control and the

problem of sludge generation. Most case studies and assessments of compound transformation and mineralization rates of actual, or simulated, industrial waste streams are bench-scale treatability studies for determining optimum doses of reagents.

5.1.1. DYE WASTES

Waste streams from dye manufacture and dyeing operations are strongly colored and contain high concentrations of salts and organic matter. Kuo (1992) demonstrated that process waste streams from dyeing operations could be treated with $FeSO_4$ and H_2O_2 at pH 3. After a 5-h reaction time, 99% decolorization was achieved, with up to 83% removal of COD (chemical oxygen demand). Kang and Chang (1997) attempted to optimize reagent doses for treating a simulated waste stream containing polyvinyl alcohol (PVA, 90% COD) and R94H dyestuff (10% COD). Using the optimized reagent concentrations of 200 mg/L Fe^{2+} and 200 mg/L H_2O_2 with actual textile effluent, 96% color removal but only 79% COD removal, was obtained. The thermal Fenton reaction was also shown to meet the regulatory discharge limit of 200 mg/L COD for a simulated waste stream containing direct and reactive dyes and 0.2% PVA (Lin and Lo, 1997). Direct, reactive and acid dyes were removed by treatment of a waste with H_2O_2 and iron powder (Tang and Chen, 1996); however, the primary removal mechanism at low pH was dye adsorption to the iron solids. At pH above 3, dye removal increased from 16–40% to greater than 91% with addition of H_2O_2 and iron powder. Fenton treatment increased the biodegradability of waste streams from the manufacture of dye intermediates (Wanpeng et al., 1996; Yu et al., 1998).

5.1.2. PULP BLEACHING WASTES

The effluent quality of pulp bleaching wastes is normally based on tests for toxicity, color and adsorbable organo-halogen compounds (AOX). The addition of ferrous iron and H_2O_2 (concentrations not reported) to bleaching effluent from *Eucalyptus globulus* pulp reduced AOX by 60% and MICROTOX toxicity by 75% (Rodriguez et al., 1999). The addition of catechols to the effluent increased the fraction of AOX removed in the order: 2,3-dihydroxybenzoic acid $\gg$ 3,4-dihydroxybenzoic acid $\approx$ catechol $\approx$ iron only. Only 2,3-dihydroxylbenzoic acid gave improved toxicity removal over iron and hydrogen peroxide alone. Catechols have been shown to enhance the degradation of organic compounds in the presence of ferric ions and hydrogen peroxide by reducing Fe(III) to Fe(II) (Chen and Pignatello, 1997; Iwahashi et al., 1989). Furthermore, the quinone oxidation products of catechols and hydroquinones also assist degradation by acting as electron shuttles in the Fenton reaction (sections 2.4 and 2.5). Degradation of pulp mill effluents with iron and hydrogen peroxide in the presence of catechols is said to mimic the mechanism by which brown rot fungi degrade cellulose and lignin in wood tissue (Goodell et al., 1997; Paszczynski et al., 1999). Perez

et al. (2002) concluded that Fenton and photo-Fenton reactions were highly effective for the treatment of paper pulp effluents.

5.1.3. AGRICULTURAL EFFLUENTS

Wine distilleries and black olive production plants generate wastes containing phenolic acids and aldehydes. These waste streams are treated conventionally using biological processes; however, the success of these treatments is frequently hampered by the toxicity or inhibitory nature of phenolic compounds. The efficacy of Fenton oxidation for treating agricultural effluents was demonstrated using model compounds (Benitez et al., 2000b; DeHeredia et al., 2001). Bimolecular rate constants for reaction of phenolic acids with hydroxyl radical were found to be in the range $(0.7 = 3.8) \times 10^9 \ M^{-1} \, s^{-1}$.

5.1.4. LANDFILL LEACHATES

Landfill leachate contains degradation-resistant high-molecular-weight organic compounds, as well as high concentrations of inorganic salts. Fenton oxidation has been coupled with conventional physicochemical and biological treatment to reduce BOD (biological oxygen demand) and COD of landfill leachate. Classical Fenton treatment following activated sludge treatment of leachate increased COD removal by about 20% over coagulation (Kang and Hwangm, 2000). Fenton treatment following nitrification and denitrification reduced COD by greater than 60% (Bae et al., 1997). Fenton pre-treatment increased the biodegradability (BOD/COD ratio) of leachates with high ammonia concentration (Kim and Huh, 1997; Kochany and Lugowski, 1998); this was attributed to reduction of inhibitory compounds, such as benzothiozols (Kochany and Lugowski, 1998).

5.1.5. SURFACTANTS

Batch studies have been used to assess oxidation of surfactants by the thermal Fenton reaction. Oxidation of linear alkylbenzene sulfonates (10 mg/L) followed first-order reaction kinetics under optimal conditions of 90 mg/L $FeSO_4$, 60 mg/L H_2O_2 and pH 3 (Lin et al., 1999). Over 95% compound removal was attained in 50 min. The products of Fenton oxidation of polyethoxy sulfate surfactants contained hydroxyl and epoxy groups resulting from random $HO^{\cdot}$ attack on the alkyl chain (Cuzzola et al., 2000). Ether-soluble ethoxylated compounds were formed by loss of the sulfonate group. The oxidation process also yielded volatile aliphatic aldehydes with carbon numbers between 8 and 14.

5.1.6. INDUSTRIAL WASTEWATER

Photographic developer wastes contain aminophenols and characteristically have low BOD/COD ratios. Metol (*N*-methyl-*p*-aminophenol) was studied as a model compound by Lunar et al. (2000a). Under optimal conditions of

0.9 mM Fe^{2+} and 0.2 M H$_2$O$_2$ and pH 3–5, the initial COD of 5 mM was reduced by 50% in 2 h. Additional COD removal was very slow (<20% in 5 days) unless the solution was illuminated. By-products were identified as partially oxidized aromatic species, dimers and polymers (Lunar et al., 2000b). Actual photo-processing wastewater was treated using sulfate-reducing bacteria, followed by activated carbon adsorption and Fenton oxidation (Lin et al., 1998a). No net change in BOD or COD removal was observed with the addition of a Fenton oxidation step in this case.

Oliveros et al. (1997) reported the successful treatment of an industrial wastewater highly contaminated with xylidines (initial TOC of 2900 mg L^{-1}) on a large pilot scale (500 L). Xylidines (dimethyl anilines) are toxic intermediates in the synthesis of pharmaceuticals, dyes, and pigments that are difficult to eliminate from wastewaters by conventional techniques (e.g., activated carbon adsorption). An initial pH between 2 and 3 yielded optimal results. The thermal Fenton reaction was almost as efficient as the photoassisted reaction. However, the thermal reaction led to a plateau in the TOC removal not observed under UV-visible irradiation, presumably due to buildup of organic acids that can be photodecarboxylated (section 3.1). Modeling and optimization of reagents for xylidine and DOC disappearance were carried out under field conditions, using the experimental design methodology (see section 4.2). Under the optimal conditions, xylidine was eliminated in 30 min and more than 90% of the initial DOC was removed after 2 h of irradiation. Biological tests showed that as soon as xylidine was completely transformed the dissolved organic matter remaining was biodegradable and not toxic toward the sludge of the communal biological treatment station. Approximately 20 m^3 of wastewater per day (in batches of 0.5 m^3) could be treated with a 10-kW medium pressure mercury arc. About 4 moles of H$_2$O$_2$ and 0.4 mole of Fe^{2+} were used per mole of xylidine degraded. The temperature of the wastewater increased from 10°C to about 70°C during treatment. No cooling system was necessary.

Gernjak et al. (2002) investigated the degradation of biorecalcitrant model phenolic compounds found in high concentrations in agro-industrial wastewaters by the photo-Fenton reaction. Vanillin, protocatechuic acid, syringic acid, *p*-coumaric acid, gallic acid, and L-tyrosine could be completely mineralized under artificial light in laboratory experiments and under sunlight in pilot-plant experiments at the Plataforma Solar de Almeria (Spain).

Enhanced reductions in dissolved organic compound concentrations could be achieved with minor modifications by addition of Fenton reagents to industrial wastewater treatment processes that currently include coagulation and flocculation steps.

5.2.7. WATER TREATMENT

The thermal Fenton reaction was investigated as a method to remove priority pollutants from surface-water sources. The fractions of phenol and polycyclic

aromatic compounds removed from water containing Suwanee River fulvic acid (NOM) were greater than expected based on a model assuming that the fraction of compound bound to fulvic acid is unreactive (Lindsey and Tarr, 2000ab). In addition, Fenton oxidation has been assessed as a method for removing trihalomethane by-products of drinking water chlorination (Tang and Tassos, 1997). The pseudo-first-order reaction rate constant decreased in the expected order with increasing chlorine substitution for bromine: bromoform > dibromochloromethane > dichlorobromomethane. Chloroform did not react within a contact time of 2 min.

Fenton oxidation is also effective for removing trace levels of inorganic contaminants from water sources. Krishna et al. (2001) lowered arsenic levels in municipal water and groundwater to below the U.S. Environmental Protection Agency (EPA) guideline of 10 μg/L with a combination of Fenton oxidation and zero valent iron. Ferrous ammonium sulfate (100 mg/L) and hydrogen peroxide (100 μl of 30% solution/L) were added to waters containing 2 mg/L of arsenic(III). Fenton oxidation was allowed to proceed for 10 min and the water was then passed over zero valent iron to remove the product arsenic(V). Arsenic removal was also achieved by Fenton oxidation using electrochemical methods to generate Fe^{2+} in the presence of H_2O_2 (Arienzo et al., 2001a). Arsenic concentrations were decreased by adsorption of arsenic(V) to hydrous ferric oxide. The concentrations of other trace metals in the water were similarly reduced by adsorption.

5.1.9. TREATMENT OF GAS STREAMS

Membrane applications of Fenton oxidation may have potential for treatment of gas streams containing volatile organic compounds. Fenton oxidation is used industrially to produce low-molecular-weight oxygenates from propane by such a process (Espro et al., 2000). A Nafion membrane separates the gas phase from a liquid phase containing ferrous iron and hydrogen peroxide. Propane diffuses across the membrane and undergoes oxidation in the aqueous phase. A potential limitation of this technology is that some oxidation products (e.g., aldehydes and alcohols) may diffuse back into the gas stream.

5.2. Adaptation to Soil and Aquifer Treatment

5.2.1. OVERVIEW

Fenton oxidation is a potential alternative to incineration or landfilling of contaminated soil and represents a possible choice for in situ remediation of aquifers. Obviously, only thermal Fenton processes are applicable since light cannot penetrate soil beyond a few millimeters.

On the face of it, Fenton technologies applied to the cleanup of natural solids face serious obstacles: interference by soil components, the pH

limitation typical of Fenton reactions, difficulties in effective dispersal of reagents, and potential alteration of the soil environment.

If conditions are aggressive enough, degradation of almost any oxidizable compound in soil can be achieved.

However, the amount of hydrogen peroxide needed to transform, and especially mineralize, a given concentration of contaminant in soil is often far greater than in aqueous systems. If the soil contains appreciable organic matter, the required H_2O_2:contaminant molar ratios can be on the order of 10^2–10^3 (compared to 10^0–10^1 in water), and H_2O_2 concentrations up to 15 M (50%!) in the aqueous phase must sometimes be employed (Tyre et al., 1991; Li et al., 1997b; Watts and Stanton, 1999). Elevated temperatures (Figure 15), or stepped as opposed to single addition of peroxide (Figure 16) help reduce peroxide demand. It should be noted that the use of high H_2O_2 concentrations and acidity renders the soil "sterile" (Miller et al., 1996), at least temporarily. This can be a hurdle to employing sequential chemical-biological degradation strategies.

The high oxidant demand is due to (1) the presence of natural organic matter (NOM), (2) nonproductive catalyzed decomposition of H_2O_2 to O_2 and H_2O, or (3) the presence of inorganic reductants in soil that consume H_2O_2.
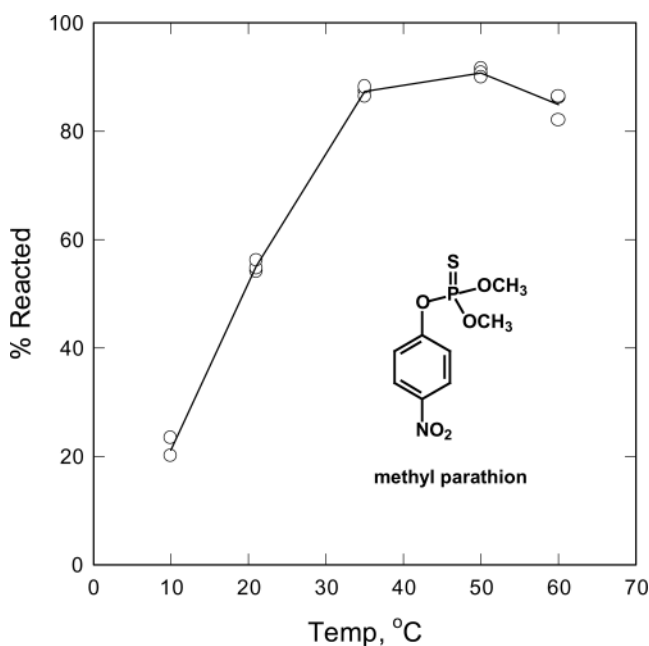

FIGURE 15. Temperature dependence of chelated Fenton reaction of methyl parathion (0.01 mole/kg) in Cheshire fsl soil (1.6% organic carbon). Conditions: 0.01 mol/kg Fe-nitrilotriacetate complex; 1 mol/kg H_2O_2; pH 6; 3 h reaction time. From Pignatello and Day (1996) with permission.
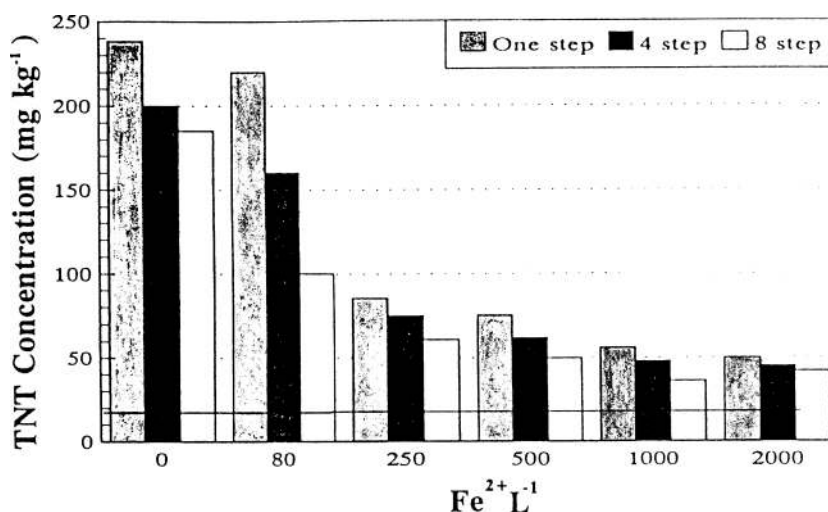
FIGURE 16. Soil concentrations of 2,4,6-trinitrotoluene (TNT) after 48 h of slurry (0.2 kg/L) reaction by Fenton oxidation. Equivalent amounts of Fenton reagents were added proportionately as 1, 4, or 8 steps every 4 h. The total effective concentration of hydrogen peroxide was 1% in all cases and pH of the slurry was adjusted to 3 prior to reagent addition. The initial soil concentration was 400 mg/kg and the cleanup goal of 17 mg/kg is designated by the horizontal line. Figure from Arienzo et al. (1998) with permission.

NOM is capable of scavenging HO$^\cdot$ and offers protective sorption sites for the contaminant. The second-order rate constant for reaction of HO$^\cdot$ with dissolved organic matter (DOM) is $\sim 2 \times 10^4$ s^{-1} (mg C/L)$^{-1}$ (Goldstone et al., 2002). Contaminant removal rate decreases with increasing DOM content. Aquifer materials generally contain much lower levels of NOM than surface soil horizons, and degradation can be reasonably facile in these media (Ravikumar and Gurol, 1994). Most organic compounds sorb predominantly to the NOM component of soils. The mechanism of sorption is by partitioning into the three-dimensional, polymerlike phase of NOM. Since Fenton reagents are hydrophilic and do not partition in NOM, most HO$^\cdot$ will be generated in the aqueous phase, where it reacts before diffusing very far (on the order of micrometers). Contaminant molecules, on the other hand, will tend to be imbedded in the NOM phase, where they are surrounded by matrix that is itself reactive with HO$^\cdot$. The probability that HO$^\cdot$ formed in solution will encounter a sorbed molecule is thus extremely small. It follows that degradation of contaminants that undergo primarily partitioning would be rate-limited by desorption. This prediction has not been adequately tested, however. Evidence for oxidation of contaminants in the sorbed state is weak. Watts et al. (1994) found that hexachlorobenzene deposited on silica sand, which is presumably very low in NOM content, was degraded at a faster rate than it could be desorbed (by air sparging) when H$_2$O$_2$ exceeded 30 mM, suggesting oxidation of surface-sorbed hexachlorobenzene. On the other hand,

addition of ethanol to artificially contaminated soil increased the transformation of anthracene to anthraquinone (Lee et al., 1998), ostensibly by enhancing desorption thermodynamically or kinetically. Few studies have reported treatment of historically-contaminated soil (Li et al., 1997a, 1997b; Arienzo et al., 1998), which often contains a large fraction in a highly desorption-resistant state (Pignatello and Xing 1996; Luthy et al., 1997). Further efforts to distinguish surface from solution reactions in soil media are required.

Decomposition of H_2O_2 in "clean" soil in batch suspension can be complete in as short as a few minutes (Baciocchi et al., 2003). Ravikumar and Gurol (1994) found that 5 mM H_2O_2 was ∼80% decomposed after a 12-min passage through a coarse-grained sand column containing 800 mg/kg natural Fe and 0.04% natural organic carbon. Decomposition was accelerated by $FeSO_4$ addition to the influent. Much of H_2O_2 decomposition in soil is nonproductive and catalyzed by microbial peroxidases and oxidases (Petigara et al., 2002) or transition metal sites on clays and oxyhydroxides (Petigara et al., 2002; Baciocchi et al., 2003). Petigara et al. (2002) found that in soils with high NOM or Mn content H_2O_2 decomposed rapidly, mainly through nonproductive processes; in other soils where decomposition was slower, processes leading to HO· were predominant. At least some of the nonproductive decomposition was enzymatic. Baciocchi et al. (2003) determined that the degradation potential of 3-chlorophenol correlates with the lifetime of H_2O_2 in a given soil under various conditions (but not among different soils). The lifetime of H_2O_2 could be increased by lowering the pH of the suspension, or by addition of $H_2PO_4^-$, which presumably binds to catalytically active surface sites. Dihydrogen phosphate has been added as a stabilizer in aquifer remediation applications (U.S. EPA, 2001).

In addition to nonproductive catalytic decomposition, H_2O_2 may react with inorganic reducing species in soil such as low-valent metal ions besides iron, such as, Mn(II) (Li et al., 1997a).

Another obstacle is the requirement for acidic conditions. Lowering the pH not only keeps Fe(III) soluble but reduces nonproductive decomposition of H_2O_2 (Baciocchi et al., 2003). The natural pH of soils lies in the region 4–8. Acidification of soil is difficult due to the high buffering capacity of soil, and is potentially polluting itself. Ferric complexes with natural and synthetic organic chelating agents were found to catalyze the transformation of pesticides (Baehr and Pignatello, 1994; Pignatello and Day, 1996; Pignatello, 2000) and PAHs (Nam et al., 2001) in soils at about pH 6, eliminating the need to acidify. One example concerns of methyl parathion with ferric nitrilotriacetate (NTA), previously shown in Figure 15; at 35°C methyl parathion gave quantitative yield of sulfate and nitrate ions, while P was recovered partially as dimethylphosphate. Similar results were obtained with a structurally similar chelating agent, hydroxyethylenimine diacetate (HEIDA).

Since Fe occurs naturally, one could hope to avoid having to add it. However, addition of peroxide alone is usually insufficient to achieve degradation

before it decomposes nonproductively (Baehr and Pignatello, 1994; Miller et al., 1996). While iron minerals (goethite, magnetite, hematite) can catalyze the Fenton reaction, they are much less reactive than soluble iron, especially when the pH is not lowered (e.g., Teel et al., 2001). The adsorption of added iron to soil surfaces may also affect the rate at which soil contaminants are transformed. The transformation rate constant of TNT was increased from 437 min^{-1} to 1613 min^{-1} by the addition of Ca-montmorillonite clay (2% by weight) to soil slurries (Li et al., 1997b). The rate enhancement was thought to be due to a surface reaction between iron and TNT. Addition of kaolinite, a clay with no appreciable ability to sorb iron, did not increase the transformation rate constant. Neither clay affected the rate of TNT conversion to CO_2.

Application of Fenton AOPs in the field for in situ decontamination of aquifers may also suffer from problems related to effective dispersal of reagents. Iron(III) sorbs strongly to mineral surfaces and NOM depending on pH (Baehr and Pignatello, 1994) and may not travel very far from the point of injection. Aquifer plugging from precipitated iron oxyhydroxides has been an issue in some cases. Another problem is the rapid decomposition of peroxide near the point of injection (Chen et al., 2001a), which sometimes resulted in gas eruption on the surface. An additional concern of gas evolution in shallow aquifers is sparging of volatile organic compounds (e.g., chlorinated solvent contaminants) into the unsaturated zone (Chen et al., 2001a). Addition of phosphate stabilizers are thought to help in this regard (Kakarla and Watts, 1997), but after a while phosphate may be depleted by adsorption. Destruction of nonaqueous phase liquids (NAPLs) by Fenton reagents likely occurs indirectly by dissolution of the NAPL into the aqueous phase because the reagents are not soluble in the NAPL.

5.2.2. SOIL TREATABILITY STUDIES

Successful Fenton treatment of soils on a laboratory scale has been demonstrated for chlorinated solvents (Leung et al., 1992; Ravikumar and Gurol, 1994), polycyclic aromatic hydrocarbons (Lee et al., 1998), polychlorinated biphenyls (Aronstein and Rice, 1995), pesticides (Tyre et al., 1991; Baehr and Pignatello, 1994; Pignatello and Day, 1996; Ravikumar and Gurol, 1994), explosives (Li et al., 1997a, 1997b; Arienzo et al., 1998), fuels (Chen et al., 1998; Kong et al., 1998) and fuel components (Tyre et al., 1991; Kakarla and Watts, 1997; Watts and Stanton, 1999). Commonly such reactions are carried out in soil slurry, but column studies have also been performed (e.g., Ravikumar and Gurol, 1994).

Arienzo et al. (1998) reported both batch-scale and pilot-scale treatments of TNT-contaminated soil (show previously in Figure 16). At a soil-to-water ratio of 0.2 kg/L, the optimal Fenton reagent concentrations were found to be 640 mg/L Fe^{2+} and 1% H_2O_2. TNT concentrations were reduced from 400 mg/kg to 50 mg/kg in 24 h. Incremental addition of reagents provided better removal than batch addition; however, neither achieved the cleanup

goal of 17.2 mg/kg. In the pilot-scale test, faster TNT removal was achieved using a 60-L air-lift reactor. Only the equivalent of 0.625% H_2O_2 was required and TNT concentration was reduced to 12 mg/kg after 24 h.

Commercial-scale systems based on Fenton technologies have been explored for the treatment of groundwater and soils by in situ and ex situ approaches (U.S. EPA, 2001; U.S. DOE, 1999). The general flow configuration for in situ treatment consists of a mixing head that combines catalyst and hydrogen peroxide solutions from separate reservoirs in the injection well. Positive displacement of reaction solutions into the aquifer are maintained by externally applied compressed air or the back pressure from CO_2 and O_2 generated from the oxidation reactions. In-place soil mixing has been used to increase contact between oxidants and contaminants, but limits applications to shallow aquifer systems. Ex situ commercial Fenton treatments consist of screw-type mixing apparatus that combine soil with Fenton reagents from reservoirs. The mixing apparatus may be contained within a mixing chamber as a stationary reactor, or attached to a vehicle that is driven through soil windrows.

Field trials conducted at sites with chlorinated solvent contamination have shown some success at reducing groundwater contaminant concentrations (U.S. DOE, 1999). Subsequent 'rebound' of groundwater contaminant concentrations is likely attributable to poor contact between oxidant and contaminant zones. Oxidant addition initially reduced aquifer microbial populations greatly, but population levels can rebound within 6 months (Ferguson et al., 2004; Chapelle et al., 2005). The formation of large amounts of iron oxyhydroxide solids can induce shifts in microbial communities to this solid as a terminal electron acceptor from another one (e.g., SO_4^{2-}) (Chapelle et al., 2005), which could slow the natural attenuation of contaminant.

Fenton-based groundwater treatment may be more suitable for aromatic hydrocarbon contamination (e.g., BTEX: benzene, toluene, ethylbenzene, xylenes). Here, the autocatalytic effect of quinone formation may accelerate contaminant degradation. Sites with chlorinated solvent DNAPLs may generate enough chloride ion to compete for HO$^{\cdot}$. Careful control of reagent addition is critical at sites with the possible presence of solvents with lower density than water, such as BTEX, as the high heats of reaction with Fenton reagents may increase temperatures to the point of soil vapor ignition (U.S. DOE, 1999).

Chiarenzelli et al. (2001) avoided the many limitations of Fenton soil treatment by steam distillation of polychlorinated biphenyl (PCB) contaminants from sediments followed by electrochemical oxidation of the distillate with nested steel electrodes and added H_2O_2. This process removed >95% of the dissolved PCBs within 30 min, preferentially removing the lower-molecular-weight congeners, which comprised 85% of the original PCB mass. It may be less effective for sediments contaminated with the heavier congeners.

6. FENTON PROCESSES IN RELATION TO OTHER TREATMENT TECHNOLOGIES

6.1. Fenton Enhancement of Other Treatment Processes

Addition of Fenton reagents along with the components of other waste treatment process often leads to enhanced degradation or degradation rate. Combined treatment processes should be considered carefully, however, because the cost per unit mass degraded may actually increase after introducing ancillary operations associated with Fenton reactions (e.g., pH control, sludge removal) and because of the possibility of interfering chemistries.

Ultrasonic degradation of phenol (Jiang and Waite, 2003) and of 2-chlorophenol (Lin and Ma, 2000) was modestly enhanced by the addition of Fenton reagents, presumably by increasing the concentration of HO⋅ from added or ultrasonically formed H_2O_2. Ferrous ions were added during ozonation of aniline or 4-chlorophenol to boost HO⋅ by eq. (71) (Sauleda and Brillas, 2001):

$$Fe^{2+} + O_3 \rightarrow FeO^{2+} + O_2$$

$$FeO^{2+} + H_2O \rightarrow Fe^{3+} + OH^{\cdot} + OH^{-} \tag{71}$$
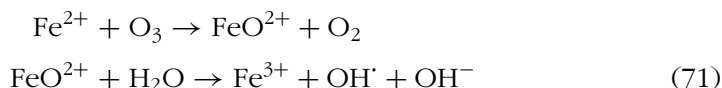
Rates of compound removal were unchanged. TOC was removed faster during the first hour, but thereafter only slow changes in TOC were observed because ferric ion was complexed by oxidation products such as oxalic acid.

The performance of biological wastewater treatment has been augmented by the addition of Fenton reagents to solutions containing microbial cultures. Using Fenton reagent (0.15–0.45 mM Fe(II)–NTA, 25–100 mg/L H_2O_2) and *Xanthobacter flavus*, tetrachloroethylene mineralization increased from 20% (culture only) to 45% (Fenton reagent only) to 54% (simultaneous treatment) after 72 h (Büyüksönmez et al., 1999). Addition of Fenton reagents to polychlorobiphenyl-spiked soil and sediment slurries increased mineralization of ^{14}C-labeled 2-chlorobiphenyl by a factor of 3 to 7 compared to microbial treatment alone (Aronstein and Rice, 1995).

6.2. Sequential Processes With the Fenton Reaction as One of the Steps

The most common employment of the Fenton reaction in a sequential mode is Fenton treatment followed by a biotic process. This strategy rests on the expectation that the parent molecule is usually more reactive chemically than

biologically, while the opposite is true for the Fenton oxidation products due to introduction of functional groups such as $-OH$ and $-CO_2H$.

Target pollutant $\xrightarrow{\text{Fenton}}$ organic intermediates $\xrightarrow{\text{microbes}}$ CO_2, mineral acids

(more oxidizable; less biodegradable)   (less oxidizable; more biodegradable)
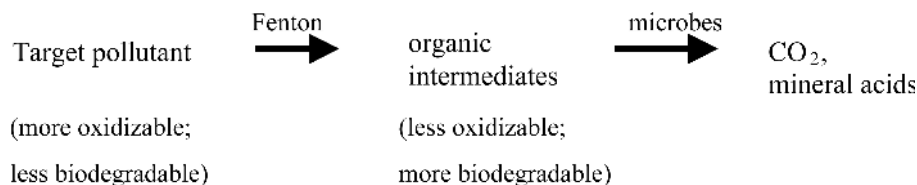
Many wastewaters—for example, from landfill leachate, agricultural processing, pulp bleaching, and chemical manufacture—contain compounds that are recalcitrant, inhibitory, or toxic in biological treatment steps. Since removal of target compounds in Fenton reactions is typically faster than the decrease in TOC, BOD, or COD, a Fenton-biological sequential treatment strategy seems to be a rational approach toward meeting effluent standards.

Fenton pretreatment has been shown in several cases to improve biodegradability under aerobic and anaerobic conditions: dye intermediates by mixed cultures (Wanpeng et al., 1996; Yu et al., 1998); ethylene oxide/propylene oxide block copolymers (Kitis et al., 1999); polyvinyl alcohol by a white rot fungus (*Pyncnoponus cinnabarinus*) (Larking et al., 1999); 2-chlorobiphenyl and 51% 2,2′,4,4′-tetrachlorobiphenyl by *Pseudomonas* sp. strain LB400 and *Algaligenes eutrophus* strain H850 (Aronstein et al., 1995); and chlorophenols and chlorobenzoates by methanogens in digester sludge (Koyama et al., 1994).

Fenton treatment has also been used along with traditional physical–chemical wastewater treatment methods. Fenton treatment followed by a coagulation step improved COD removal to greater than 90% for dye manufacture wastewater (Yu et al., 1998; Kang et al., 2002). Coagulation plus Fenton treatment increased COD removal from landfill leachate over coagulation alone (Yoon et al., 1998; Kang and Hwang, 2000; Lau et al., 2001). Poor floc formation and settling characteristics have been noted when Fenton oxidation is coupled with coagulation (Lin and Lo, 1997). Fenton pretreatment decreases the quantity of sludge generated by coagulation and yields sludges with lower toxicity and improved dewatering ability (Yoo et al., 2001; Neyens et al., 2002).

While a Fenton pretreatment step may improve biodegradability, when Fenton conditions are optimized the biological step might be unnecessary. For example, Hess and Schrader (2002) found that, under otherwise similar conditions, percent mineralization of 2,4,6-trinitrotoluene (TNT) followed the order photo-Fenton alone (99%) > thermal Fenton/biotic sequential (75–80%) > thermal Fenton alone (43%) > biotic alone (<2%). In this case, photo-Fenton alone was clearly superior. However, in deciding which strategy to employ one would have to balance costs with treatment objectives.

6.3. Comparison of Fenton Reactions With Other AOPs or Other Treatment Technologies

Numerous studies have compared the classical Fenton reaction to other AOPs. Usually these comparisons are rather favorable to the Fenton process in terms of effectiveness, but most often costs and possible limitations are not discussed. Since different AOPs require different reagents and conditions, it is difficult to generalize without an economic analysis.

Thermal Fenton reaction degraded chlorophenol and nitrophenol faster than did H_2O_2/UV (Lipczynska-Kochany 1992; Benitez et al., 2000a; Trapido and Kallas, 2000) or O_3/UV (Benitez et al., 2000a). The time required to remove 90% of atrazine was the same for Fenton reaction as for H_2O_2/UV (DeLaat et al., 1999). Fenton reaction (0.1–0.75 g/L $FeSO_4$, 0.1 or 1% H_2O_2, pH 3) was more effective than TiO_2 (0.1–0.8 g/L)/UV for removing the explosive 5-nitro-1,2,4-triazol-3-one (NTO) (LeChampion et al., 1999). Electrochemical Fenton reaction with 600 mg/L Fe^{2+} and 600 mg/L H_2O_2 at pH 3.8 achieved 86% COD removal from photographic waste, while ozone (146 mg/L) with H_2O_2 (100 mg/L) achieved less than 4% COD removal for the same reaction time (Huang et al., 1999). Irradiation of Fenton reaction mixtures nearly always increases compound transformation rates or removal efficiencies (section 3.1).

Many factors are important in selecting a treatment technology—amortized investment, installation costs, operating costs, regulations, effluent quality goals, maintenance, safety, robustness, effluent disposal, and so on—but economic factors related to daily operation are often decisive. Economic comparisons among AOPs and between AOPs and conventional treatments have been attempted. The value of many such comparisons is limited, however, due to the following.

1. The reaction conditions of each AOP used for the cost analysis are often not optimized.
2. The outcome of the analysis is often not linked to a real treatment goal.
3. Some analyses consider only electrical energy consumption and ignore the costs of reagents; this would, for example, make the Fenton reaction carried out in the dark free.
4. Some analyses ignore costs of ancillary operations, such as neutralization and filtration.
5. The outcome can change when solar light is used because it eliminates part of the electrical costs.
6. Projection from one type of waste stream to another is difficult.

Clearly, economic comparisons require definition of a standard measure of treatment efficiency. Bolton et al. (2001) proposed "Figures-of-Merit" for AOPs based on electrical energy consumption, since electrical energy

represents a major fraction of operating costs of many AOPs. In addition to providing cost comparisons, Figures-of-Merit may also provide data useful for treatment scaleup.

The Figures-of-Merit approach is based on the observation that degradation of a specific organic contaminant (C) can often be described by a simple second-order rate law between HO˙ and C and between HO˙ and scavengers with specific rate constants. Technically, TOC depletion does not follow the analogous rate law because the nature of TOC changes over time.

At high [C] where scavenging is negligible and rate is pseudo zero-order in C, Bolton et al. propose the *electrical energy per unit of mass* (EE/M), the electrical energy required to bring about degradation of 1 kg of C having a molecular weight M (g/mol) and initial and final concentrations $[C]_{init}$ and $[C]_{final}$ (moles/L) in V (L) of polluted water or air after time t (min):

$$\text{EE/M (kW} \cdot \text{h} \cdot \text{kg}^{-1}) = \frac{1000Pt}{60VM([C]_{init} - [C]_{final})} \tag{72}$$

where P is electrical power input (kW). At low [C], where scavenging is important and the reaction tends to be pseudo first-order in C, Bolton et al. proposed the *electrical energy per order* (EE/O), which is the electrical energy required to bring about degradation of C by one order of magnitude in 1 m^3 of water or air. For a batch operation this is given by

$$\text{EE/O (kW per order per m}^3) = \frac{1000Pt}{60V \ \log([C]_{init}/[C]_{final})} \tag{73}$$

Based on the EE/O Figures-of-Merit, Fenton was superior to UV/H$_2$O$_2$ for treatment of water containing various pollutants, and considerable savings could be achieved by including oxalate in the Fenton reaction mixture (Safarzadeh-Amiri et al., 1996). Nevertheless, costs related to pH adjustments were not taken into account.

The Figures-of-Merit approach provides a good semi–mechanistic way to compare treatment procedures. Still to be answered is whether Figures-of-Merit developed under one set of operating conditions can be applied to others, given the complex relationship between initial reagent concentrations, compound conversion, and competing reactions.

Despite their potential utility, Figures-of-Merit or any other standard economic measures of treatment efficiency have not been widely adopted. Instead, treatment costs are usually reported on a per-unit liquid volume or per-unit solids mass basis and do not take into account the concentration of the contaminant, nor the treatment goal to be achieved. Pulgarin and Kiwi (1996) investigated Fenton removal of *p*-coumaric acid representing constituents in wine and cooking oil refining effluent. The estimate cost of USD 6/m^3 of solution was within the range of costs for nondestructive flocculation and filtration processes. Cooper and Nicell (1996) compared the cost of

Fenton reaction versus a horseradish peroxidase–H_2O_2 system for polymerizing phenol wastes from foundry operations. At doses of 15 mM H_2O_2 and 1.5 mM ferrous ion, Fenton oxidation, not including acidification to pH 3.3 or subsequent neutralization, was about six times less expensive. A lower per-liter energy requirement was realized for electro-Fenton using Pt anodes (20 W · h/L), than for photo-Fenton oxidation (520 W · h/L) of flavor manufacture wastewater (Ribordy et al., 1997). Goi and Trapido (2002) compared the energy costs of various AOPs for 90% reduction of 0.4 mM nitrophenols. Photo-Fenton reaction was 2–3 times more expensive than thermal Fenton. Even including iron oxide sludge disposal, the Fenton AOPs were less expensive than UV/H_2O_2 or UV alone. Perez et al. (2002) compared various AOPs for removing TOC in a bleaching Kraft mill effluent. They found that Fenton, Fenton-like, and photo-Fenton reactions achieved better TOC removal at lower costs than did photocatalysis (TiO$_2$, with or without additives). Bauer and Fallmann (1997) compared chemical and energy costs for removal of TOC in a landfill leachate. Both chemical and energy costs per kilogram TOC decreased in the order: O_3 alone > UV/O_3 > UV/H_2O_2 > photo-Fenton > solar photo-Fenton.

7. CONCLUDING STATEMENTS

Fenton-based reactions are capable of extensively degrading organic contaminants in a variety of wastewater streams and soils. They usually perform favorably when compared to other hydroxyl radical-generating AOPs. Rigorous economic comparisons using an accepted standard measure of treatment efficiency are scarce, however. Fenton reactions can be performed at ambient temperature and do not require illumination, although they usually enhanced by it. The reagents are readily available, easy to store, relatively safe to handle, and non–threatening to the environment. Biological wastewater treatment may be improved with the addition of a Fenton pretreatment step.

Fenton AOPs have a number of drawbacks that limit their widespread acceptance, however. The major drawbacks are: the instability of the reagent mixture; waste of a significant fraction of the bulk oxidant by nonproductive conversion to oxygen; the requirement in most Fenton variants for mildly acidic conditions; interference by some substances that complex iron ions; and the production of iron oxide sludge that interferes with the process (e.g., aquifer remediation) or has to be removed prior to discharge of the treated water. Some of these drawbacks are intrinsic; others may be alleviated after further research and development. In addition, Fenton AOPs suffer from the same disadvantages that other hydroxyl radical-AOPs do: namely, they are susceptible to scavenging of hydroxyl radicals by nontarget substances (e.g., natural organic matter, halides), and are unsuitable for certain compounds (such as perchlorinated compounds) that resist attack by hydroxyl radicals.

In homogeneous aqueous solution the fundamental reaction steps of Fenton-based AOPs are fairly well understood and multistep kinetic models assuming the conventional mechanisms do a good job of predicting trends. However, it is still difficult to predict the transformation and mineralization rates of particular compounds without conducting treatability studies. Considering the complexity of the Fenton reaction, empirical optimization strategies should be advantageous in technical and commercial scaleup. Even more difficult to predict are the appearance and decay profiles of organic intermediates. The nonselectivity of the hydroxyl radical leads to a variety of products whose distribution is sensitive to reaction conditions. No one, to our knowledge, has attempted to deal with a changing wastestream composition.

Emphasis is needed on many aspects of Fenton chemistry in order to achieve breakthroughs in technical development identification of appropriate complexing ligands to boost reactivity and assist in iron recycling; clarification of the role of ferryl species in the degradation of relevant contaminants; more attention to characterizing reactions of halogen radical and dihalogen radical anions resulting from halideions in the treated water with organic compounds; studies designed to limit or exploit, as the case may be, side reactions that result from iron or organic radical chemistry, for example, the autocatalytic effect of quinones; development of reactive immobilized forms of iron that perform at neutral pH, or, alternatively, reactors that recycle the sludge; research devoted to sorting out the roles of surface and solution-phase reactions in designed heterogeneous catalysts and solid sources of iron, such as minerals and zero valent iron; advances in the development of electro-Fenton systems; efforts to differentiate and quantify the roles of surface and solution-phase reactions in soil media; more attention to identifying and characterizing situations in which Fenton reactions can synergize with other AOPs; and technological development of efficient solar reactors designed for Fenton applications, particularly reactors equipped with supplemental illumination around the clock and full-time operation. Lastly, for successful applications of Fenton-based treatment processes for aquifer remediation, researchers and engineers must find ways to overcome mass transfer limitations associated with reagent delivery, which are particularly limiting in the case of Fenton due to the instability of the reagent mixture and decomposition of the bulk oxidant by the matrix.

ACKNOWLEDGMENTS

J. J. Pignatello et al.

REFERENCES

Ahmad, S., McCallum, J.D., Shiemke, A.K., Appelman, E.H., Loehr, T.M., and Sanders-Loehr, J. Raman spectroscopic evidence for side-on binding of peroxide to Fe(III)(edta), *Inorg. Chem.* 27, 2230–2233, 1988.

Ali, M.A., Yasui, F., Matsugo, S., and Konishi, T. The lactate-dependent enhancement of hysroxyl radical generation by the Fenton reaction, *Free Radical Res.* 32, 429–438, 2000.

Ali, M., and Konishi, T. Enhancement of hydroxyl radical generation in the fenton reaction by alpha-hydroxyl acid, *Biochem. Mol. Biol. Int.* 46, 137–145, 1998.

Anbar, M., Meyerstein, D., and Neta, P.J. The reactivity of aromatic compounds toward hydroxyl radicals, *J. Phys. Chem.* 70, 2660–2662, 1966.

Andreozzi, R., Caprio, V., Insola, A., and Marotta, R. Advanced oxidation processes (AOP) for water purification and recovery, *Catalysis Today* 53, 51–59, 1999.

Andrianirinaharivelo, S., Mailhot, G., and Bolte, M. Photodegradation of organic pollutants induced by complexation with transition metals (Fe^{3+} and Cu^{2+}) present in natural waters, *Solar Energy Mater. Solar Cells* 38, 459–474, 1995.

Arasasingham, R.D., Cornman, C.R., and Balch, A.L. Detection of alkylperoxo and ferryl, $(FeIV{=}O)^{2+}$, intermediates during the reaction of *tert*-butyl Hydroperoxide with iron porphyrins in toluene solution, *J. Am. Chem. Soc.* 111, 7800–7805, 1989.

Arienzo, M. Oxidizing 2,4,6-trinitrotoluene with pyrite–H_2O_2 suspensions, *Chemosphere* 39, 1629–1638, 1999.

Arienzo, M., Chiarenzelli, J., and Scrudato, R. Remediation of metal-contaminated aqueous systems by electrochemical peroxidation: An experimental investigation, *J. Haz. Mater.* 87, 187–198, 2001a.

Arienzo, M., Chiarenzelli, J., Scrudato, R., Pagano, J., Falanga, L., and Connor, B. Iron-mediated reactions of polychlorinated biphenyls in electrochemical peroxidation process (ECP), *Chemosphere* 44, 1339–1346, 2001b.

Arienzo, M., Comfort, S.D., Zerkoune, M. Li, Z.M., and Shea, P.J. Pilot-scale devices for remediation of munitions contaminated soils, *J. Environ. Sci. Health A* 33, 1515–1531, 1998.

Arnold, S.M., Talaat, R.E., Hickey, W.J., and Harris, R.F. Identification of Fentons-reagent-generated atrazine degradation products by high performance liquid-chromatography and megaflow electrospray-ionization tandem mass-spectrometry, *J. Mass Spectrom.* 30, 452–460, 1995.

Aronstein, B.N., and Rice, L.E. Biological and integrated chemical-biological treatment of PCB congeners in soil/sediment containing system, *J. Chem. Technol. Biotechnol.* 63, 321–328, 1995.

Aronstein, B.N., Paterek, J.R. Kelley R.L., and Rice, L.E. The effect of chemical pretreatment on the aerobic microbial degradation of PCB congeners in aqueous systems, *J. Ind. Microbiol.* 15, 55–59, 1995.

Arslan, I., and Balcioglu, I.A. Degradation of commercial reactive dyestuffs by heterogenous and homogenous advanced oxidation processes: A comparative study, *Dyes Pigments* 43, 95–108, 1999.

Atkinson, R. *Kinetics and Mechanisms of the Gas-Phase Reactions of the Hydroxyl Radical with Organic Compounds,* American Institute of Physics, New York, 1989.

Augusti, R., Dias, A.O., Rocha, L.L., and Lago, R.M. Kinetics and mechanism of benzene derivative degradation with Fenton's reagent in aqueous medium studied by MIMS, *J. Phys. Chem. A* 102, 10723–10727, 1998.

Baciocchi, R., Boni, M.R., and D'Aprile, L. Hydrogen peoxide lifetime as an indiator of the efficiency of 3-chlorophenol Fenton's and Fenton-like oxidation in soils, *J. Haz. Mater.* B96, 305–329, 2003.

Bae, J.-H., Kim, K.S., and Chang, H.-S. Treatment of landfill leachates: Ammonia removal via nitrification and denitrification and further COD reduction via Fenton's treatment followed by activated sludge, *Water Sci. Technol.* 36, 341–348, 1997.

Baehr, K., and Pignatello, J.J. Ferric complexes as catalysts for "Fenton" degradation of 2,4-D and metolachlor in soil, *J. Environ. Qual.* 23, 365-370, 1994.

Balanosky, E., Herrera, F., Lopez, A., and Kiwi, J. Oxidative degradation of textile waste water. Modeling reactor performance, *Water Res.* 34, 582–596, 2000.

Balanosky, E., Fernandez, J., Kiwi, J., and Lopez, A. Degradation of membrane concentrates of the textile industry by Fenton like reactions in iron-free solutions at biocompatible pH values (pH ≈ 7–8), *Water Sci. Technol.* 4(4–5), 417–424, 1999.

Balanosky, E., and Kiwi, J. Mathematical modeling of the photochemical reactor degradation of *p*-nitrotoluenesulfonate, *Ind. Eng. Chem. Res.* 37, 347–356, 1998a.

Balanosky, E., Lopez, A., and Kiwi, J. Degradation of naphthalene-1,5-disulphonate in a flow reactor. Modelling via reduced dimensionless centered variables, *J. Photochem. Photobiol. A Chem.* 119, 151–164, 1998b.

Balzani, V., and Carassiti, V. *Photochemistry of Coordination Compounds,* Academic Press, New York, 1970.

Bandara, J., Nadtochenko, V. Kiwi, J., and Pulgarin, C. Dynamics of oxidant addition as a parameter in the modelling of dye mineralization (orange II) via advanced oxidation technologies, *Water Sci. Technol.* 35, 87–93, 1997.

Bandara, J., Morrison, C., Kiwi, J., Pulgarin, C., and Peringer, P.J. Degradation/decoloration of concentrated solutions of orange II. Kinetics and quantum yield for sunlight induced reactions via Fenton type reagents, *Photochem. Photobiol. A Chem.* 99, 57–66, 1996.

Barb, W.G., Baxendale, J.H., George, P., and Hargrave, K.R. Reactions of ferrous and ferric ions with hydrogen peroxide, *Nature* 163, 692–694, 1949.

Barb, W.G., Baxendale, J.H., George, P., and Hargrave, K.R. Reactions of ferrous and ferric ions with hydrogen peroxide. Part I.—The ferrous ion reaction, *Trans. Faraday Soc.* 47, 462–500, 1951a.

Barb, W.G., Baxendale, J.H., George, P., and Hargrave, K.R. Reactions of ferrous and ferric ions with hydrogen peroxide. Part II.—The ferric ion reaction, *Trans. Faraday Soc.* 47, 591–616, 1951b.

Bärsch, S., Schröder, D., and Schwarz, H. Extreme differences in the interactions of "bare" Fe^+ and Fe^{2+} with hydrogen peroxide: Fenton chemistry in the gas phase, *Helv. Chim. Acta* 83, 827–835, 2000.

Bauer, R., and Fallmann, H. The photo-fenton oxidation—A cheap and efficient wastewater treatment method, *Res. Chem. Intermed.* 23, 341–354, 1997.

Behar, B., and Stein, G. Photochemical evolution of oxygen from certain aqueous solutions, *Science* 154, 1012–1013, 1986.

Benitez, F.J., Beltran-Heredia, J., Acero, J.L., and Rubio, F.J. Contribution of free radicals to chlorophenols decomposition by several advanced oxidation processes, *Chemosphere* 41, 1271–1277, 2000a.

Benitez, F.J., Beltran-Heredia, J., Rea, F., and Acero, J.L. Phenolic contaminant acids oxidation by Fenton's reagent, *Fresenius Environ. Bull.* 9, 144–151, 2000b.

Benkelberg, H.-J., and Warneck, P. Photodecomposition of iron(III) hydroxo and sulfato complexes in aqueous solution: Wavelength dependence of OH and SO_4^- quantum yields, *J. Phys. Chem.* 99, 5214–5221, 1995.

Bielski, B.H.J., Cabelli, D.E., Arudi, R.L., and Ross, A.B. Reactivity of HO_2/O_2^- Radicals in aqueous solution, *J. Phys. Chem. Ref. Data* 14, 1041–1051, 1985.

Bielski, B.H.J., and Cabelli, D.E. Highlights of current research involving superoxide and perhydroxyl radicals in aqueous solutions, *Int. J. Radiat. Biol.* 59, 291–319, 1991.

Bishop, D.F., Stern, G., Fleischman, M., and Marshall, L.S. Hydrogen peroxide catalytic oxidation of refractory municipal waste waters, *I&EC Proc. Design Dev.* 7, 110–117, 1968.

Bolton, J.R., Ravel, M., Cater, S.R., and Safarzadeh-Amiri, A. Homogeneous solar photodegradation of contaminants in water, *Proceedings of the ASME 1996 International Solar Energy Conference* 53–60, 1996.

Bolton, J.R., Bircher, K.G., Tumas, W., and Tolman, C.A. Figures-of-merit for the technical development and application of advanced oxidation technologies for both electric- and solar-driven systems, *Pure Appl. Chem.* 73, 627–637, 2001.

Bossmann, S.H., Oliveros, E., Goeb, S., Kantor, M., Goeppert, A., Braun, A.M., Lei, L., and Yue, P.L. Oxidative degradation of polyvinyl alcohol by the photochemically enhanced Fenton Reaction. Evidence for the formation of supermacromolecules, *Prog. Reaction Kin. Mech* 26, 113–137, 2001a.

Bossmann, S.H., Oliveros, E., Goeb, S., Kantor, M., Goeppert, A., Lei, L., Yue, P.L., and Braun, A.M. Degradation of polyvinylalcohol (PVA) by homogeneous and heterogeneous catalysis applied to the photochemically enhanced Fenton reaction, *Water Sci. Technol.* 44, 257–262, 2001b.

Bossmann, S.H., Oliveros, E., Goeb, S., Siegwart, S., Dahlen, E.P., Pavayan, L., Jr., Straub, M., Wörner, M., and Braun, A.M. New evidence against hydroxyl radicals as reactive intermediates in the thermal and photochemically enhanced Fenton reaction, *J. Phys. Chem. A* 102, 5542–5550, 1998.

Bossmann, S.H., Thanh, H.L., Shahin, N., Bonfill, A., Woerner, M., and Braun, A.M. $Fe(bpy)_3^{2+}/TiO_2$-codoped zeolites: Synthesis, characterization, and first application in photocatalysis, *Chem. Phys. Phys. Chem* 3, 401–407, 2002.

Box, G.E.P., Hunter, W.G., and Hunter, J.S. *Statistics for Experimenters: An Introduction to Design, Data Analysis and Model Building*, Wiley, New York, 1978.

Brand, N., Mailhot, G., and Bolte, M. Degradation photoinduced by Fe(III): Method of alkylphenolethoxylates removal in water, *Environ. Sci. Technol.* 32, 2715–2720, 1998.

Brand, N., Mailhot, G., and Bolte, M. The interaction "light, Fe(III)" as a tool for pollutant removal in aqueous solution: Degradation of alcohol ethoxylates, *Chemosphere* 40, 395–401, 2000a.

Brand, N., Mailhot, G., Sarakha, M., and Bolte, M. Primary mechanism in the degradation of 4-octylphenol photoinduced by Fe(III) in water-acetonitrile solution, *J. Photochem. Photobiol. A Chem.* 135, 221–228, 2000b.

Braun, A.M., Jakob, L., Oliveros, E., and Nascimento, C.A.O. Up-scaling photochemical reactions, *Adv. Photochem.* 18, 235–313, 1993.

Braun, A.M., Maurette, M.-T., and Oliveros, E. *Photochemical Technology*, Wiley & Sons, New York, 77–81, 1991 (and references cited therein.)

Bigda, R.J. Consider Fenton's chemistry for wastewater treatment, *Chem. Eng. Prog.* 12, 62–66, 1995

Brillas, E., Mur, E., Sauleda, R., Sanchez, L., Peral, J., Domenech, X., and Casado, J. Aniline mineralization by AOP's: Anodic oxidation, photocatalysis, electro-Fenton and photoelectro-Fenton processes, *Appl. Catal. B Environ.* 16, 31–42, 1998a.

Brillas, E., Sauleda, R., and Casado, J. Degradation of 4-chlorophenol by anodic oxidation, electro-Fenton, photo-electro-Fenton, and peroxy coagulation processes, *J. Electrochem. Soc.* 145, 759–765, 1998b.

Brillas, E., Calpe, J.C., and Casado, J. Mineralization of 2,4-D by advanced oxidation electrochemical oxidation processes, *Water Res.* 34, 2253–2262, 2000.

Burkitt, M.J. Chemical, biological and medical controversies surrounding the Fenton reaction, *Prog. Reaction Kinet. Mechanism* 28, 75–103, 2003.

Buxton, G.V., and Green, J.C. Reactions of some simple α- and β-hydroxyalkyl radicals with Cu^{2+} and Cu^+ ions in aqueous solution. A radiation chemical study, *J. Chem. Soc. Faraday Trans.* 1(74), 697–714, 1978.

Buxton, G.V., Greenstock, C.L., Helman, W.P., and Ross, A.B. Critical review of rate constants for reactions of hydrated electrons, hydrogen atoms and hydroxyl radicals ($\cdot OH/\cdot O^-$) in aqueous solutions, *J. Phys. Chem. Ref. Data* 17, 513–886, 1988.

Büyüksönmez, F., Hess, T.F., Crawford, R.L., Paszczynski, A., and Watts, R.J. Optimization of simultaneous chemical and biological mineralization of perchloroethylene, *Appl. Environ. Microbiol.* 65, 2784–2788, 1999.

Casado, J., Fornaguera, J., and Galán, M.I. Mineralization of aromatics in water by sunlight-assisted electro-Fenton technology in a pilot reactor, *Environ. Sci. Technol.* 39, 1843–1847, 2005.

Catrinescu, C., Teodosiu, C., Macoveanu, M., Miehe-Brendlé, J., and Le Dred, R. Catalytic wet peroxide oxidation of phenol over Fe-exchanged pillared beidellite, *Water Res.* 37, 1154–1160, 2003.

Cermenati, L., Pichat, P., Guillard, C., and Albini, A. Probing the TiO_2 photocatalytic mechanisms in water purification by use of quinoline, photo-Fenton generated OH* radicals and superoxide dismutase, *J. Phys. Chem. B* 101, 2650–2658, 1997.

Chen, C.T., Tafuri, A.N., Rahman, M., and Foerst, M.B. Chemical oxidation treatment of petroleum contaminated soil using Fenton's reagent, *J. Environ. Sci. Health A* 33, 987–1008, 1998.

Chen, G., Hoag, G.E., Chedda, P., Nadim, F., Woody, B.A., and Dobbs, G.M. The mechanism and applicability of in situ oxidation of trichloroethylene with Fenton's reagent, *J. Hazard. Mater.* B87, 171–186, 2001a.

Chen, F., Xie, Y., He, J., and Zhao, J. Photo-Fenton degradation of dye in methanolic solution under both UV and visible irradiation, *J. Photochem. Photobiol. A Chem.* 138, 139–146, 2001b.

Chen, S.-T., Stevens, D.K., and Kang, G. Pentachlorophenol and crystal violet degradation in water and soils using heme and hydrogen peroxide, *Water Res.* 33, 3657–3665, 1999.

Chen, R., and Pignatello, J.J. Role of quinone intermediates as electron shuttles in Fenton and photoassisted Fenton oxidations of aromatic compounds, *Environ. Sci. Technol.* 31, 2399–2406, 1997.

Chen, R., and Pignatello, J.J. Structure-activity study of electron-shuttle catalysis by quinones in the oxidation of aromatic compounds by the Fenton reaction, *J. Adv. Oxidation Technol.* 4, 447–453, 1999.

Chiarenzelli, J.R., Scrudato, R.J., Wunderlich, M.L., and Pagano, J.J. Combined steam distillatoin and electrochemical peroxidation (ECP) treatment of river sediment contaminated by PCBs, *Chemosphere* 45, 1159–1165, 2001.

Chou, S.S., Huang, Y.H., Lee, S.N. Huang, G.H., and Huang, C.P. Treatment of high strength hexamine-containing wastewater by electro-Fenton method, *Water Res.* 33, 751–759, 1999.

Christensen, H., Sehested, K., and Løgager, T. The reaction of hydrogen peroxide with Fe(II) ions at elevated temperatures, *Radiat. Phys. Chem.* 41, 575–578, 1993.

Cochran, W.G., and Cox, G.M. *Experimental Design*, Wiley, New York, 1992.

Cooper, V.A., and Nicell, J.A. Removal of phenols from a foundry wastewater using horseradish peroxidase, *Water Res.* 30, 954–964, 1996.

Cuzzola, A., Raffaelli, A., Saba, A., and Salvadori, P. Identification and characterization of Fenton oxidation products of surfactants by electrospray mass spectrometry and by solid phase microextraction gas chromatography mass spectrometry. 2. Fatty acid alcohol polyethoxy sulfates, *Rapid Commun. Mass Spectrom.* 14, 834–839, 2000.

DeHeredia, J.B., Torregrosa, J., Dominguez, J.R., and Peres, J.A. Kinetic model for phenolic compound oxidation by Fenton's reagent, *Chemosphere* 45, 85–90, 2001.

De Laat, J., and Gallard, H. Catalytic decomposition of hydrogen peroxide by Fe(III) in homogenerous aqueous solution: Mechanism and kinetic modeling, *Environ. Sci. Technol.* 33, 2726–2732, 1999.

De Laat, J., Gallard, H. Ancelin, S., and Legube, B. Comparative study of the oxidation of atrazine and acetone by H_2O_2/UV, Fe(III)/UV, Fe(III)/H_2O_2, and Fe(II) or Fe(III)/H_2O_2, *Chemosphere* 39, 2693–2706, 1999.

De Laat, J., and Le, T.G. Kinetics and modeling of the Fe(III)/H_2O_2 system in the presence of sulfate in acidic aqueous solutions, *Environ. Sci. Technol.* 39, 1811–1818, 2005.

Dhananjeyan, M.R., Kiwi, J., Albers, P., and Enea, O. Photo-assisted immobilized Fenton degradation up to pH 8 of azo dye orange II mediated by Fe^{3+}/Nafion/glass fibers, *Helvet. Chim. Acta* 84, 3433–3445, 2001.

Dong, Y., Fujii, H., Hendrich, M.P., Leising, R.A., Pan, G., Randall, C.R., Wilkinson, E.C., Zang, Y., Que, L., Jr., Fox, B.G., Kauffmann, K., and Munck, E. A high-valent nonheme iron intermediate. Structure and properties of [Fe_2(u-O)2(5-Me-TPA)$_2$](ClO$_4$)$_3$, *J. Am. Chem. Soc.* 117, 2778–2792, 1995.

Droesbeke, J.-J., Fine, J., and Saporta, G. eds., *Plans d'expériences. Applications à l'entreprise*. Editions Technip, Paris, 1997.

Duesterberg, C.K., Cooper, W.J., and Waite, T.D. Fenton-mediated oxidation in the presence and absence of oxygen, *Environ. Sci. Technol.* 39, 5052–5058, 2005.

Eisenhauer, H.R. Oxidation of phenolic wastes, *J. Water Pollut. Contr. Fed.* 36, 1116–1128, 1964.

Espro, C., Frusteri, F., Arena, F., and Parmaliana, A. Selective oxidation of propane on a Nafion-based catalytic membrane mediated by Fe^{II}-H_2O_2 Fenton system, *J. Mol. Catal. A Chem.* 159, 359–364, 2000.

Evans, M.G., George, P., and Uri, N. The $[Fe(OH)]^{+2}$ and $[Fe(O2H)]^{+2}$ complexes, *Trans. Faraday Soc.* 34, 230–234, 1949.

Faust, B.C., and Hoigne, J. Photolysis of Fe(III)-hydroxyl complexes as sources of OH radicals in clouds, fog, and rain, *Atmos. Environ.* 24A, 79–89, 1990.

Feig, A.L., and Lippard, S.J. Mechanistic studies of the reaction of dioxygen with dinuclear iron(II) compound to form (u-peroxo)diiron(III) complexes, *J. Am. Chem. Soc.* 116, 8410–8411, 1994.

Feng, J., Hu, X., Yue, P.L., Zhu, H.Y., and Lu, G.Q. A novel laponite clay-based Fe nanocomposite and its photo-catalytic activity in photo-assisted degradation of orange II, *Chem. Eng. Sci.* 58, 679–685, 2003.

Fenton, H.J.H. Oxidation of tartaric acid in presence of iron, *J. Chem. Soc.* 65, 899–910, 1894.

Fernandez, J., Bandara, J., Lopez, A., Buffat, P., and Kiwi, J. Photoassisted Fenton degradation of nonbiodegradable azo dye (orange II) in Fe-free solutions mediated by cation transfer membranes, *Langmuir* 15, 185–192, 1999.

Feuerstein, W., Gilbert, E., and Eberle, S.H. Modellversuche zur Oxidation aromatischer Verbindungen mittels Wasserstoffperoxid in der Abwasserbehandlung, *Vom Wasser*, 56 35–54, 1981.

Fish, R.H., Oberhausen, K., Chen, S., Richardson, J.F., Pierce, W., and Buchanan, R.M. Biomimetic oxidation studies. 7. Alkane functionalization with a MMO structural model, $[Fe_2O(OAc)(tris((1-methylimidazol-2-yl)methyl)amine)_2]^{3+}$, in the presence of *t*-butyl hydroperoxide and oxygen gas, *Catal. Lett.* 18, 357–365, 1993.

Francis, K.C., Cummins, D., and Oakes, J. Kinetic and structural investigations of [Fe(III)(edta)]- [edta = ethylenediaminetetraacetate(4-)] catalysed decomposition of hydrogen peroxide, *J. Chem. Soc. Dalton Trans.* 493–501, 1985.

Fujii, H., Yoshimura, T., and Kamada, H. ESR Studies of A_{1u} and A_{2u} oxoiron(IV) porphyrin pi–cation radical complexes. Spin coupling between ferryl iron and A_{1u}/A_{2u} orbitals, *Inorg. Chem.* 35, 2373–2377, 1996.

Fukushima, M., and Tatsumi, K. Degradation pathways of pentachlorophenol by photo-Fenton systems in the presence of iron(III), humic acid, and hydrogen peroxide, *Environ. Sci. Technol.* 35, 1771–1778, 2001.

Fukushima, M., Tatsumi, K., and Morimoto, K. The fate of aniline after a photo-Fenton reaction in an aqueous system containing iron(III), humic acid, and hydrogen peroxide, *Environ. Sci. Technol.* 34, 2006–2013, 2000.

Gallard, J., and De Laat, J. Kinetics of oxidation of chlorobenzenes and phenyl-ureas by $Fe(II)/H_2O_2$ and $Fe(III)/H_2O_2$. Evidence of reduction and oxidation reactions of intermediates by Fe(II) or Fe(III), *Chemosphere* 42, 405–413, 2001.

Gallard, H., and De Laat, J. Kinetic modelling of Fe(III)/H$_2$O$_2$ oxidation reactions in dilute aqueous solution using atrazine as a model organic compound, *Water Res.* 34, 3107–3116, 2000.

Gallard, H., de Laat, J., and Legube, B. Influence du pH sur la vitesse d'oxydation de composés organiques par FeII/H$_2$O$_2$: Mécanismes réactionnels et modélisation, *N. J. Chem.* 22, 263–268, 1998.

Gallard, H., De Laat, J., and Legube, B. Spectrophotometric study of the formation of iron(III)–hydroperoxy complexes in homogeneous aqueous solutions, *Water Res.* 33, 2929–2936, 1999.

Gernjak, W., Krutzler, T., Glaser, A., Malato, S., Caceres, J., Bauer, R., and Fernandez-Alba, A.R. Photo-Fenton treatment of water containing natural phenolic pollutants, *Chemosphere* 50, 71–78, 2002.

Goeb, S., Oliveros, E., Bossmann, S.H., Braun, A.M., Guardani, R., and Nascimento, C.A.O. Modeling the kinetics of a photochemical water treatment process by means of artificial neural networks, *Chem. Eng. Proc.* 38, 373–382, 1999.

Goeb, S., Oliveros, E., Bossmann, S.H., Braun, A.M., Nascimento, C.A.O., and Guardani, R. Optimal experimental design and artificial neural networks applied to the photochemically enhanced Fenton reaction, *Water Sci. Technol.* 44, 339–345, 2001.

Gogate, P.R., and Pandit, A.B. A review of imperative technologies for wastewater treatment I: Oxidation technologies at ambient conditions, *Adv. Environ. Res.* 8, 501–551, 2004a.

Gogate, P.R., and Pandit, A.B. A review of imperative technologies for wastewater treatment II: Hybrid methods, *Adv. Environ. Res.* 8, 553–597, 2004b.

Goi, A., and Trapido, M. Hydrogen peroxide photolysis, Fenton reagent and photo-Fenton for the degradation of nitrophenols: A comparative study, *Chemosphere* 46, 913–922, 2002.

Goldstein, S., Meyerstein, D., and Czapski, G. The Fenton reagents, *Free Radical Biol. Med.* 15, 435–445, 1993.

Goldstone, J. V., Pullin, M. J., Bertilsson, S., and Voelker, B. M. Reactions of hydroxyl radical with humic substances: Bleaching, mineralization, and production of bioavailable carbon substrates, *Environ. Sci. Technol.* 36, 364–372, 2002.

Gonzalez, M.G., Oliveros, E., Wörner, M., and Braun, A.M. Vacuum-ultraviolet photolysis of aqueous reaction systems, *J. Photochem. Photobiol. C Photochem. Rev.* 5, 225–246, 2004.

Goodell, B., Jellison, J., Liu, J., Daniel, G., Paszczunski, A., Fekete, F., Krishnamurthy, S., Jun, L., and G. Xu. Low molecular weight chelators and phenolic compounds isolated from wood decay fungi and their role in the fungal biodegradation of wood, *J. Biotechnol.* 53, 133–162, 1997.

Graf, E., Mahoney, J.R., Bryant, R.G., and Eaton, J.W. Iron-catalyzed hydroxyl radical formation, *J. Biol. Chem.* 259, 3620–3624, 1984.

Haber, F., and Weiss, J. The catalytic decomposition of hydrogen peroxide by iron salts, *Proc. Roy. Soc. A.* 134, 332–351, 1934.

Hamilton, G.A., Hanifin, J.W., Jr., and Friedman, J.P. The hydroxylation of aromatic compounds by hydrogen peroxide in the presence of catalytic amounts of ferric ion and catechol. Product studies, mechanism, and relation to some enzymic reactions, *J. Am. Chem. Soc.* 88, 5269–5272, 1966.

Hatchard, C.G., and Parker, C.A. A new sensitive chemical actinometer. II. Potassium ferrioxalate as a standard chemical actinometer, *Proc. Roy. Soc.* A235, 518–536, 1956.

Herrera, F., Lopez, A., and Kiwi, J. Photochemically activated degradation of reactive dyes. Statistical modeling of the reactor performance, *J. Photochem. Photobiol. A Chem.* 135, 45–51, 2000.

Hess, T.F., and Schrader, P.S. Coupled abiotic-biotic mineralization of 2,4,6-trinitrotolute (TNT), *J. Environ. Qual.* 31, 736–744, 2002.

Hislop, K.A., and Bolton, J.R. The photochemical generation of hydroxyl radicals in the UV-vis/ferrioxalate/H_2O_2 System, *Environ. Sci. Technol.* 33, 3119–3126, 1999.

Howsawkeng, J., Watts, R., Washington, D., Teel, A., Hess, T., and Crawford, R. Evidence for simultaneous abiotic-biotic oxidations in a microbial-fenton's system, *Environ. Sci. Technol.* 35, 2961–2966, 2001.

Hsaio, Y.L., and Nobe, K. Oxidative reactions of phenol and chlorobenzene with in situ electrogenerated Fenton's reagent, *Chem. Eng. Commun.* 126, 97–110, 1993.

Huang, Y.-H., Chou, S., Perng, M.-G. Huang, G.-H., and Cheng, S.-S. Case study on the bioeffluent of petrochemical wastewater by electro-Fenton method, *Water Sci. Technol.* 39, 145–149, 1999.

Huston, P.L., and Pignatello, J.J. Reduction of perchloroalkanes by ferrioxalate-generated carboxylate radical preceding mineralization by the photo-Fenton reaction, *Environ. Sci. Technol.* 30, 3457–3463, 1996.

Iwahashi, H., Morishita, H., Ishii, T., Sugata, R., and Kido, R. Enhancement by catechols of hydroxyl-radical formation in the presence of ferric ions and hydrogen peroxide, *J. Biochem.* 105, 429–434, 1989.

Iwahashi, H., Kawamori, H., and Fukushima, K. Quinolinic acid, picolinic acid, fusaric acid, and 2,6-pyridinedicarboxylic acid enhance the fenton reaction in phosphate buffer, *Chem. Biol. Interact.* 118, 201–215, 1999.

Iwahashi, H., Ishii, T., Sugata, R., and Kido, R. The effects of caffeic acid and its related catechols on hydroxyl radical formation by 3-hydroxyanthranilic acid, ferric chloride, and hydrogen peroxide, *Arch. Biochem. Biophys.* 276, 242–247, 1990.

Jacobsen, F., Holcman, J., and Sehested, K. Activation parameters of ferryl ion reactions in aqueous acid solutions, *Int. J. Chem. Kinet.* 29, 17–24, 1997.

Jacobsen, F., Holcman, J., and Sehested, K. Reactions of the ferryl ion with some compounds found in cloud water, *Int. J. Chem. Kinet.* 30, 215–221, 1998.

Jayson, G.G., Parsons, B.J., and Swallow, A.J. Some simple, highly reactive, inorganic chlorine derivatives in aqueous solution, *J. Chem. Soc.* 1597–1607, 1973.

Jiang, J., Bank, J.F., and Scholes, C.P. Subsecond time-resolved spin trapping followed by stopped-flow EPR of Fenton reaction products, *J. Am. Chem. Soc.* 115, 4742–4746, 1993.

Jiang, Y., and Waite, T.D. Degradation of trace contaminants using coupled sonochemistry and Fenton's reagent, *Water Sci. Technol.* 47, 85–92, 2003.

Jones, P., Tobe, M.L., and Wynne-Jones, W.F.K. Behavior of mixtures of hydrogen peroxide + water. V. Stabilization against the iron perchlorate-catalyzed decomposition of hydrogen peroxide, *Trans. Faraday Soc.* 55, 91–97, 1959.

Joo, S.H., Feitz, A.J., Sedlak, D.L., and Waite, T.D. Quantification of the oxidizing capacity of nanoparticulate zero-valent iron, *Environ. Sci. Technol.* 39, 1263–1268, 2005.

Kakarla, P.K.C., and Watts, R.J. Depth of Fenton-like oxidation in remediation of surface soil, *Journal of Environmental Engineering* 123, 11–17, 1997.

Kang, S.F., Liao, C.H., and Chen, M.C. Pre-oxidation and coagulation of textile wastewater by the Fenton process, *Chemosphere* 46, 923–928, 2002.

Kang, S.-F., and Chang, H.-M. Coagulation of textile secondary effluents with Fenton's reagent, *Water Sci. Technol.* 36, 215–222, 1997.

Kang, Y.W., and Hwang, K.-Y. Effects of reaction conditions on the oxidation efficiency in the Fenton process, *Water Res.* 10, 2786–2790, 2000.

Katsumata, H., Kaneco, S., Suzuki, T., Ohta, K., and Yobiko, Y. Degradation of linuron in aqueous solution by the photo-Fenton reaction, *Chem. Eng. J.* 108, 269–276, 2005.

Kavitha, V., and Palanivelu, K. Degradation of nitrophenols by Fenton and photo-Fenton processes, *J. Photochem. Photobiol. A Chem.* 170, 83–95, 2005.

Kawaguchi, H., and Inagaki, A. Kinetics of ferric ion promoted photodecomposition of 2-chlorophenol, *Chemosphere* 28, 57–62, 1994.

Khuri, A.I., and Cornell, J.A. *Response Surfaces, Designs and Analyses*, Marcel Dekker, New York, 1987.

Kim, S.-M., and Vogelpohl, A. Degradation of organic pollutants by the photo-Fenton process, *Chem. Eng. Technol.* 21, 187–191, 1998.

Kim, Y.-K., and Huh, I.-R. Enhancing biological treatability of landfill leachate by chemical oxidation, *Environ. Eng. Sci.* 14, 73–79, 1997.

King, D.W. Role of carbonate speciation on the oxidation rate of Fe(II) in aquatic systems, *Environ. Sci. Technol.* 32, 2997–3003, 1998.

Kitis, M., Adams, C.D., and Daigger, G.T. The effects of Fenton's reagent pretreatment on the biodegradability of nonionic surfactants, *Water Res.* 33, 2561–2568, 1999.

Kiwi, J., Denisov, N., Gak, Y., Ovanesyan, N., Buffat, P., Suvorova, E., Gostev, F., Titov, A., Albers, P., and Nadtochenko, V. Catalytic Fe^{3+} clusters and complexes in Nafion active in photo-Fenton processes. High-resolution electron microscopy and femtosecond studies, *Langmuir* 18, 9054–9066, 2002.

Kiwi, J., Lopez, A., and Nadtochenko, V. Mechanism and kinetics of the OH-radical intervention during Fenton oxidation in the presence of a significant amount of radical scavenger (Cl^-), *Environ. Sci. Technol.* 34, 2162–2168, 2000.

Kiwi, J., Pulagarin, C., and Peringer, P. Effect of Fenton and photo-Fenton reactions on the degradation and biodegradability of 2- and 4-nitrophenols in water treatment, *Appl. Catal. B Environ.* 3, 335–350, 1994.

Kochany, J., and Lugowski, A. Application of Fenton's reagent and activated carbon for removal of nitrification inhibitors, *Environ. Technol.* 19, 425–429, 1998.

Kong, S.-H., Watts, R., and Choi, J.-H. Treatment of petroleum-contaminated soils using iron mineral catalyzed hydrogen peroxide, *Chemosphere* 37, 1473–1482, 1998.

Koppenol, W.H., Butler, J., and van Leeuwen, J.W. The Haber–Weiss cycle, *Photochem. Photobiol.* 28, 655–660, 1978.

Koyama, O., Kamagata, Y., and Nakamura, K. Degradation of chlorinated aromatics by Fenton oxidation and methanogenic digester sludge, *Water Res.* 28, 895–899, 1994.

Kremer, M.L. "Complex" versus "free radical" mechanism for the catalytic decomposition of H_2O_2 by ferric ions, *Int. J. Chem. Kinet.* 17, 1299–1314, 1985.

Kremer, M.L. Mechanism of the Fenton reaction. Evidence for a new intermediate, *Phys. Chem. Chem. Phys.* 1, 3595–3605, 1999.

Kremer, M.L. Is OH the active Fenton intermediate in the oxidation of ethanol? *J. Inorg. Biochem.* 78, 255–257, 2000.

Krishna, M.V.B., Chandrasekaran, K., Karunasagar, D., and Arunchalam, J. A combined treatment approach using Fenton's reagent and zero valent iron for the removal of arsenic from drinking water, *J. Hazard. Mater.* 84, 229–240, 2001.

Kunai, A., Hata, S., Ito, S., and Sasaki, K. The role of oxygen in the hydroxylation reaction of benzene with Fenton's reagent. Tracer study, *J. Am. Chem. Soc.* 108, 6012–6016, 1986.

Kuo, W.G. Decolorizing dye wastewater with Fenton's reagent, *Water Res.* 26, 881–886, 1992.

Langford C.H., and Carey, J.H. The charge transfer photochemistry of the hexaaquoiron(III) ion, the chloropentaaquoiron(III) ion, and the μ-dihydroxy dimer explored with *tert*-butyl alcohol scavenger, *Can. J. Chem.* 53, 2430–2435, 1975.

Larking, D.M., Crawford, R.J., Christie, G.B.Y., and Lonergan, G.T. Enhanced degradation of polyvinyl alcohol by *Pycnoporus cinnabainus* after pretreatment with Fenton's reagent, *Appl. Environ. Microbiol.* 65, 1798–1800, 1999.

Larson, R.A., Schlauch, M.B., and Marley, K.A. Ferric ions promoted photodecomposition of triazines, *J. Agric. Food Chem.* 39, 2057–2062, 1991.

Lau, I.W.C., Wang, P., and Fang, H.H.P. Organic removal of anaerobically treated leachate by Fenton coagulation, *J. Environ. Eng.* 127, 666–669, 2001.

LeChampion, L., Giannotti, C., and Ouazzani, J. Photo-catalytic degradation of 5-nitro-1,2,4-triazon-3-one NTO in aqueous suspension of TiO_2. Comparison with Fenton oxidation, *Chemosphere* 38, 1561–1570, 1999.

Lee, B.-D., Iso, M., and Hosomi, M. Prediction of Fenton oxidation positions in polycyclic aromatic hdyrocarbons by Frontier electron density, *Chemosphere* 42, 431–435, 2001.

Lee, B.-D., Hosomi, M., and Murakami, A. Fenton oxidation with ethanol to degrade anthracene into biodegradable 9,10-anthraquinone: A pretreatment method for anthracene contaminated soil, *Water Sci. Technol.* 38, 91–97, 1998.

Lei, L., Hu, X., Yue, P.L., Bossmann, S.H., Göb, S., and Braun, A.M. Oxidative degradation of polyvinyl alcohol by the photochemically enhanced Fenton reaction, *J. Photochem. Photobiol. A Chem.* 116, 159–166, 1998.

Leising, R.A., Brennan, B.A., Que, L., Jr., Fox, B.G., and Münck, E. Models for non-heme iron oxygenases: A high-valent iron-oxo intermediate, *J. Am. Chem. Soc.* 113, 3988–3990, 1991.

Leung, S.W., Watts, R.J., and Miller, G.C. Degradation of perchloroethylene by Fenton's reagent: Speciation and pathway, *J. Environ. Qual.* 21, 377–381, 1992.

Lewis, T.J., Richards, D.H., and Salter, D.A. Peroxy-complexes of inorganic ions in hydrogen peroxide–water mixtures. Part I. Decomposition by ferric ions, *J. Chem. Soc.* 2434–2446, 1963.

Li, Y.-S., Liu, C.-C., and Fang, Y.-Y. Decolorization of dye wastewater by hydrogen peroxide in the presence of basic oxygen furnace slag, *J. Environ. Sci. Health A* 34, 1205–1221, 1999.

Li, Z.M., Comfort, S.D., and Shea, P.J. Destruction of 2,4,6-trinitrotoluene by Fenton oxidation, *J. Environ. Qual.* 26, 480–487, 1997a.

Li, Z.M., Shea, P.J., and Comfort, S.D. Fenton oxidation of 2,4,6-trinitrotoluene in contaminated soil slurries, *Environ. Eng. Sci.* 14, 55–66, 1997b.

Lide, D.R., ed. *Handbook of Chemistry and Physics,* CRC Press, Boca Raton, FL, 1998.

Lin, B., Yamaguchi, R., Hosomi, M., and Murakami, A. A new treatment process for photo-processing waste using a sulfur-oxidizing bacteria/granular activated carbon system followed by Fenton oxidation, *Water Sci. Technol.* 38, 163–170, 1998.

Lin, J.-G., and Ma, Y.-S. Oxidation of 2-chlorophenol in water by ultrasound/Fenton method, *J. Environ. Qual.* 126, 130–137, 2000.

Lin, S.H., and Lo, C.C. Fenton process of treatment of desizing wastewater, *Water Res.* 31, 2050–2056, 1997.

Lin, S.H., Lin, C.M., and Leu, H.G. Operating characterisitics and kinetic studies of surfactant wastewater treatment by Fenton oxidation, *Water Res.* 33, 1735–1741, 1999.

Lindsey, M.E., and Tarr, M.A. Inhibited hydroxyl radical degradation of aromatic hydrocarbons in the presence of dissolved fulvic acid, *Water Res.* 34, 2385–2389, 2000a.

Lindsey, M.E., and Tarr, M.A. Inhibition of hydroxyl radical reaction with aromatics by dissolved natural organic matter, *Environ. Sci. Technol.* 34, 444–449, 2000b.

Lipcznska-Kochany, E. Degradation of aqueous nitrophenols and nitrobenzene by means of the Fenton reaction, *Chemosphere* 22, 529–536, 1991.

Lipczynska-Kochany, E. Novel method for a photocatalytic degradation of 4-nitrophenol in homogeneous aqueous solution, *Environ. Technol.* 12, 87–92, 1991.

Lipczynska-Kochany, E. Degradation of nitrobenzene and nitrophenols by means of advanced oxidation processes in a homogeneous phase: Photolysis in the presence of hydrogen peroxide versus the Fenton reaction, *Chemosphere* 24, 1369–1380, 1992.

Lloyd, R.V., Hanna, P.M., and Mason, R.P. The origin of the hydroxyl radical oxygen in the Fenton reaction, *Free Radical Biol. Med.* 22, 885–888, 1997.

Lu, M.C., Chen, J.N., and Chang, C.P. Effect of inorganic ions on the oxidation of dichlorovos insecticide with Fenton's reagent, *Chemosphere* 35, 2285–2293, 1997.

Lu, M.-C. Oxidation of chlorophenols with hydrogen peroxide in the presence of goethite, *Chemosphere* 40, 125–130, 2000.

Lucking, F., Koser, H., Jank, M., and Ritter, A. Iron powder, graphite and activated carbon as catalysts for the oxidation of 4-chlorophenol with hydrogen peroxide in aqueous solution, *Water Res.* 32, 2607–2614, 1998.

Lunar, L., Sicilia, D., Rubio, S., Perez-Bendito, D., and Nickel, U. Degradation of photographic developers by Fenton's reagent: Condition optimization and kinetics for metol oxidation, *Water Res.* 34, 1791–1802, 2000a.

Lunar, L., Sicilia, D., Rubio, S. Perez-Bendito, D., and Nickel, U. Identification of metol degradation products under Fenton's reagent treatment using liquid chromatography-mass spectrometry, *Water Res.* 34, 3400–3412, 2000b.

Luthy, R.G., Aiken, G.R., Brusseau, M.L., Cunningham, S.D., Gschwend, P.M., Pignatello, J.J., Reinhard, M., Traina, S.J., Weber, W.J. Jr., and Westall, J.C. Sequestration of hydrophobic organic contaminants by geosorbents, *Environ. Sci. Technol.* 31, 3341–3347, 1997.

MacFaul, P.A., Wayner, D.D.M., and Ingold, K.U. A radical account of "oxygenated Fenton Chemistry", *Accounts Chem. Res.* 31, 159–162, 1998.

MacKay, A.A., and Pignatello, J.J. Application of Fenton-based reactions for treating dye wastewaters: Stability of sulfonated azo dyes in the presence of Fe(III), *Helvet. Chim. Acta* 84, 2589–2600, 2001.

Mailhot, G., Astruc, M., and Bolte, M. Degradation of tributyltin chloride in water photoinduced by iron(III), *Organomet. Chem.* 13, 53–61, 1999.

Mansano-Weiss, C., Cohen, H., and Meyerstein, D. Reactions of peroxyl radicals with $Fe(H_2O)_6^{2+}$, *J. Inorg. Biochem.* 91, 199–204, 2002.

Martire, D.O., Caregnato, P., Furlong, J., Allegreti, P., and Gonzalez, M.C. Kinetic study of the reactions of oxoiron(IV) with aromatic substrates in aqueous solutions, *Int. J. Chem. Kinet.* 34, 488–494, 2002.

Masarwa, M., Cohen, H., Meyerstein, D., Hickman, D.L., Bakac, A., and Espensen, J.H. Reactions of low-valent transition-metal complexes with hydrogen peroxide. Are they "Fenton-like" or not? 1. The case of Cu_{aq}^+ and Cr_{aq}^{2+}, *J. Am. Chem. Soc.* 110, 4293–4297, 1988.

Mazellier, P., Mailhot, G., and Bolte, M. Photochemical behavior of the iron(III)/2,6-dimethylphenol system, *N. J. Chem.* 21, 389–397, 1997.

Mazellier, P., Sarakha, M., and Bolte, M. Primary mechanism for the iron(III) photoinduced degradation of 4-chlorophenol in aqueous solution, *N. J. Chem.* 23, 133–135, 1999.

Mazellier, P., and Sulzberger, B. Diuron degradation in irradiated, hetergeneous iron/oxalate systems: The rate-determining step, *Environ. Sci. Technol.* 35, 3314–3320, 2001.

McGinnis, B.D., Adams, V.D., and Middlebrooks, E.J. Degradation of ethylene glycol in photo Fenton systems, *Water Res.* 34, 2346–2354, 2000.

Merz, J.H., and Waters, W.A. Electron-transfer reactions. A. The mechanism of oxidation of alcohols with Fenton reagent, *Disc. Faraday Soc.* 2, 179–188, 1947.

Meunier, B. In *Metalloporphyrins catalyzed oxidations*, Montanari, F., Casella, L., Eds., Kluwer Academic, Dordrecht, 1994, chap. 1.

Miller, C.M., Valentine, R.L., Roehl, M.E., and Alvarez, P.J.J. Chemical and microbiological assessment of pendimethalin-contaminated soil after treatment with Fenton's reagent, *Water Res.* 30, 2579–2586, 1996.

Nadtochenko, V., and Kiwi, J. Photoinduced adduct formation between orange II and $[Fe^{3+}(aq)]$ or $Fe(ox)_3^{3-}$–H_2O_2, *J. Chem. Soc. Faraday Trans.* 93, 2373–2378, 1997.

Nam, W., Ho, R., and Valentine, J.S. Iron–cyclam complexes as catalysts for the epoxidation of olefins by 30% hydrogen peroxide in acetonitrile and methanol, *J. Am. Chem. Soc.* 113, 7052–7054, 1991.

Nam, K., Rodriguez, W., and Kukor, J. Enhanced degradation of polycyclic aromatic hydrocarbons by biodegradation combined with a modified Fenton rection, *Chemosphere* 45, 11–20, 2001.

Nascimento, C.A.O., Oliveros, E., and Braun, A.M. Neural network modelling for photochemical processes, *Chem. Eng. Proc.* 33, 319–324, 1994

Natrajan, A., Hecht, S.M., van der Marel, G.A., and van Boom, J.H. Activation of Fe(III)-bleomycin by 10-hydroperoxy-8,12-octadecadienoic acid, *J. Am. Chem. Soc.* 112, 4532–4538, 1990.

Neta, P., Grodkowski, J., and Ross, A.B. Rate constants for reactions of aliphatic carbon-centered radicals in aqueous solution, *J. Phys. Chem. Ref. Data* 25, 709–1050, 1996.

Neyens, E., and Baeyens, J. A review of the classic Fenton's peroxidation as an advanced oxidation technique, *J. Hazard. Mater.* 98, 33–50, 2003.

Neyens, E., Baeyens, J., Weemaes, M., and DeHeyder, B. Advanced biosolids treatment using H_2O_2-oxidation, *Environ. Eng. Sci.* 19, 27–35, 2002.

Oliveros, E., Benoit-Marquié, F., Puech-Costes, E., Maurette, M.-T., and Nascimento, C.A.O. Neural network modeling of the photocatalytic degradation of 2,4-dihydroxybenzoic acid in aqueous solution, *Analysis* 26, 326–332, 1998.

Oliveros, E., Goeb, S., Bossmann, S.H., Braun, A.M., Nascimento, C.A.O., and Guardani, R. Waste water treatment by the photochemical enhanced Fenton reaction: Modeling and optimization using experimental design and artificial neural networks. In *Sustainable Energy and Environmental Technology*, Proceedings of the Third Asia Pacific Conference, Hu, X., Yue, P.L. eds., World Scientific, Singapore, 577–581, 2000.

Oliveros, E., Legrini, O., Braun, A.M., Hohl, M., and Müller, T. Large scale development of a light-enhanced Fenton reaction by optimal experimental design, *Water Sci. Technol.* 35, 223–230, 1997a.

Oliveros, E., Legrini, O., Hohl, M., Müller, T., and Braun, A.M. Industrial waste water treatment: Large scale development of a light-enhanced Fenton reaction, *Chem. Eng. Proc.* 36, 397–405, 1997b.

Oturan, M.A., Aaron, J.J., Oturan, N., and Pinson, J. Degradation of chlorophenoxy herbicides in aqueous media, using a novel electrochemical method, *Pestic. Sci.* 55, 558–562, 1999.

Oturan, M.A., Oturan, N., Lahitte, C., and Trevin, S. Production of hydroxyl radicals by electrochemically assisted Fenton's reagent—Application to the mineralization of an organic micropollutant, pentachlorophenol, *J. Electroanal. Chem.* 507, 96–102, 2001.

Oturan, M.A., Peiroten, J., Chartrin, P., and Acher, A.J. Complete destruction of *p*-nitrophenol in aqueous medium by electro-Fenton method, *Environ. Sci. Technol.* 34, 3474–3479, 2000.

Park, J.S.B., Wood, P.M., Gilbert, B.C., and Whitwood, A.C. A kinetic and ESR investigation of iron(II) oxalate oxidation by hydrogen peroxide and dioxygen as a source of hydroxy radicals, *Free Radical Res.* 27, 447–458, 1997.

Paszczynski, A., Crawford, R., Funk, D., and Goodell, B. De novo synthesis of 4,5-dimethoxycatechol and 2,5-dimethoxyhydroquinone by the brown rot fungus *Gloeophyllum trabeum Appl. Environ. Microbiol.* 65, 674–679, 1999.

Perez, M., Torrades, F., Garcia-Hortal, J.A., Domenech, X., and Perel, J. Removal of organic contaminants in paper pulp treatment effluents under Fenton and photo-Fenton conditions, *Appl. Catal. B Environ.* 36, 63–74, 2002.

Petigara, B.R., Blough, N.V., and Mignerey, A.C. Mechanisms of hydrogen peroxide decomposition in soils, *Environ. Sci. Technol.* 36, 639–645, 2002.

Peyton, G.R., Bell, O.J., Girin, E., and Lefaivre, M.H. Reductive destruction of water contaminants during treatment with hydroxyl radical processes, *Environ. Sci. Technol.* 29, 1710–1712, 1995.

Pignatello, J. Dark and photoassisted Fe^{3+}-catalyzed degradation of chlorophenoxy herbicides by hydrogen peroxide, *Environ. Sci. Technol.* 26, 944–951, 1992.

Pignatello, J.J. Soil decontamination using ferric chelates and peroxide. U.S. Patent No 6,160,194, December 12, 2000.

Pignatello, J.J., Liu, D., and Huston, P. Evidence for an additional oxidant in the photoassisted Fenton reaction, *Environ. Sci. Technol.* 33, 1832–1839, 1999.

Pignatello, J.J., and Xing, B. Mechanisms of slow sorption of organic chemicals to organic particles, *Environ. Sci. Technol.* 30, 1–11, 1996.

Pignatello, J.J., and Day, M. Mineralization of methyl parathion insecticide in soil by hydrogen peroxide activated with iron(III)–NTA or –HEIDA complexes, *Haz. Waste. Haz. Mater.* 13, 237–244, 1996.

Pohl, K., Wieghardt, K., Kaim, W., and Steenken, S. Redox reactivity of bis(1,4,7-triazacyclononane)iron(II/III) complexes in alkaline solution and characterization of a deprotonated species: Amidoiron(III) vs aminyliron(II) ground-state formulation. EPR, kinetic, pulse radiolysis, and laser photolysis study, *Inorg. Chem.* 27, 440–447, 1988.

Pratap, K., and Lemley, A.T. Electrochemical peroxide treatment of aqueous herbicide solutions, *J. Agric. Food Chem.* 42, 209–215, 1994.

Pratap, K., and Lemley, A.T. Fenton electrochemical treatment of aqueous atrazine and metachlor, *J. Agric. Food Chem.* 46, 3285–3291, 1998.

Pulgarin, C., and Kiwi, J. Overview on photocatalytic and electrocatalytic pretreatment of industrial non-biodegradable pollutants and pesticides, *Chimia* 50, 50–55, 1996.

Qiang, Z., Chang, J.-H., and Huang, C.-P. Electrochemical regeneration of Fe^{2+} in Fenton oxidation processes, *Water Res.* 37, 1308–1319, 2003.

Rahhal, S., and Richter, H. W. Reduction of hydrogen peroxide by the ferrous iron chelate of diethylenetriamine-N,N,N′,N″,N″-pentaacetate, *J. Am. Chem. Soc.* 110, 3126–3133, 1988.

Ravikumar, J.X., and Gurol, M.D. chemical oxidation of chlorinated organics by hydrogen peroxide in the presence of sand, *Environ. Sci. Technol.* 28, 394–400, 1994.

Ribordy, P., Pulgarin, C. Kiwi, J., and Peringer, P. Electrochemical versus photochemical pretreat of industrial wastewaters, *Water Sci. Technol.* 35, 293–302, 1997.

Rigg, T., Taylor, W., and Weiss, J. The rate constant of the reaction between hydrogen peroxide and ferrous ions, *J. Chem. Phys.* 22, 575–577, 1954.

Rios-Enriquez, M.A., Shahin, N., Durán-de-Bazúa, C., Lang, J., Oliveros, E., Bossmann, S.H., and Braun, A.M. Optimization of the heterogeneous Fenton-oxidation of the model pollutant 2,4-xylidine using the experimental design methodology, *Solar Energy* 77, 491–501, 2004.

Rodriguez, J., Contreras, D., Parra, C., Freer, J., Baeza, J., and Duran, N. Pulp mill effluent treatment by Fenton-type reactions catalyzed by iron complexes, *Water Sci. Technol.* 40, 351–355, 1999.

Roe, B.A., and Lemley, A.T. Treatment of two insecticides in an electrochemical Fenton system, *J. Environ. Sci. Health B* 32, 261–281, 1997.

Ronco, S.E., and Aymonino, P.J. Kinetics of the thermal and photochemical decomposition of aquapentacyanoferrate(III) in aqueous solution, *Transition Met. Chem.* 12, 174–178, 1987.

Rumelhart, D.E., Hinton, G.E., and Williams, R.J. In *Parallel Distributed Processing: Explorations in the Microstructure of Cognition*, J.L. McClelland, ed., MIT Press, Cambridge, MA, Vol. 1, chapt. 8, 1986.

Ruppert, G., Bauer, R., and Heisler, G. The photo-Fenton reaction—an effective photochemical wastewater treatment process, *J. Photochem. Photobiol. A Chem.* 73, 75–78, 1993.

Rush, J.D., and Bielski, B.H.J. Decay of ferrate(V) in neutral and acidic solutions. A premix pulse radiolysis study, *Inorg. Chem.* 33, 5499–5502, 1994.

Rush, J.D., and Bielski, B.H.J. Pulse radiolysis of alkaline Fe(III) and Fe(IV) solutions. Observation of transient iron complexes with intermediate oxidation states, *J. Am. Chem. Soc.* 108, 523–525, 1986.

Rush, J.D., and Koppenol, W.H. Oxidizing intermediates in the reaction of ferrous EDTA with hydrogen peroxide, *J. Biol. Chem.* 261, 6730–6733, 1986.

Sabhi, S., and Kiwi, J. Degradation of 2,4-dichlorophenol by immobilized iron catalysts, *Water Res.* 35, 1994–2002, 2001.

Safarzadeh-Amiri, A., Bolton, J. R., and Cater, J. R. Ferrioxalate-mediated photodegradaation of organic pollutants in contaminated water, *Water Res.* 31, 787–798, 1997.

Safarzadeh-Amiri, A., Bolton, J.R., and Cater, S.R. The use of iron in advanced oxidation technologies, *J. Adv. Oxid. Technol.* 1, 18–26, 1996.

Saltmiras, D.A., and Lemley, A.T. Anodic Fenton treatment of treflan MTF (R), *J. Environ. Sci. Health A* 36, 261–274, 2001.

Saltmiras, D.A., and Lemley, A.T. Degradation of ethylene thiourea (ETU) with three Fenton treatment processes, *J. Agric. Food Chem.* 48, 6149–6157, 2000.

Sandström, B.E., Svoboda, P., Granström, M., Harms-Ringdahl, M., and Candeias, L.P. H_2O_2-Driven reduction of the Fe^{3+}-quin2 chelate and the subsequent formation of oxidizing species, *Free Radical Biol. Med.* 23, 744–753, 1997.

Sauleda, R., and Brillas, E. Mineralization of aniline and 4-chlorophenol in acidic solution by ozonation catalyzed by Fe^{2+} and UVA light, *Appl. Catal. B Environ.* 29, 135–145, 2001.

Savall, A. Electrochemical treatment of industrial organic effluents, *Chimia* 49, 23–27, 1995.

Sawyer, D.T., Kang, C., Llobet, A., and Redman, C., Fenton reagents (1:1 $Fe^{II}L_x$/HOOH) react via $[L_xFe^{II}OOH(BH^+)]$ as hydroxylases, not as generators of free hydroxyl radicals (HO·) *J. Am. Chem. Soc.* 115, 5817–5818, 1993.

Sawyer, D.T., Sobkowiak, A., and Matsushita, T. Metal [MLx, M = Fe, Cu, Co, Mn]/hydroperoxide-induced activation of dioxygen for the oxygenation of hydrocarbons: Oxygenated Fenton chemistry, *Acc. Chem. Res.* 29, 409–416, 1996.

Sawyer, D.T., and Valentine, J.S. How super is superoxide, *Acc. Chem. Res.* 14, 393–400, 1981.

Schröder, D., Bärsch, S., and Schwarz, H. Second ionization energies of gaseous iron oxides and hydroxides: the $FeO_mH_n^{2+}$ dications ($m = 1, 2; n$ less than or equal to 4), *J. Phys. Chem. A* 104, 5101–5110, 2000.

Sedlak, D.L., and Andren, A.W. Aqueous-phase oxidation of polychlorinated biphenyls by hydroxyl radicals, *Environ. Sci. Technol.* 25, 1419–1427, 1991.

Sheldon, R.A., and Kochi, J.K. *Metal-Catalyzed Oxidations of Organic Compounds*, Academic Press, New York, 1981.

Shen, Z., Yang, J., Hu, X., Lei, Y., Ji, X., Jia, J., and Wang, W. Dual electrodes oxidation of dye wastewater with gas diffusion cathode, *Environ. Sci. Technol.* 39, 1819–1826, 2005.

Sheu, C., Richert, S.A., Cofré, R.B., Jr., Sobkowiak, A., Sawyer, D.T., and Kanofsky, J.R., Iron-induced activation of hydrogen peroxide for the direct ketonization of methylenic carbon [c-C_6H_{12} to c-$C_6H_{10}(O)$] and the dioxygenation of acetylenes and arylolefins, *J. Am. Chem. Soc.* 112, 1936–1942, 1990.

Sheu, C., and Sawyer, D.T. Activation of dioxygen by PA-iron(II) for the bromination (via $BrCCl_3$) and monoxygenation (via PhNHNHPh) of saturated hydrocarbons: Reaction mimic for the methane monoxygenase proteins; *J. Am. Chem. Soc.* 112, 8212–8214, 1990a.

Sheu, C., Sobkowiak, A., Jeon, S., and Sawyer, D.T. Activation of dioxygen by bis(2,6-dicarboxylatopyridine)iron(II) for the ketonization of methylenic carbons and the dioxygenation of acetylenes, aryl olefins, and catechols: Reaction mimics for dioxygenase proteins, *J. Am. Chem. Soc.* 112, 879–881, 1990b.

Sillén, L.G., and Martell, A.E. *Stability Constants of Metal-ion Complexes*, The Chemical Society, London, 1964.

Sima, J., and Makanova, J. Photochemistry of iron(III) complexes, *Coord. Chem. Rev.* 160, 161–189, 1997.

Smith, M.B., and March, J. *March's Advanced Organic Chemistry*, 5th ed. J. Wiley & Sons, New York, 2001.

Song, Y., Yang, C.-M., and Kluger, R. Monoxygenase-like activity of methemoglobin with sodium sulfite as an efficient reductant, *J. Am. Chem. Soc.* 115, 4365–4366, 1993.

Sorokin, A., Seris, J., and Meunier, B. Efficient oxidation dechlorination and aromatic ring cleavage of chlorinated phenols catalyzed by iron sulfophthalocyanine, *Science* 268, 1163–1166, 1995.

Sudoh, M., Kodera, T., Sakai, K., Zhang, J.Q., and Koide, K. Oxidative degradation of aqueous phenol effluent with electrogenerated Fenton's reagent, *J. Chem. Eng. Jpn.* 19, 513–518, 1986.

Sugimoto, H., Tung, H.-C., and Sawyer, D.T. Formation, characterization, and reactivity of the oxene adduct of [tetrakin(2,6-dichlorophenyl) porphrinato]iron(III) perchlorate in acetonitrile. Model for the reactive intermediate of cyrtochrome P-450, *J. Am. Chem. Soc.* 110, 2465–2470, 1988.

Sun, Y., and Pignatello, J.J. Chemical treatment of pesticide wastes. Evaluation of Fe(III) chelates for catalytic hydrogen peroxide oxidation of 2,4-D at circum-neutral pH, *J. Agric. Food Chem.* 40, 322–327, 1992.

Sun, Y., and Pignatello, J.J. Activation of hydrogen peroxide by iron(III) chelates for abiotic degradation of herbicides and insecticides in water, *J. Agric. Food Chem.* 41, 308–312, 1993a.

Sun, Y., and Pignatello, J.J. Organic intermediates in the degradation of 2,4-dichlorophenoxyacetic acid by Fe^{3+}/H_2O_2 and $Fe^{3+}/H_2O_2/UV$, *J. Agric. Food Chem.* 41, 1139–1142, 1993b.

Sun, Y., and Pignatello, J.J. Photochemical reactions involved in the total mineralization of 2,4-D by Fe3+/H_2O_2/UV, *Environ. Sci. Technol.* 27, 304–310, 1993c.

Sun, Y., and Pignatello, J.J. Complete oxidation of metolachlor and methyl parathion in water by the photoassisted Fenton reaction, *Water Res.* 29, 1837–1844, 1995.

Sylva, R.N. The hydrolysis of iron(III). *Rev. Pure Appl. Chem.* 22, 115–130, 1972.

Szulbinski, W.S. Fenton reaction of iron chelates involving polyazacyclononane. The ligand structure effect, *Polish J. Chem.* 74, 109–124, 2000.

Takemura, Y., Seno-o, K., Mukai, T., and Suzzuki, M. Decomposing organic chlorine compounds in dry cleaning wastewater by Fenton's reaction on recticulated iron, *Water Sci. Technol.* 30, 129–137, 1994.

Tang, W.Z., and Chen, R.Z. Decolorization kinetics and mechanisms of commercial dyes by H_2O_2/iron powder system, *Chemosphere* 32, 947–958, 1996.

Tang, W.Z., and Huang, C.P. 2,4-Dichlorophenol oxidation kinetics by Fenton's reagent, *Environ. Technol.* 17, 1371–1378, 1996.

Tang, W.Z., and Huang, C.P. Stoichiometry of Fenton's reagent in the oxidation of chlorinated aliphatic organic pollutants, *Environ. Technol.* 18, 13–23, 1997.

Tang, W.Z., and Tassos, S. Oxidation kinetics and mechanisms of trihalomethanes by Fenton's reagent, *Water Res.* 5, 1117–1125, 1997.

Tarr, M.A. Chemical degradation methods for wastes and pollutants. In *Environmental Science and Pollution Control Series*, Vol. 26 (Chemical Degradation Methods for Wastes and Pollutants), 165–200, 2003.

Teel, A.L., Warberg, C.R., Atkinson, D.A., and Watt, R.J. Comparison of mineral and soluble iron Fenton's catalysts for the treatment of trichloroethylene, *Water Res.* 35, 977–984, 2001.

Teixeira, A.C.S.C., Guardani, R., and Nascimento, C.A.O. Solar photochemical degradation of aminosilicones contained in liquid effluents, *Ind. Eng. Chem. Res.* 42, 5751–5761, 2003.

Teixeira, A.C.S.C., Guardani, R., and Nascimento, C.A.O. Photo-Fenton remediation of wastewaters containing silicones: Experimental study and neural network modeling, *Chem. Ing. Technol.* 27, 800–810, 2004.

Trapido, M., and Kallas, J. Advanced oxidation processses for the degradation and detoxification of 4-nitrophenol, *Environ. Technol.* 21, 799–808, 2000.

Tung, H.-C., Kang, C., and Sawyer, D.T. Nature of the reactive intermediates from the iron induced activation of hydrogen peroxide: Agents for the ketonizaton of methylenic carbons, the monoxygenation of hydrocarbons, and the dioxygenation of arylolefins, *J. Am. Chem. Soc.* 114, 3445–3455, 1992.

Tyre, B.W., Watts, R.J., and Miller, G.C. Treatment of four biorefractory contaminants in soils using catalyzed hydrogen peroxide, *J. Environ. Qual.* 20, 832–838, 1991.

U.S. Environmental Protection Agency. *Handbook on Advanced Nonphotochemical Oxidation Processes.* U.S. EPA, National Risk Management Research Laboratory, Cincinnati, OH, 1991.

Utset, B., Garcia, J., Casado, J., and Domènech, X. Replacement of H_2O_2 by O_2 in Fenton and photo-Fenton reactions, *Chemosphere* 41, 1187–1192, 2000.

Van der Zee, J., Krootjes, B.B.H., Chignell, C.F., Dubbelman, T.M.A.R., and Van Steveninck, J. Hydroxyl radical generation by a light dependent Fenton reaction, *Free Radical Biol. Med.* 14, 105–113, 1993.

Voelker, B.M., and Sulzberger, B. Effects of fulvic acid on Fe(II) oxidation by hydrogen peroxide, *Environ. Sci. Technol.* 30, 1106–1114, 1996.

Von Sonntag, C., and Schuchmann, H.P. Elucidation of peroxyl radical reactions in aqueous solution with radiation chemistry technology, *Angew. Chem. Int. Ed. Engl.* 30(10), 1229–1253, 1991.

Von Sonntag, C., and Schuchmann, H.P. Peroxyl radicals in aqueous solutions. In *Peroxyl Radicals*, Z. B. Alfassi, ed., John Wiley and Sons, New York, 173–234, 1997.

Walling, C. Fenton's reagent revisited, *Acc. Chem. Res.* 8, 125–131, 1975.

Walling, C. Intermediates in the reactions of Fenton type reagents, *Acc. Chem. Res.* 31, 155–157, 1998.

Walling, C., and Amarnath, K. Oxidation of mandelic acid by Fenton's reagent, *J. Am. Chem. Soc.* 104, 1185–1189, 1982.

Walling, C., and Goosen, A. Mechanism of the ferric ion catalyzed decomposition of hydrogen peroxide. Effect of organic substrates, *J. Am. Chem. Soc.* 95, 2987, 1973.

Walling, C., Kurz, M., and Schugar, H.J. The iron(III)-ethylenediaminetetraacetic acid–peroxide system, *Inorg. Chem.* 9, 931–937, 1970.

Wang, Q.Q., and Lemley, A.T. Kinetic model and optimization of 2,4-D degradation by anodic Fenton treatment, *Environ. Sci. Technol.* 35, 4509–4514, 2001.

Wanpeng, Z., Zhihua, Y., and Li, W. Application of ferrous-hydrogen peroxide for the treatment of H-acid manufacturing process wastewater, *Water Res.* 30, 2949–2954, 1996.

Watts, R.J., Bottenberg, B.C., Hess, T.F., Jensen, M.D., and Teel, A.L. Role of reductants in the enhanced desorption and transformation of chloroaliphatic compounds by modified Fenton's reactions *Environ. Sci. Technol.* 33, 3432–3437, 1999.

Watts, R., Kong, S., Dippre, M., and Barnes, W.T. Oxidation of sorbed hexachlorobenzene in soils using catalyzed hydrogen peroxide, *J. Hazard. Mater.* 39, 33–47, 1994.

Watts, R.J., and Stanton, P.C. Mineralization of sorbed and NAPL-phase hexadecane by catalyzed hydrogen peroxide, *Water Res.* 33, 1405–1414, 1999.

Wells, C.F., and Salam, M.A. Hydrolysis of ferrous ions: A kinetic method for deermination of the Fe(II) species, *Nature* 205, 690–692, 1965.

Wells, C.F., and Salam, M.A. Complex formation between iron(II) and inorganic anions. Part I. Effect of simple and complex halide ions on the reaction of Fe(II) + H_2O_2 reaction, *Trans. Faraday Soc.* 63, 620–629, 1967.

Wells, C.F., and Salam, M.A. The effect of pH on the kinetics of the reaction of iron(II) with hydrogen peroxide in perchlorate media, *J. Chem. Soc. A* 24–29, 1968a.

Wells, C.F., and Salam, M.A. Complex formation between iron(II) and inorganic anions. Part II. The effect of oxyanions on the reaction of iron(II) with hydrogen peroxide, *J. Chem. Soc. A* 308–315, 1968b.

Wink, D.A., Nims, R.W., Saavedra, J.E., Utermahlen, W.E. Jr., and Ford, P.C. The Fenton oxidation mechanism: reactivities of biologically relevant substrates with two oxidizing intermediates differ from those predicted for the hydroxyl radical, *Proc. Natl. Acad. Sci. USA* 91, 6604–6608, 1994.

Xie, Y., Chen, F., He, J., Zhao, J., and Wang, H. Photoassisted degradation of dyes in the presence of Fe^{3+} and H_2O_2 under visible irradiation, *J. Photochem. Photobiol. A Chem.* 136, 235–240, 2000.

Yoo, H.C., Cho, S.H., and Ko, S.O. Modification of coagulation and Fenton oxidation processes for cost-effective leachate treatment, *J. Environ. Sci. Health A* 36, 39–48, 2001.

Yoon, J., Cho, S., Cho, Y., and Kim, S. The characteristics of coagulation of Fenton reaction in the removal of landfill leachate organics, *Water Sci. Technol.* 38, 209–214, 1998.

Yu, G., Zhu, W., and Yang, Z. Pretreatment and biodegradability enhancement of DSD acid manufacturing wastewater, *Chemosphere* 37, 487–494, 1998.

Zehavi, D., and Rabani, J. The oxidation of aqueous bromide ions by hydroxyl radicals. A pulse radiolytic investigation, *J. Phy. Chem.* 76, 312–319, 1972.

Zupan, J., and Gasteiger, J, *Neural Networks for Chemists: An Introduction*, VCH, Weinheim, 1993.